TIMING, DISTRIBUTION AND CLIMATIC IMPLICATIONS

OF LATE QUATERNARY EOLIAN DEPOSITS:

NORTHERN COLUMBIA PLATEAU, WA

By:

KURT ALAN DALMAN

A thesis submitted in partial fulfillment of
the requirements for the degree of

MASTER OF GEOLOGY

WASHINGTON STATE UNIVERSITY
School of Earth and Environmental Sciences

MAY 2007

To the Faculty of Washington State University:

The members of the Committee appointed to examine the thesis of KURT ALAN DALMAN find it satisfactory and recommend that is be accepted.

_____

Chair

_____

_____

Finally, I would like to thank my family for their encouragement and patience in this part of my life's journey. Thanks mostly to Anna for her listening ears and editing eyes with a subject she has hopefully grown to appreciate. Thanks also to Camas for his comedic relief, his foot warming, and his giving me an excuse to take breaks and go for walks.

TIMING, DISTRIBUTION AND CLIMATIC IMPLICATIONS

OF LATE QUATERNARY EOLIAN DEPOSITS:

NORTHERN COLUMBIA PLATEAU, WA

Abstract

by Kurt Alan Dalman, MS
Washington State University
May 2007

Chair: David R. Gaylord

Eolian sedimentation on the northern Columbia Plateau, WA is intimately tied to last glacial maximum (LGM) outburst flooding. Post-LGM, L1, loess on the northern plateau never exceeds 3 m while coeval loess on the southern plateau reaches thicknesses of 8 m (Sweeney, 2004). Similarly, post-LGM mass accumulation rates (MARs) for loess on the northern plateau are one to two orders of magnitude less than those of the southern plateau. Relatively thin loess deposits on the northern plateau are a product of source-limiting factors. These factors include: 1) a lack of fine-grained material within source deposits due to the bypassing of fine-grained particles over the northern plateau during glacial outburst flooding, 2) the presence of coarse-grained deposits stratigraphically above fine-grained deposits preventing eolian remobilization of fine-grained deposits, 3) the erosional removal of loess and soil during glacial outburst flooding, which left large portions of the region bare bedrock and unsuitable for vegetative growth and sediment accumulation.

Glacial outburst flooding on the northern Columbia Plateau deposited a diverse mixture of clay- to boulder-sized sediment. The fine-grained sediment fraction is held in

deposits associated with narrow passageways along the flood path and in back flooded tributary valleys. The coarse sediment was deposited within and at the terminuses of flood channels and formed gravel bars and alluvial fans. Adequate fine-grained material required to produce the relatively thin loess deposits of Wilbur Plateau and east of Quincy Basin is present within Quincy Basin. The Columbia River Valley, Grand Coulee, Wilson Creek Valley and Lind Coulee were also identified as likely local sources of loess on the northern plateau.

The stratigraphy of the northern Columbia Plateau sediments gives insight into the outburst flood and climatic history of eastern Washington. Tephras and paleosols are major stratigraphic markers on the plateau. Tephras indicate outburst-flooding episodes occurred following the Mount St. Helens "S" eruption (ca. 15.4 ka) and preserved Glacier Peak tephra suggests extensive eolian activity prior to and following ca. 13.2 ka. MARs determined from paleosols and tephra data suggest cold and dry glacial episodes marked by accelerated eolian activity during and following glacial ice retreat.

TABLE OF CONTENTS

LIST OF FIGURES

LIST OF TABLES

CHAPTER ONE

INTRODUCTION

The Quaternary Period in Eastern Washington was marked by cold and dry glacial periods followed by increasingly wet interglacial times. Sediment deposited on the Columbia Plateau by glacial outburst floods and the redistribution of this glacial sediment by wind and water during interglacial periods produced the complex stratigraphy recorded on the northern Columbia Plateau. Glacial sediments were derived from glacial outwash, glacio-lacustrine, and glacio-fluvial processes. The most prominent depositional and erosional features resulted from immense and catastrophic glacial outburst floods or jökulhlaups (Björnsson, 1974), that periodically occurred during previous glaciations (Bretz, 1923; 1969; Bretz et al., 1956; Baker, 1973; Waitt, 1980; 1985; Baker and Bunker, 1985). The floods stripped much of the existing sediment cover and carved coulees into the bedrock of the northern plateau during creation of the Channeled Scabland (Bretz, 1923); (Figure 1.1).

The catastrophic outburst floods were capable of carrying a wide range of sediment from clay- to house-sized boulders (Bretz, 1923; 1969; Bretz et al., 1956; Baker, 1973; Baker and Bunker, 1985). Narrow passageways along the floods' path caused large bodies of water to be ponded for days to a week (Baker, 1973; Baker and Bunker, 1985). The ponding of water behind narrow passageways and within tributary valleys encouraged the deposition of fine sediment consisting primarily of silt and fine sand as slackwater deposits. These slackwater deposits are interstratified with, or cap, coarser sands and gravels thus forming normally graded rhythmite accumulations.

Late-stage glacial periods and early interglacial periods on the plateau provided a favorable environment for widespread eolian redistribution of the fine-grained sediments into the sand dune, sand sheet and loess deposits (Berger and Busacca, 1995; Richardson et al., 1997; 1999; Gaylord et al., 2003), that blanket much of the plateau. The stratigraphy of these eolian deposits holds key information on the post-glacial eolian and climatic history of the plateau. Paleosols within loess deposits record episodes of land surface stabilization and relatively decreased sediment input. Thick beds of mostly unaltered eolian sediment accumulate during relatively dry episodes when large volumes of unconsolidated fine-grained sediment is available for entrainment into the lower atmosphere (Berger and Busacca, 1995; Richardson et al., 1997; 1999, Sweeney, 2004).

The combination of silt and sand, which dominate the rhythmite deposits, makes these the main source for loess in eastern Washington (Sweeney, 2004; Gaylord et al., 2004). Other sources of silt include the partially cemented Ringold Formation (Packer, 1979; Ludwig, 1987), and Recent sedimentary deposits found within the Columbia River drainage system (Waitt, 1983; Gaylord et al., 2001). Loess deposits accumulated over the duration of the Pleistocene reach thicknesses of 75 m where they were not removed by glacial outburst floods (Busacca et. al., 1992). The major source of the northern plateau loess is thinner, less continuous and more coarse-grained glacial outwash and outburst flood deposits. This is unlike the southern Columbia Plateau, where loess is sourced primarily from three large relatively coarse-depleted slackwater concentrations of the Yakima Basin, Umatilla Basin and Walla Walla Valley (Sweeney, 2004; Sweeney et. al., 2004; 2005).

The higher flow competence of the outburst floods through the northern Scabland, including Grand Coulee and Quincy Basin, led to deposits of fines-depleted sand- and gravel-rich sediment (Baker, 1973). Only in local depocenters, such as behind point bars, in flood-scoured depressions or in back-flooded river and creek valleys, were the flood current velocities sufficiently slowed to deposit volumetrically significant fine-grained rhythmite deposits. The bypassing of finer-grained sediment created more coarsely grained deposits leading to greater expanses of gravel bars, alluvial fans, sand dunes and sand sheets on the northern plateau.

Saltating sand is the most effective mechanism for the entrainment of silt and fine-grained sand particles, and the production of loess deposits (Pye, 1987). Extensive sand dune migration on the northern Columbia Plateau would have promoted large-scale ejection of silt and clay into the atmosphere (Pye, 1987). However, loess deposits on the northern plateau are less than half as thick as those on the southern plateau (Sweeney, 2004). Reasons for thinner loess deposits on the northern plateau relative to the southern plateau include: 1) a lack of fine-grained material within the source deposits caused by the higher flood velocities and the bypassing of more mobile fine-grained sediment during outburst flooding, 2) a mantling of coarse-grained deposits overlying fine-grained deposits prevented the eolian redistribution of the fine-grained sediment and 3) the absence of a soil layer on flood scoured basalt bedrock, therefore, a less suitable ground surface for plant growth and loess accumulation.

This study sheds light on why northern plateau loess is relatively thin compared to coeval southern plateau loess. Determination of eolian sources and their characteristics provide insights into this observation. Eolian deposits on the northern

3

Columbia Plateau including their stratigraphies also provide key information required for the determination and further resolution of paleoclimatic fluctuations since the last glacial maximum.
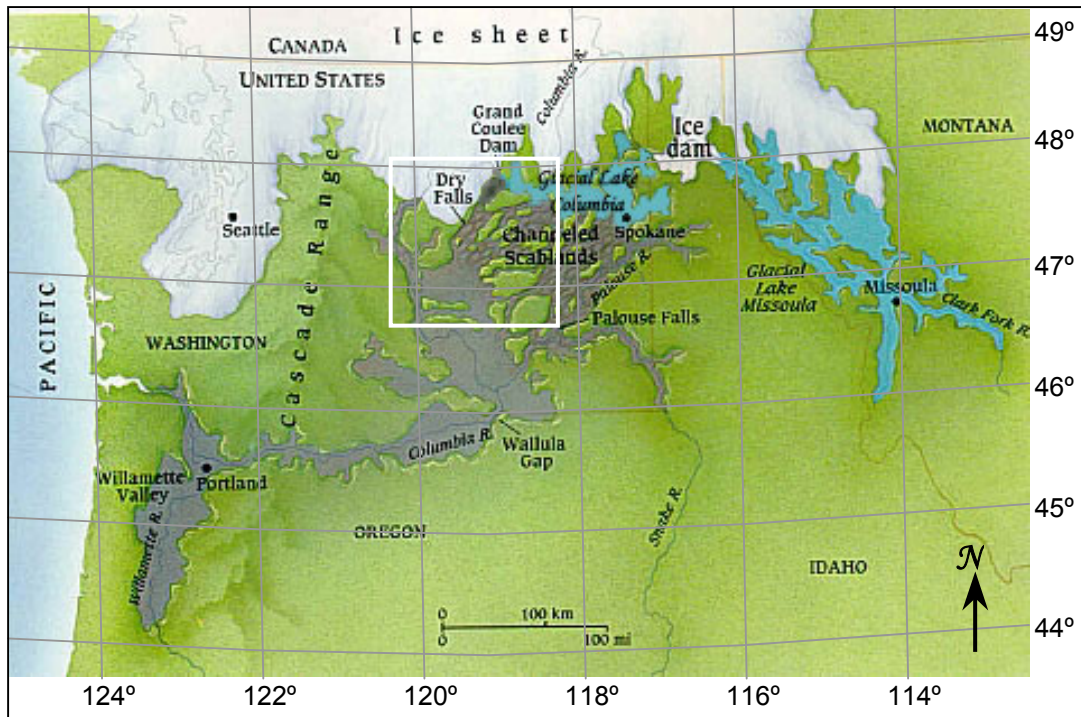
Figure 1.1. Map showing the region affected by glacial outburst flooding from Lake Missoula. Areas inundated during flooding are shaded gray. Study locality occurs within white box.

CHAPTER TWO

GEOLOGIC SETTING

The Quaternary eolian deposits on the Columbia Plateau of eastern Washington are closely linked to its Cenozoic history. The plateau was a major depocenter for widespread flood basalt during the Miocene (Figure 2.1). These flood basalts were termed the Columbia River Basalt Group (Swanson et al., 1979), and they cover an area on the order of 160,000 km^2 (Tolan et al., 1987). Since the emplacement of these thick sheets of basalt, they were locally deformed into east-west trending anticlinal and monoclinal ridges (Reidel, 1984). The ridges of most interest for this study are the Beezley Hills and the Frenchman Hills (Figure 2.2). The Beezley Hills extend across 350 km^2 on the northern plateau and rise 300 m above the northern margin of the Quincy Basin; the Frenchman Hills cover >200 km^2 and rise 200 m above the southern margin of the Quincy Basin. The Ringold Formation (ca. 3.4-8.5 Ma), a succession of continental siliciclastic sedimentary deposits from the Late Tertiary that discontinuously overlies the region's basalt flows and is best exposed along the Columbia River near Hanford, WA (Newcomb et al., 1972; Gustafson, 1978).

The Columbia Plateau was inundated and sculpted by catastrophic glacial outburst floods during the Late Pleistocene (Bretz et al., 1956; Baker, 1973; Waitt, 1980; 1985; Baker and Bunker, 1985). The sedimentary record indicates substantial flood deposits from the most recent flooding associated with the last glacial maximum (LGM) that occurred ca. 14.5-18.0 ka (Baker, 1973; Waitt, 1980; 1985; 1994; Atwater, 1984; 1986; 1987; Baker and Bunker, 1985; Smith, 1993; Bjornstad et al., 2001). Glacial flooding also occurred during previous glaciations with evidence of flood deposits prior

to the last magnetic reversal, ca. 1.1 Ma (McDonald and Busacca, 1992; Busacca and McDonald, 1994; Berger and Busacca, 1995; Pluhar et al., 2006). The question of how many floods and the source of these floods is still being debated. Shaw et al. (1999) propose a single outburst from beneath the Cordilleran ice sheet; however, most researchers agree that there were multiple outburst floods originating from glacial Lake Missoula (Figure 1.1); (Baker, 1973; Waitt, 1980; 1985; 1994; Atwater, 1984; 1986; 1987; Baker and Bunker, 1985; Smith, 1993; Clague et al., 2003; Pluhar et al., 2006; Smith, 2006).

Floodwaters with discharges up to 21×10^6 m^3/sec and velocities reaching 16 m/s brought with them a large volume of poorly sorted sediment (Baker, 1973; Baker and Bunker, 1985). The sediment deposited consists of boulders as large as houses down to fine silt- and clay-sized glacial flour. Much of the northern plateau, including the Wilbur Plateau, was almost entirely stripped of post-Miocene sedimentary deposits as the outburst flood waters rushed over the surface leaving only small loess capped basalt plateaus or loess islands (Kiver et al., 1991; Bjornstad et al., 2001). This highly dissected region was termed the Channeled Scabland by Bretz (1926). As the floodwaters continued south, they were obstructed and slowed by the anticlinal ridges that directed floodwaters through narrow channels. The ridges impeded the floodwaters progress, and sometimes acted like natural weirs locally pooling water in lower lying basins and back flooding river valleys. Where water pooled, the finer-grained sediment accumulated as rhythmites, deposits of alternating fine- and courser-grained material, indicative of the changing water velocities.

Paleoclimatic History

The climate on the Columbia plateau has been consistently arid to semi-arid since the LGM, ca. 15 ka (Bartlein et al., 1998; Blinnikov et al., 2001; 2002; Gaylord et al., 2001; O'Geen and Busacca, 2001). The Cascade Mountains to the west create a rain shadow over the Columbia Plateau. The rain shadow creates a precipitation gradient with mean annual precipitation ranging from <150 mm on the western margin of the plateau to 800 mm on the eastern margin (Busacca, 1989). Currently the majority of the precipitation falls during the winter and spring while summers and autumns typically are dry (Gentry, 1979; Busacca and Montgomery, 1992).

Loess grain-size distributions and thicknesses indicate prevailing south and southwest winds since 75 ka (Busacca and McDonald, 1994). Glacial advances modified atmospheric circulation patterns resulting in the formation of a possible anticyclone and subdued prevailing southwest winds and a decrease in eolian activity (Bartlein et al., 1998; Sweeney, 2004; Sweeney, et al., 2004). Dune morphologies in the Quincy Basin indicate a present day west-southwest prevailing wind direction (Figure 2.4).

Episodes of glacial advance were marked by cold and dry conditions that promoted sagebrush steppe expansion and soil formation (Blinnikov et al., 2001; 2002; O'Green and Busacca, 2001). Sagebrush steppe expansion and decreased eolian activity during the LGM led to the formation of the Washtucna soil in many areas of the Columbia Plateau (Franklin and Dyrness, 1988; Berger and Busacca, 1995; Richardson et al., 1997; 1999; O'Geen and Busacca, 2001; Sweeney et al., 2004). The reestablishment of prevailing southwest winds during the subsequent glacial ice retreat

8

along with large volumes of newly introduced fine-grained outburst flood sediment promoted eolian activity and relatively thick accumulations of loess across much of the Columbia Plateau (Busacca and Mc Donald, 1994; Bartlein et al., 1998; Sweeney, 2004; Sweeney, et al., 2004).

Eolian activity on the plateau increased again during the mid-Holocene in response to decreased precipitation and slightly increased temperature (Whitlock and Bartlein, 1997; Gaylord et al., 2001; O'Green and Busacca, 2001). The current hot, dry summer climate of the Columbia Plateau region (Gentry, 1979) points toward the potential for sustained eolian activity. An apparent decrease in eolian activity and stabilization of much of the plateau's sand dune and sand sheet deposits could be a result of the introduction of irrigation farming to the region.

Late Quaternary Eolian History

Eolian deposits on the northern Columbia Plateau include near source sand dunes and sand sheets and a variably thick downwind blanket of loess. The histories of these eolian deposits were determined using tephra chronology, paleosols, paleomagnetic orientation and thermal and optically stimulated luminescence dating. The primary source of northern plateau eolian deposits is fine-grained outburst flood sediment.

The largest eolian sand deposit on the northern plateau consists of two dune fields and associated sand sheets and covers approximately 780 km^2 within Quincy Basin (Figure 2.3). A sand sheet also covers approximately 50 km^2 of Arbuckle Flat on the southwest corner of Wilbur Plateau (Figure 2.3). Silt and fine sand is entrained in

the atmosphere from these eolian sand deposits due to saltation making them the major sources for down-wind loess deposits (Figure 2.3).

Loess deposited on the plateau during the late Pleistocene was subdivided into two units: L1 (0-15 ka) and L2 (15-75 ka) (Busacca and McDonald, 1994). Mount St. Helens (MSH) tephra from the 'S' eruptive phase, ca. 15.4 ka (Millineaux, 1986), is the principle division between L1 and L2. The Washtucna paleosol, the soil developed during the LGM, can also be used to indicate the upper limit of L2 loess where MSH set 'S' is not present.

Tephra Chronology and Age Dating

Stratigraphic age-determination on the Columbia Plateau, especially in eolian deposits, is difficult mostly due to a lack of datable material present in these deposits. Both thermal and optically stimulated luminescence dating are being used to date eolian deposits but little data is available for the northern plateau. Volcanoes upwind of the Columbia Plateau in the Cascade Range have intermittently distributed tephra over the plateau. Ages of tephra were determined using radiometric dating, lake core stratigraphies and pollen records. Stratigraphic age determination using magnetostratigraphy and luminescence dating has further helped resolve the ages of volcanic eruptions. Lenses of ash can be correlated using their chemical signatures and have become essential for further development of the loess stratigraphy.

Geologic Map of Study Area
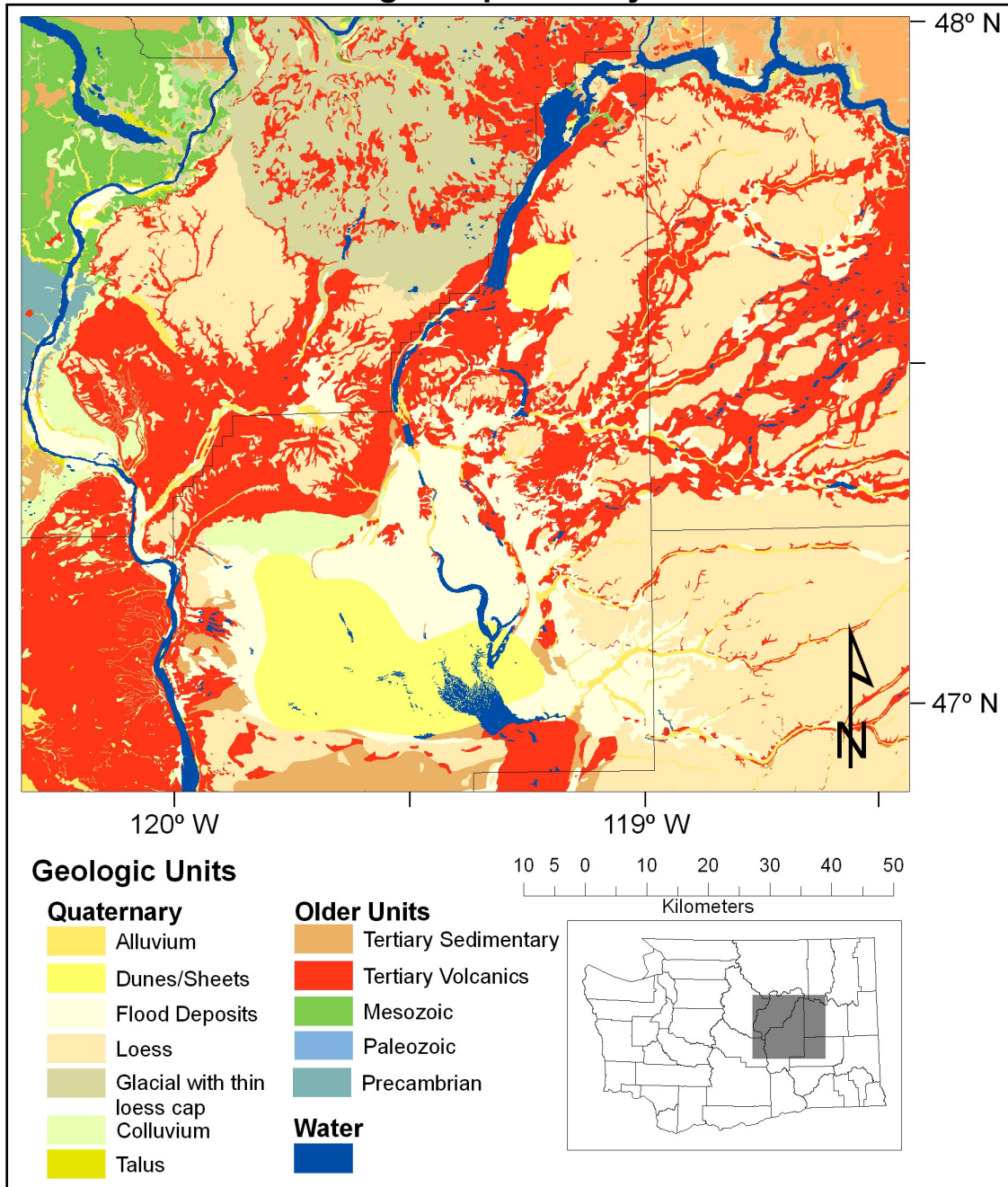
Figure 2.1. The geology of the region with emphasis on Quaternary deposits. Also important are the Tertiary volcanics (Columbia River Basalt) shown in red.

Map of Geographic Areas and Prominent Physiographic Features
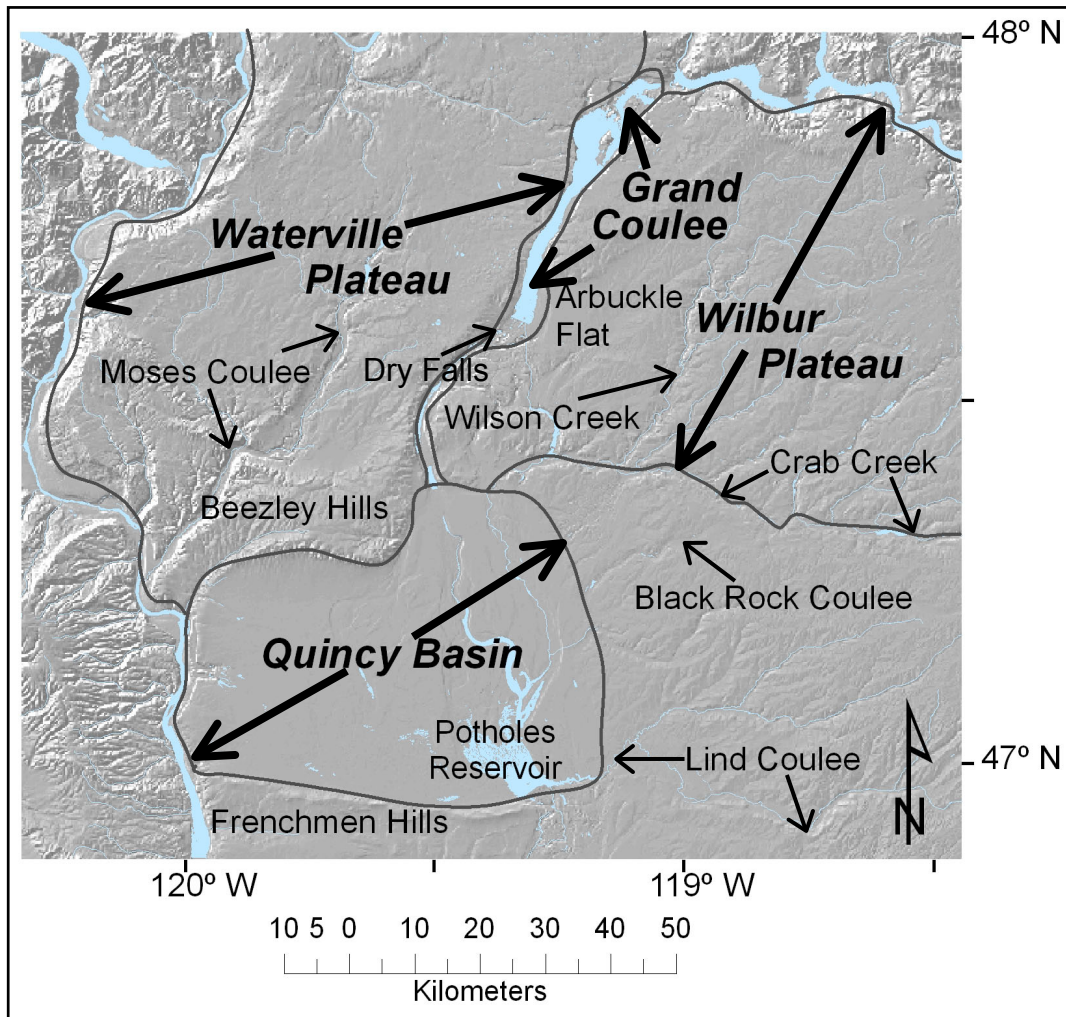
Figure 2.2. Map indicating location of prominent physiographic features and extent of geographic subdivisions within the study area.

Distribution of Quaternary Eolian and Alluvial Deposits

Figure 2.3. Generalized distribution of surface sediment types on the northern plateau. Cross hatch pattern indicates loess, dark diagonal pattern represents eolian sand dunes and sheets, and light diagonal pattern indicates outburst flood gravels.
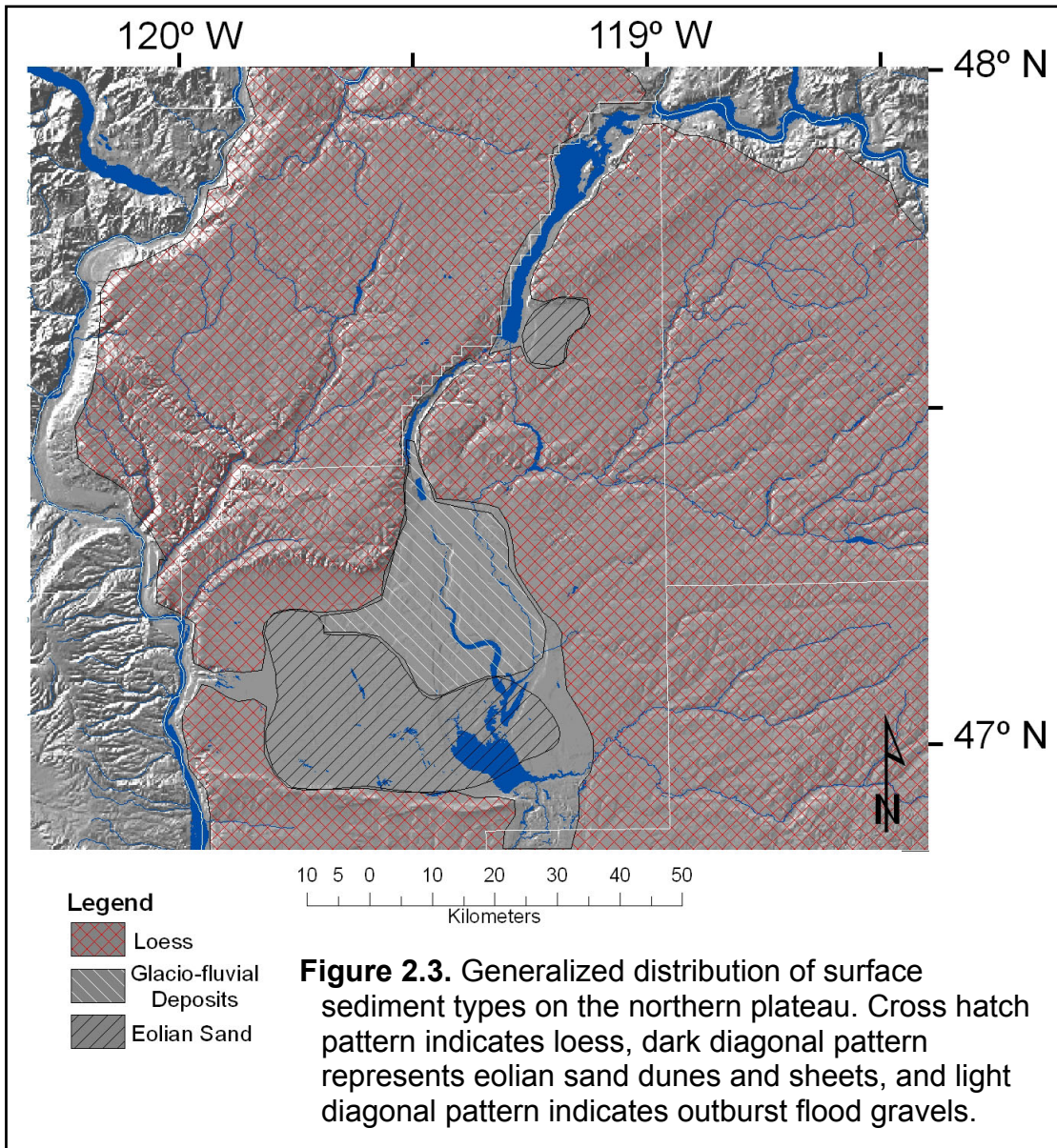
Air Photograph of Moses Lake Dunes
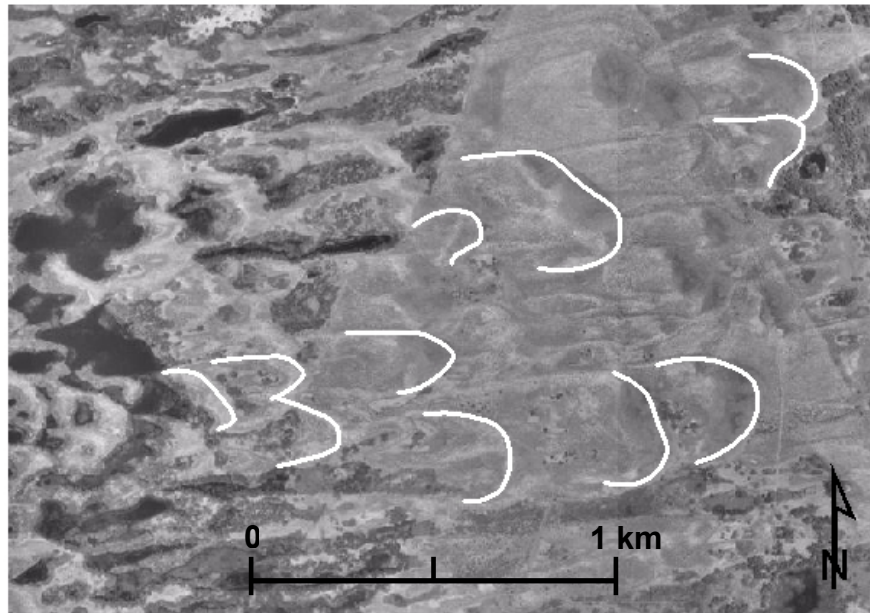
Figure 2.4. Aerial photograph of Moses Lake dunes
approximately 2 km northwest of Potholes Reservoir
(Seamless Data Distribution System). White lines highlight
crests and associated vegetated linear dune limbs of semi-
active to active parabolic dunes and correspond to a
modern WSW prevailing wind direction.

CHAPTER THREE

METHODS

Sample Collection

Samples were collected on an approximate six-mile grid that covered the entire field area. This sampling strategy was designed to accurately represent the distribution of unconsolidated eolian and glacial outburst flood sediment on the northern Columbia Plateau. Mappable units of eolian sand, flood gravel and rhythmite deposits, within the Quincy Basin, are less continuous and more interspersed with other eolian and flood deposits. The discontinuous distribution of unique deposits within the Quincy Basin requires a higher density of sample locations. The closer-spaced sample sites based on an approximate three-mile grid provide a more representative sample set of the Quincy Basin.

The existing public land survey (PLS) system of townships and ranges provided a convenient framework for this sampling strategy. Sample site numbers are assigned by combining the township number and the range number where the sampling site is located. For example, site 1827 is located in township 18 and range 27. Sample sites were further modified to place them within each township. Samples collected at the northwest corner of each township are labeled "A" and provide all the sample locations on a six-mile grid. Sites within Quincy basin and those sites northeast of Arbuckle Flat that are sampled on a three-mile grid, were collected at the northwest corners of sections 6, 3, 19 and 22, and labeled "A," "B," "C" and "D" respectively (Figure 3.1). Sites that provided exposure of relevant information were studied in addition to the predetermined six- and three-mile grid sampling locations. Sampling density and

coverage of the entire field area can be seen on Figure 3.2 and Appendix E provides a map showing all sampling sites and corresponding sample numbers.

Pertinent information including location, type of vegetative cover, landscape, slope, and aspect were recorded for each site (Appendix D). Locations were determined using a Garmin eTrax handheld GPS unit. The type of landscape is a function of topography and landform type. Slope and aspect of sample site surface was determined using a Brunton compass. Samples were obtained from hand auger cuttings, placed in a bag and labeled. Properties of each sample including color, texture, moisture, and presence of carbonate were recorded. An initial sample was collected at a depth of 30 cm, less if coarse sediment or bedrock prevented augering to this depth. Additional samples were taken at depths where noticeable changes in sediment color, texture, pedologic morphology, and carbonate characteristics occurred. The next sample was taken approximately 100 cm below the previous if there were no distinct changes in any of these characteristics.

Augering and sample collection was continued until a depth where augering was no long possible. Augering was not possible when partially consolidated layers were encountered, when the sediment became too coarse to be retrieved by the auger, or when bedrock was reached. Auguring was also halted when sediment was too loose for sampling and would fall out of the auger before it could be retrieved or outside sediment refilled and contaminated the auger hole. The water table was encountered at some sampling sites as well and prevented retrieval of sediment samples. Finally, the total length of auger available was 600 cm a depth that was reached only on rare occasions.

Grain Size Analysis

Samples collected within the Moses Lake and Ritzville 1:100,000 Quadrangles were dried, disaggregated and split. Each sample was then sieved for grain size distribution >500 μm. Samples collected within the Banks Lake, Coulee Dam, Chelan and Priest Rapids quadrangles and the pan fractions of samples from Moses Lake and Ritzville quadrangles were pretreated and analyzed using a Malvern Mastersizer S laser particle diffractometer per WSU Quaternary Research Lab Protocol (2005).

All samples were air-dried and split to a weight of 10-20 g. Samples that contained carbonate were treated using approximately 10 mL of sodium acetate and heated to 75° C for one to two hours. After allowing samples to remain at room temperature for at least twelve hours, they were rinsed using de-ionized water, centrifuged and decanted twice. Samples that contained organic material were treated using 30% hydrogen peroxide and warmed to 65° C for one to two hours. After allowing samples to sit at least twelve hours, the same rinsing process that was used for carbonate treatment was performed.

To further disaggregate samples, 20 mL of 10g/L sodium hexametaphosphate dispersion solution was added to each sample after the required pretreatments. Samples were then shaken for 12-16 hours. Banks Lake, Coulee Dam, Chelan and Priest Rapids samples were then wet sieved to 850 μm. Particles >850 μm in diameter were dried and sieved. 4 mm of sample were retrieved with a wide-bore pipette from a de-ionized water and sediment mixture being agitated by a motorized propeller and placed in the laser diffractometer sample chamber for analysis.

XRF Bead Preparation

X-ray fluorescence (XRF) was used to determine bulk elemental composition of seventeen samples. Samples from sand dunes and sand sheets, loess, and glacial outwash were selected to determine the sources of the loess deposits. Eleven samples, including both source and loess deposits, were prepared using the entire grain size distribution of the sample. Six source samples were sieved to segregate grain sizes less than or equal to 250 µm to more closely match the grain size distribution of the loess deposits. All samples were then prepared using the Washington State University XRF bead lab protocol (Johnson et al, 1999).

Tephra Analysis

Tephras were prepared for glass analysis using techniques outlined by Foit et al. (1993) and were analyzed using a Cameca Camebax electron microprobe in the Geoanalytical Lab at Washington State University. Each analysis used an acceleration voltage of 15 kV, a beam current of 10 ηA and beam diameter of 6 µm. As many as 20 glass shards from each sample were analyzed for relevant oxide weight percentages and then compared to a database of Pacific Northwest tephras and other known tephra standards (Clague et al., 2003; Foit et al., 1993) based on similarity coefficients. Similarity coefficients are a weighted average of the ratios of oxide weight percents of unknown to known or vise versa to yield a value less than 1 (Borchardt et al., 1972) and were determined using the mean oxide weight percents of each tephra sample.

Maps and Spatial Analysis

 Grain size data and stratigraphic information for each sampling site was

compiled into a database to be used for geospatial analysis. ArcGIS 9.1 software was

used to draft grain size, sediment distribution, physiographic and geologic maps. Other

preexisting data layers, such as county boundaries, rivers, lakes and geologic units,

were also used to assist in the creation and analysis of these maps.

Determination of Sampling Site Locations
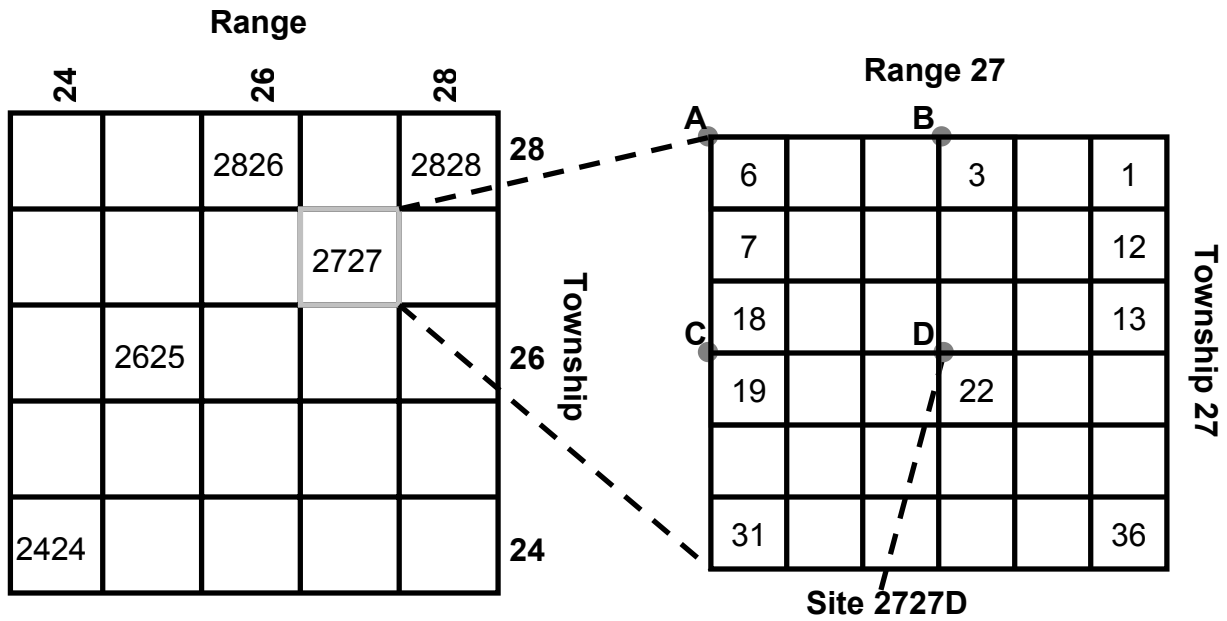
Figure 3.1. Schematic showing how sample sites were located based on the PLS system of Townships and Ranges. Site number is given based on which Township and Range it lies in. Further modification of site given by letter A, B, C or D depending on which section corner the site lies on. In this example, 2727 is highlighted and expanded to show sections within that township. Locations A, B, C and D are the northwest corners of sections 6, 3, 19 and 22 respectively. For example, as shown in the schematic a sample collected at the northwest corner of section 22 in Township 27 and Range 27 would be labeled 2727D.

Study Area Sample Site Locations

Figure 3.2. Map showing all sampling site locations (darker circles) within the study area. Labeled sampling site location map located in Appendix E.
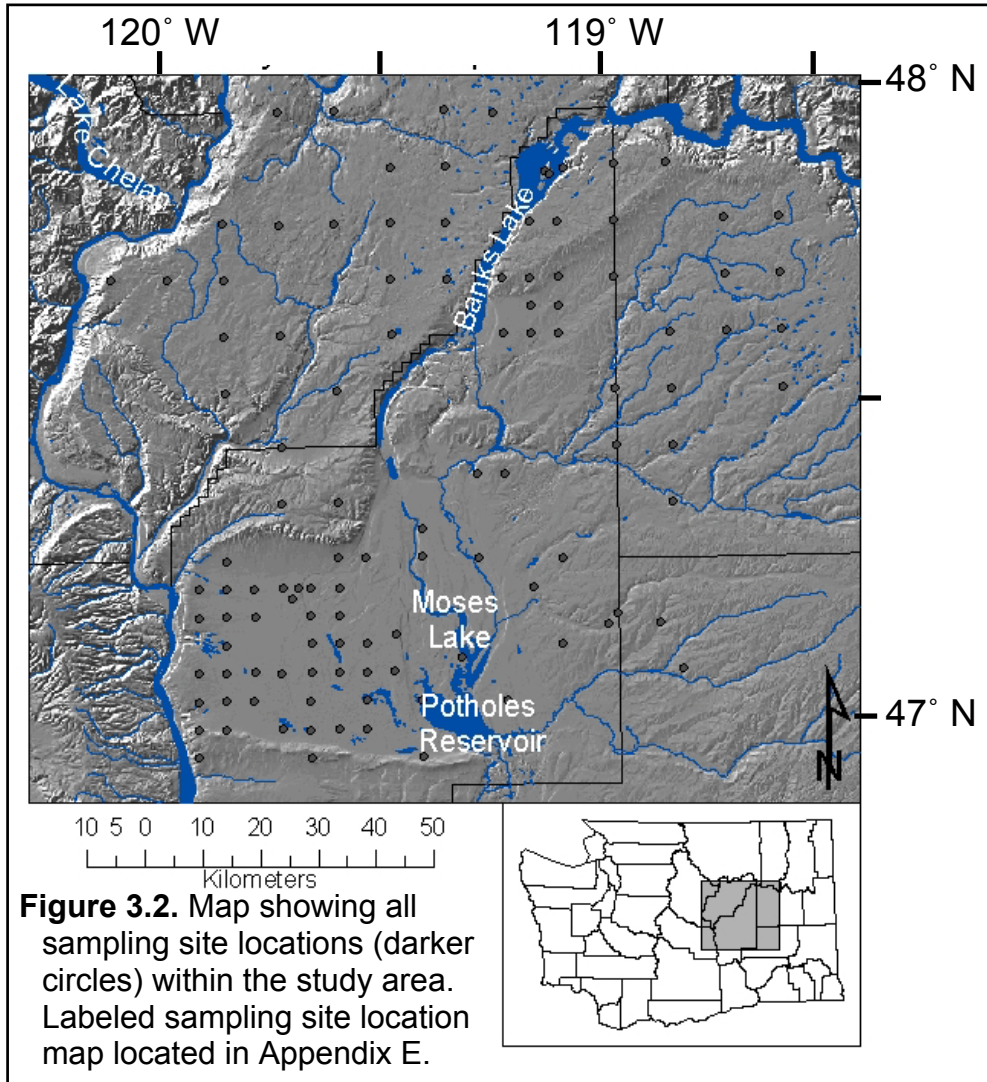
CHAPTER FOUR

RESULTS

The study area was divided into five separate physiographic areas (Figure 2.2). These areas are based on differences in sediment type and landform morphology, and are separated from each other by prominent geographic features such as steam valleys, coulees, or ridges. The five regions include: 1) Quincy Basin in the southwestern portion of the study area bounded by the Beasley Hills to the north, the Frenchman Hills to the south, the Columbia River to the west and the terminus of the eolian sand sheet just east of Moses Lake and Potholes Reservoir, 2) Waterville Plateau, the northwest region of the study area, bounded by the Columbia river on the west and north, Grand Coulee to the east, and including the Beasley Hills to the south, 3) Wilbur Plateau lying east of Grand Coulee, south of the Columbia River and north of Crab Creek in the northeast portion of the study area, 4) the region east of Quincy Basin in the southeast part of the study area bounded by Crab Creek to the north and Lind Coulee to the south and lies just east of Moses Lake and Potholes Reservoir, 5) the Grand Coulee that cuts through the northern portion of the study area and separates the Waterville Plateau from Wilbur Plateau.

Quincy Basin

Quincy Basin (Figure 2.2) contains two separate dune fields (Figure 4.1), the Moses Lake dunes and Winchester dunes, which cover nearly half of the basin's surface area (Petrone, 1970). Loess deposits are distributed along the periphery of the entire basin (Figure 2.3). Deposits from glacial outburst floods are concentrated on the

22

northern part of the basin in the area east and north of the city of Quincy; however, many locations across the basin are underlain by coarse-grained granule-rich flood sediment.

Sediment Type and Thickness

The largest of the dune field on the northern plateau is the Moses Lake dunes, which covers an area of about 650 km^2 and is partially submerged by waters impounded behind O'Sullivan Dam. The second and much smaller dune field covers an area of approximately 130 km^2 in the northern part of the basin east-southeast of the town of Quincy and is herein termed the Winchester dunes. The thickness of the sand in these localities is difficult to determine due to the dry and loose nature of the sediment and the inability to auger to the lower limit of the deposit. Using the collected sand thickness data and the vertical relief between dune crests and interdunes, a realistic average thickness of dune sand is 10 m. The sand in both of these dune fields and the sand sheets surrounding them is basalt-rich, up to 50%, and contains up to 70% quartz and feldspar. The medium- to coarse-sand fraction contains on average >70% basalt while the very fine- to fine-sand sediment fraction contains on average 30% basalt. The mean grain size of Quincy Basin sand deposits is 100 µm.

Loess covers the area of Quincy Basin surrounding the sand dunes and sand sheets. The majority of this loess is a thin veneer of <30 cm thick that covers basalt bedrock and coarse-grained gravel flood deposits. The loess is much thicker in the northwest corner and on the southern boundary of the basin (Figure 4.2). L1 loess on the north slopes of the Frenchmen Hills is 1 m thick while loess thickness in the

northwest corner of the basin southeast of the town of Quincy at site 2023D is 2.6 m.

The mean grain size of all loess deposits in the Quincy Basin is approximately 30 μm.

Sediment derived from glacial outburst flooding mantles much of the northern half of the basin. This sediment consists of gravel bars and fans, granule-rich gravel, and normally graded, fined-grained rhythmites. These deposits often are overlain by a thin veneer of loess or eolian sand deposits. Ephrata Fan (Figure 4.3) is a geomorphic and sedimentary feature generated where glacial outburst floodwaters emerged from the Grand Coulee into Quincy Basin (Baker, 1973; Grolier and Bingham, 1978). The fan consists dominantly of pebble- to boulder-sized sediment (Baker, 1973; Grolier and Bingham, 1978; Baker and Bunker, 1985). The presence of terraces on the fan indicate incision by floodwaters into the existing fan due to changing flood paths and the lowering of glacio-fluvial base level.

Another flood-derived sediment is a coarse sand/gravel deposit found at the surface at ML 3 and ML5 and beneath much of the eolian sand dune and sand sheet deposits in the central part of the basin (Figure 4.4). This deposit has a mean grain size of 1 mm and has an extent of 250 km^2. A coarse sand/gravel sample collected at site 1924B contained 50% quartz, 30% basalt and 20% feldspar. The other six locations where the coarse sand/gravel occurred, the sediment contained >90% basalt grains. The thickness of this deposit is not easily determined due to the inability to retrieve the sediment by auger. Total thicknesses of coarse basalt sand/gravel at sites ML 3 and ML 5 are approximately 12 m and 5 m respectively and site 1926C contains >3 m. Mean thickness is estimated to be 5 m with the thickest deposits to the north and gradually thinning to the south.

ML 3 (Figure 4.5), a gravel pit east of Quincy, is one of the few locations in the basin where a flood-derived, fine-grained, mean grain size of 60 μm, slackwater rhythmite was encountered. The 120 cm thick rhythmite section at ML 3 contains at least seven normally graded beds that are overlain by 12 m of coarse basalt sand/gravel.

Dune Morphology

Dunes in Quincy Basin have parabolic, stringer and blowout morphologies. Nearly 80% of the dunes are parabolic and have generated stabilized low ridges and longitudinal stringers that can be 1-10 km long (Petrone, 1970; Grolier and Bingham, 1978). More of the dunes were stabilized in recent years leading to an increase in blowout morphology and a loss of transverse and barchan morphologies documented by Petrone (1970). Possible causes of dune stabilization include greater amounts of precipitation, creation of Potholes Reservoir and the inception of extensive irrigation. Limited recent eolian activity is evident from the 1-3 cm thick lens of MSH set D (1980 eruption) preserved in the upper 30 cm of semi-active sand dunes. Examples of this occur at site 1827D where MSH set D is tens of centimeters below the surface of this active dune (Figure 4.6) and ML 2 where the tephra is 10 cm below the surface (Figure 4.7).

Eolian sands in both Quincy Basin dune fields are more dune-dominated and thickest towards their centers and merge into sheets that are thinner and featureless. A similar observation was reported for other dune fields and ergs in other parts of the world (Cooke and Warren, 1973). Flattening and thinning at dune field edges may be

due to shorter transport of the coarse-grained sands and fine gravels and the more distant transport of fine- and very fine-grained sands by similar wind velocities. Thinning in directions perpendicular to dune migration is possibly a function of prevailing wind direction, availability of loose sediment, amount of vegetation and moisture content. Thinner sand deposits will be accumulated on these margins if the wind rarely blows perpendicular to the dune migration direction. Thin dune field margins could also be a function of sediment supply. The center of the dune field will migrate downwind leaving behind thin and relatively flat sand sheets as the source area becomes depleted of sediment.

The crests of the parabolic dunes in the Moses Lake dune field are up to 25 m higher than the interdune areas (Figure 4.8) whereas the Winchester dune field has less topographic relief with dunes reaching no greater than 10 m above adjacent interdunes. Few pristine dunes remain in the Winchester dune field since most of the original dune forms were tilled and their morphologies subdued or destroyed.

Stratigraphy

Many locations in the Quincy Basin dune fields have a similar stratigraphy of coarse sand- to gravel-sized basalt fragments capped by an eolian sand unit. The stratigraphy at location 1925D (Figure 4.9) consists of >200 cm of the coarse basalt sand/gravel that is overlain by a 60 cm thick eolian sand layer containing carbonate nodules. The eolian sand bed is covered by a second coarse basalt sand/gravel layer that is 120 cm thick. This second basalt sand/gravel deposit is capped by 215 cm of eolian sand.

The stratigraphy of a parabolic dune in the Winchester dune field was studied at location ML 2 (Figure 4.7; 4.10). A small portion of the dune was excavated, but the rest remains in a mostly undisturbed state. This location contains >7 m of dune sand that consists of 60-70% sand-sized particles composed of approximately 30% basalt and 70% quartz and feldspar. The sand deposit is capped by a 50 cm thick, inversely graded, weakly calcic sand deposit with common rhizoliths. This deposit is subsequently capped by a 30 cm thick tephra-rich bed consisting of ash to medium sand-sized pumice from Glacier Peak (ca. 13.2 ka). The tephra-rich bed is covered by a 40 cm inversely graded sand bed containing few weakly cemented rhizoliths. This sand bed is covered by 40 cm of sand containing 5% basalt granules. The granule-rich sand deposit is capped by 60 cm of silty sand that contains a MSH D tephra lens at 10 cm depth.

Site ML 3 is located in a gravel pit 10 km east of Quincy, Washington (Figure 4.5). The stratigraphy of this site is characterized by a 120 cm thick normally graded rhythmite that contains an undisturbed, 2-5 cm thick, tephra bed 30 cm above the bottom of the section. This tephra was deposited during the MSH set Sg eruption (ca. 15.4 ka). The rhythmite has a sharp upper contact where it is overlain by 12 m of planar cross-stratified basalt-rich sand and gravel. The number of normally graded rhythmite beds indicates at least seven separate glacial outburst-flooding events. The presence of the undisturbed tephra layer within the rhythmite indicates it accumulated in relatively calm water following the main pulse of flooding.

ML 4 (also 1925B) in the north-central portion of the basin is an exposure of a 40 cm thick cross-stratified coarse-sand to gravel deposit that may have originated from

outburst floods or later fluvial redistribution (Figure 4.11). Three distinct, 1-5 cm thick, tephra lenses are interstratified with the gravel deposit. All three lenses were Glacier Peak tephra (ca. 13.2 ka). The gravel deposit is overlain by a 110 cm thick massive dark brown silt deposit with mean grain size of 35 μm interpreted as loess. The bottom 40 cm of loess is carbonaceous. An auger hole drilled above this exposure yielded 220 cm of basalt-rich samples containing 70-90% sand-sized grains interpreted as dune sand.

Waterville Plateau

The Waterville Plateau (Figure 2.2) is characterized by a 30 to >400 cm thick loess blanket on the southern portion of the plateau and a thin, <30 cm, loess capped glacial till deposit on the northern reaches of the plateau (Figures 2.1; 4.2). Moses Coulee, a 50-100 m deep, 1-5 km wide, glacio-fluvial carved valley, bisects the southern loess deposit (Waitt and Atwater, 1989; Kovanen and Slaymaker, 2004). Sample site 2522A, west of Moses Coulee, contains the thickest loess deposit within the entire study area. The deposit consists of >4 m of loess, containing a weakly cemented carbonate nodule-rich layer 1 m deep that is capped by L1 loess. The Waterville Plateau loess deposit gradually thins to the east and northeast where it becomes <30 cm thick.

Locations 2126A, 2324A and 2424A on the southern Waterville Plateau all have beds that contain tephra. The tephra-rich beds are up to 30 cm thick and contain low concentrations of ash to sand-sized pumice dispersed within the loess. L1 loess extended to a depth of 125 cm and contained Mount Mazama tephra (ca. 7.6 ka) in the top 30 cm at location 2126A, in the Beasley Hills east of Moses Coulee. Samples at site

2324A, west of Moses Coulee, contained a mixture of Mount Mazama and Glacier Peak tephras (ca. 13.2 ka) in a zone 30-60 cm deep. Samples collected at site 2424A, also west of Moses Coulee, incorporated Glacier Peak tephra (ca. 13.2 ka) into the loess near the loess basalt bedrock contact at 30-40 cm depth. The diffuse concentration of tephra within the well-sorted loess deposit indicates it was reworked (Rose et al., 2003).

During the last glaciation the Okanogan ice lobe deposited the glacial drift that covers the northern portion of the Waterville Plateau (Kovanen and Slaymaker, 2004). This glacial deposit includes morphologic features such as kames, eskers, end moraines and ground moraines and consists of poorly sorted, heterogeneous, clay to boulder till too coarse to sample by auger. The glacial drift is covered by a thin, <30 cm, layer of loess. Location 2825A, on the northeast margin of the plateau, contains a slightly thicker, 50 cm, loess deposit that caps a single calcic horizon at the till/loess contact. This is the only location on the northern Waterville Plateau that contained >30 cm of loess or a calcic horizon.

Wilbur Plateau

The Wilbur Plateau (Figure 2.2) lies within the Channeled Scabland and is dissected by closely spaced flood-carved coulees. A moderately thick loess deposit blankets this area. Loess deposits 100-150 cm in thickness accumulated adjacent to Grand Coulee and Arbuckle Flat, as well as Wilson Creek (Figure 4.2). Wilbur Plateau loess deposits that are <100 cm thick were deposited directly on top of basalt bedrock or flood gravels (Figure 4.12). A calcic horizon is often present at the loess-basalt

contact. The thickest loess deposits were deposited on weakly cemented carbonate nodule-rich horizons indicating soil development and the presence of vegetation.

Arbuckle Flat is a small basin that covers approximately 180 km^2 on the southwest corner of Wilbur Plateau is mantled by a thin, <1 m thick, sand sheet that covers basalt bedrock and basalt-rich gravel. Location 2429A, in the center of the flat, contains a 15 cm thick sand veneer with mean grain size of 120 μm. Site 2429B, on the southeastern edge of the flat, contains basalt gravel capped by 30 cm of sand, mean grain size 135 μm, overlain by 40 cm of sand-rich loess, mean grain size 38 μm. The northwest corner of the flat, location 2530C, has 30 cm of loess, mean grain size 20 μm, capped by 70 cm of sand-rich loess, mean grain size 50 μm, overlain by 230 cm of loess, mean grain size 18 μm. The sand-rich silt beds may indicate an increase in wind speed and/or duration, the introduction of coarser source sediment, or the migration of an eolian sand body over the area.

Thick loess deposits adjacent to Arbuckle Flat and Grand Coulee, in addition to 2530C, include locations 2430A, 2529A and 2530A. Sampling site 2430A, directly east of Arbuckle Flat, contains 100 cm of basalt gravel covered by 250 cm of silt with mean grain size 17 μm and has carbonate concentrated at the gravel/silt boundary. Location 2529A, north of Arbuckle Flat, is 20 cm of carbonate coated basalt gravel capped by 150 cm of loess, mean grain size 17 μm. Site 2530A, northeast of Arbuckle Flat, has 30 cm of carbonate-rich basalt gravels covered by 180 cm of silt, mean grain size 19 μm, that contains weakly cemented carbonate nodules near its base.

Downwind of Wilson Creek is another relatively thick, up to150 cm loess deposit. Sampling site 2332A is approximately 12 km east of Wilson Creek and contains 20 cm

of basalt gravel capped by 150 cm of loess that becomes more carbonate-rich with depth. Location 2432A, 10 km north of 2332A, contains 70 cm of basalt gravel covered by 20 cm of loess, grain size 12 μm, that is rich in carbonate nodules 1-3 cm in diameter. The nodule-rich bed is capped by 100 cm of loess, mean grain size 12 μm, containing filamentous carbonate stringers and is capped by 80 cm of non-carbonaceous loess with mean grain size of 12 μm.

The locations of the thickest loess deposits adjacent to the Grand Coulee, Arbuckle Flat and the Wilson Creek Valley indicate that these are local sources of loess on the Wilbur Plateau. The variable loess thicknesses on the Wilbur Plateau are a result of the localized loess sources and surface characteristics during loess deposition. The thickest loess deposits contain evidence of soil development indicating the presence of vegetative cover while thinner loess deposits occur directly on basalt bedrock or gravel deposits. The loess thickness differences indicate preferential deposition on vegetated surfaces.

Tephra occurs at two locations on the Wilbur Plateau. Site 2529A contains diffusely distributed Glacier Peak tephra (ca. 13.2 ka) in a bed 30-60 cm deep. Site 2432A contains two separate beds with low concentrations of tephra. The first tephra bed is deposited between 30-60 cm deep and identified as Glacier Peak tephra (ca. 13.2 ka). The second tephra bed is between 110-120 cm deep and identified as MSH So tephra (ca. 15.4 ka). Location 2432A is the only location where MSH set S tephra occurs within loess, which provides a definitive L1/L2 boundary.

Grand Coulee

The Grand Coulee bisects the northern portion of the field area separating the Wilbur Plateau from the Waterville Plateau. The coulee itself is divided into upper and lower portions by Dry Falls (Figure 2.2). The large alluvial fan near the towns of Soap Lake and Ephrata marks the terminus of the coulee. Grand Coulee, with a depth of 300 m, a width of 1 to 10 km and length of 75 km, is by far the largest coulee of the region. The upper Grand Coulee was partially filled with water in the 1950's to create Banks Lake (Department of the Interior, 2004) that is used for irrigation and recreational purposes. Banks Lake has drowned much of the sedimentary record that was left by glacial flooding. The present-day lake has eroded the banks into 2-8 m high bluffs that expose the stratigraphy of fine-grained varve and slackwater deposits that drape gravel bars deposited within the coulee by outburst floods (Atwater, 1985; 1987).

The majority of the exposed sedimentary deposits within Grand Coulee are very coarse gravel to boulder bars that are covered by lacustrine varves (Atwater, 1987). The varve deposits were documented at Northrup Point (Figure 4.13). Several fine- to coarse-sand lenses <1 cm thick with mean grain size of 117 µm are interstratified with the varves. The varves are composed of silt and clay and have a mean grain size of 10 µm.

Steamboat Rock is a large basalt plateau in the middle of the coulee that lies west of Northrup Point. A large boulder bar capped by several varves interstratified with coarse-sand layers (Figure 4.14) similar to those of Northrup Point is deposited on the south and east flanks of Steamboat Rock (Atwater, 1987). A small dune field covers the east and southeast sides of the basalt plateau. This field consists of quartz-rich

parabolic dunes from 5-15 m in height (Crosby and Carson, 1999). The top of the plateau is covered by glacial till that has been eroded to form an east west trending coulee 30 m deep and up to 500 m wide (Bretz et. al., 1956; Crosby and Carson, 1999). Much of Steamboat Rock's surface has a thin, <5 cm thick veneer of loess.

East of Quincy Basin

East of Quincy Basin is an area covered by up to 2 m of L1 loess (Figure 4.2). The thickest loess lies near the eastern edge of the Quincy Basin, northeast of Moses Lake and Potholes Reservoir. Sampling site 1930C contained 210 cm of loess, mean grain size 20 µm, which contains carbonate nodules at its base. The loess, at this location, rests on a consolidated petrocalcic horizon inferred to be the Washtucna paleosol. Site 2030A, 15 km directly north of 1930C, is very similar and contains a consolidated Washtucna paleosol overlain by 180 cm of loess with mean grain size 21 µm. Location 2229C, in the northwest corner of this area, contained 135 cm of loess with mean grain size 19 µm deposited on the consolidated petrocalcic horizon of the Washtucna paleosol. This location is isolated from other thick loess deposits and is therefore a loess island that was spared from erosion by floodwaters. The stratigraphy of the eastern portion of this area closely resembles that of Wilbur Plateau with thinner loess deposited on basalt-rich outburst flood gravels (Figure 4.12). The majority of the northeast and eastern parts of this area were therefore inundated by water during glacial outburst flooding.

The occurrence of paleosols at most sampling locations in the area indicates that the western portion of the area east of Quincy Basin was unaffected by floodwaters.

The floodwaters drained via Crab Creek and Black Rock Coulee to the north, Quincy

Basin and the Columbia River to the west and Lind Coulee, the nearest drainage to the

east and south. The proximity of this area to the Frenchman Hills cataract allowed for

back flooding of existing coulees and the deposition of thick slackwater rhythmites in the

southern portion of this area (Grolier and Bingham, 1978; Moody, 1987; Gaylord et. al.,

2004).
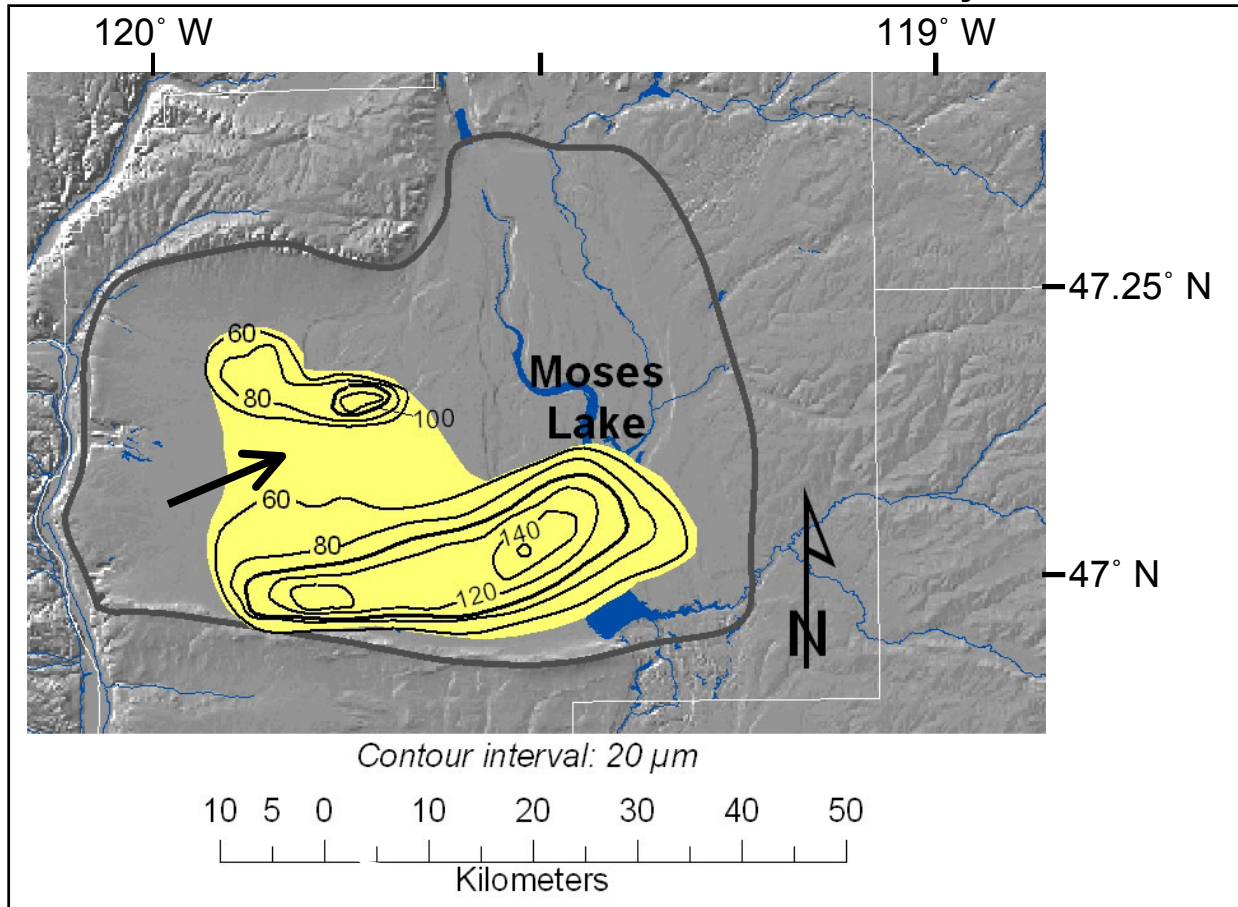
Figure 4.1. Isopach map of mean grain size and extent of sand bodies in Quincy Basin. Extent of Quincy Basin indicated by gray line. Prevailing wind indicated by black arrow.

L1 Loess Thickness within Study Area
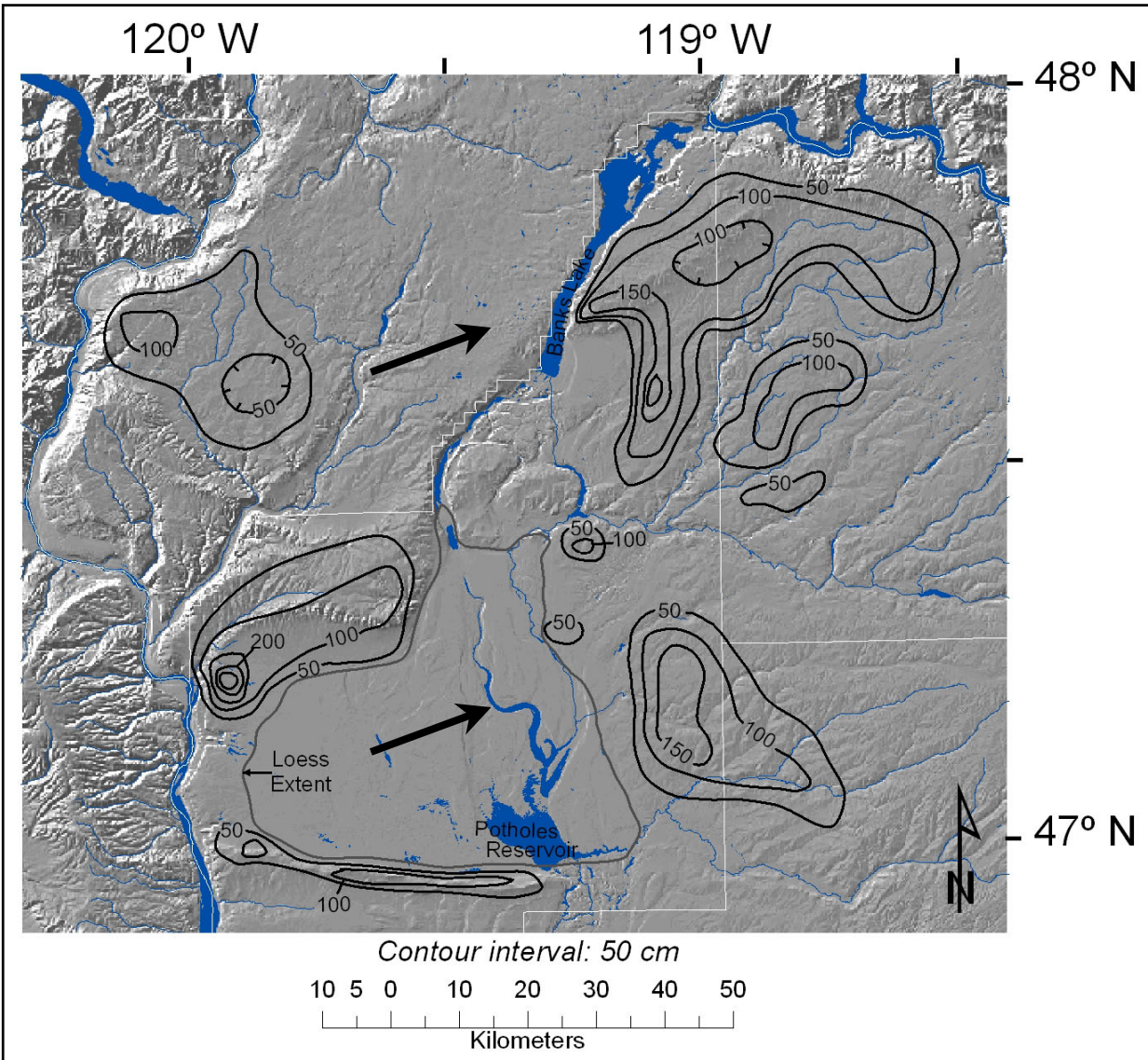
Figure 4.2. Isopach map of loess thickness across the entire study area. Large black arrows show prevailing winds across the region. The thickest loess deposit is in the northwest corner of Quincy Basin. Relatively thick loess occurs adjacent to the Columbia River on the Waterville Plateau, north and east of Arbuckle Flat on the Wilbur plateau, east of Moses Lake and in the Frenchman Hills south of Quincy Basin (Figure 2.2).
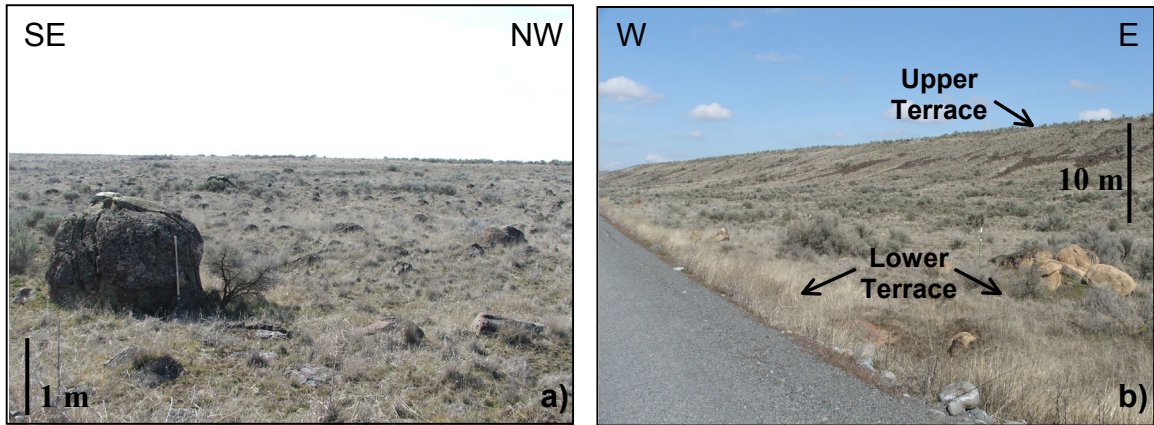
Figure 4.3. Two photographs of the Ephrata Fan that were taken 10 km southeast of the town of Ephrata at site 2027B. a) Shows the scale and abundance of boulders on the surface of the fan. b) Photograph of fluvial incision into the fan deposit forming a terrace approximately 10 m high. Both upper and lower terrace surfaces are nearly flat to shallowly dipping to the southwest.

Distribution of Gravel within Quincy Basin
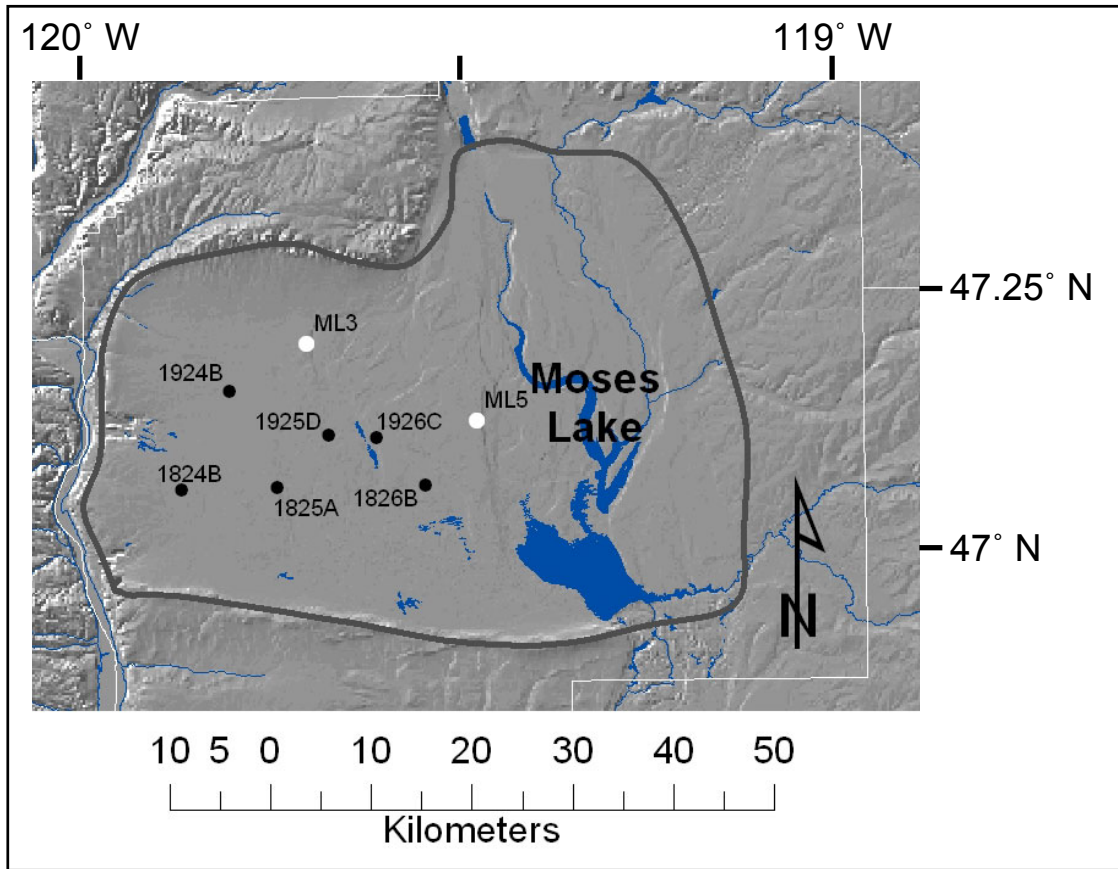
Figure 4.4. Coarse basalt sand/gravel collected at ML 5. Similar sediment is present at the surface of ML 3 indicated with white dot and in the subsurface at sites indicated by black dots. Extent of Quincy Basin shown by gray line.

ML 3
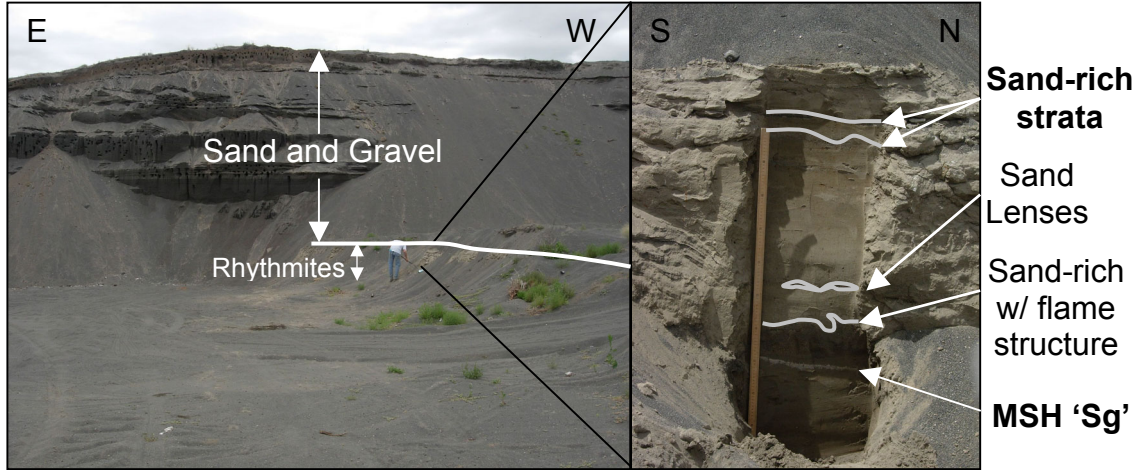
Figure 4.5. Photograph of ML3 showing stratigraphy and important features. This site contains several normally graded rhythmites overlain by 5-15 cm thick planar cross-bedded sand and gravel whose foresets dip to the SW and WSW. A 1-2 cm thick MSH set Sg tephra (ca. 15.4 ka) lies within the normally graded slackwater rhythmite succession that records six flooding episodes following this eruption. Meter stick and person for scale.
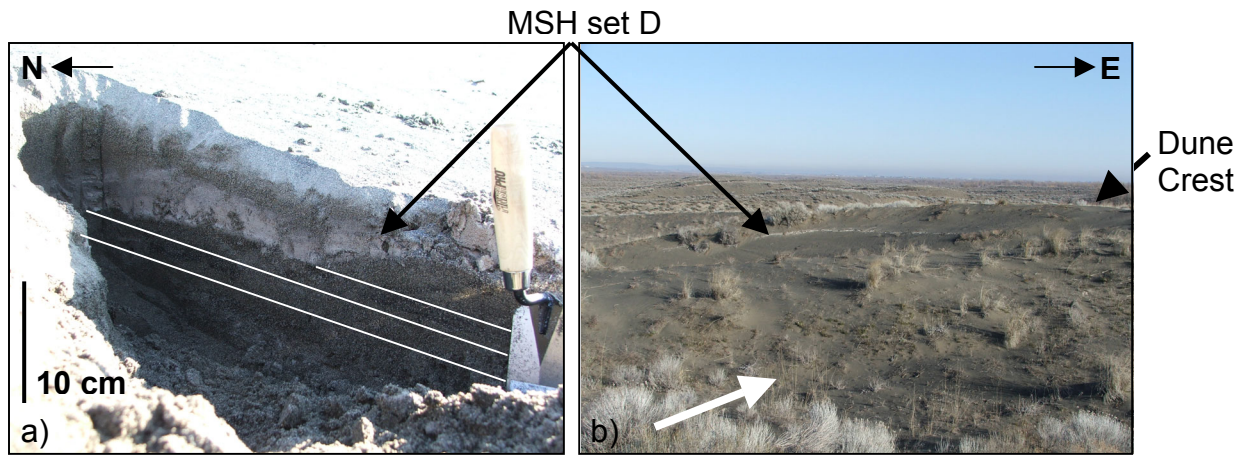
Figure 4.6. MSH set D (1980 eruption) seen incorporated into ENE facing parabolic dune in Moses Lake dune field. a) Close-up shows 5 cm thick tephra layer exposed within dune. Highlighted cross-lamination just below tephra shows slightly steeper dip angle in the same WSW direction. b) Tephra exposed on the deflationary windward side of dune 1-2 m below the dune crest. White arrow represents prevailing wind direction.

Figure 4.7. Photograph of ML 2 stratigraphy. Site consists of silty medium to coarse sand containing 40% basalt clasts with few very faint cross-strata dipping NNE. The Glacier Peak tephra (ca. 13.2 ka) consists of ash to medium sand-sized pumice and is concentrated in a 30 cm thick, light-colored bed. Two moderately calcic horizons associated with rhizoliths coincide with the burrow pattern. The black circles indicate a zone containing granule-sized basalt grains and arrows represent gradational contacts. A 620 cm auger hole was drilled directly below the exposed face and cuttings yielded fine- to coarse-grained sand, interpreted as dune sand, for the entire depth. Meter stick for scale.

Figure 4.8. Looking southwest over the eastern portion of the Moses Lake Dunes from site 1827D. Standing on the north limb of a parabolic dune looking WSW at the face of a large parabolic dune (outlined in white). Vertical relief between interdune and dune crest is approximately 15 m. Vegetation dominated by sagebrush and bunch grasses. Interdunes contain abundant trees and bushes, which probably did not become widespread until the filling of Pothole Reservoir.

1925D
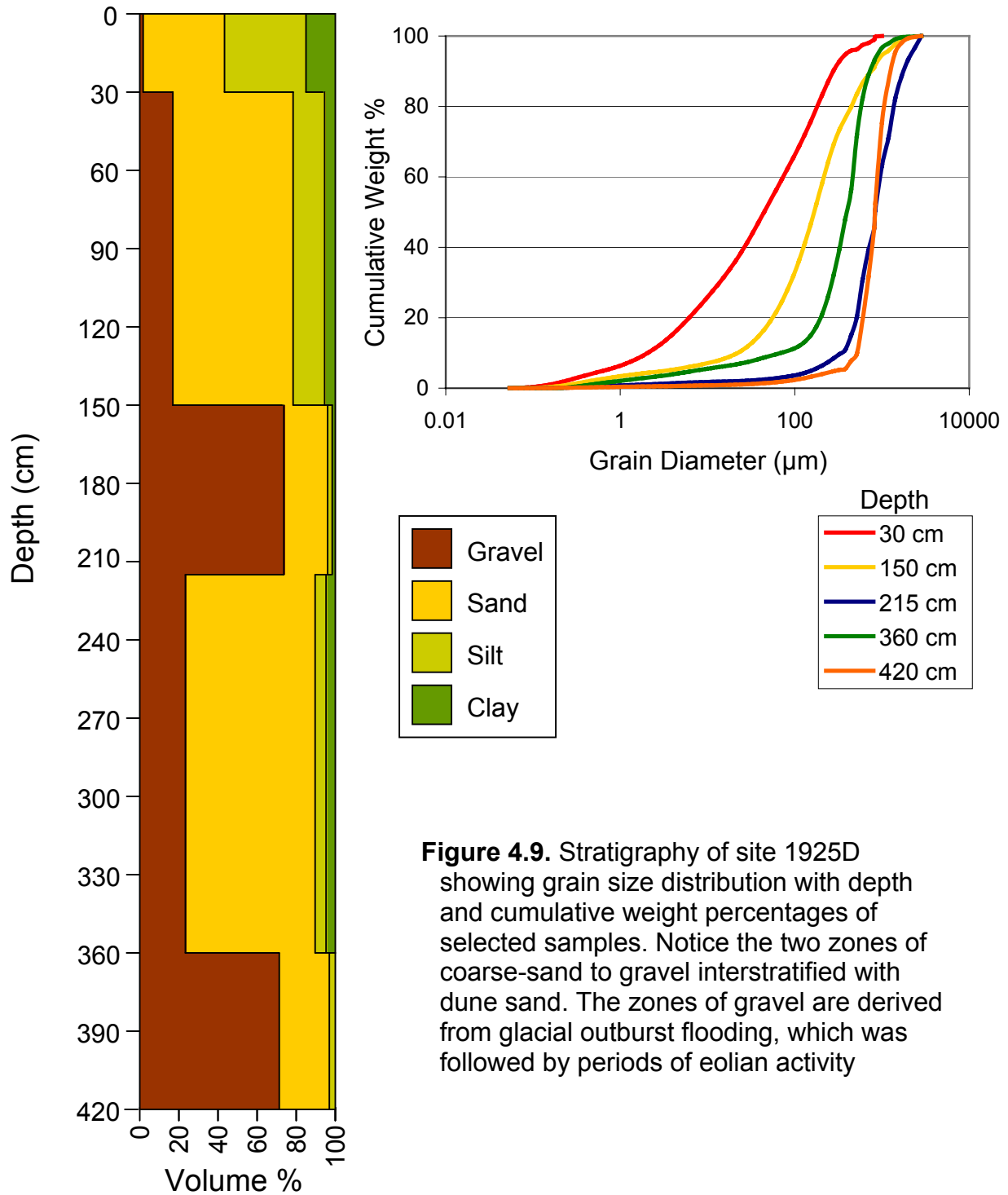
Figure 4.9. Stratigraphy of site 1925D showing grain size distribution with depth and cumulative weight percentages of selected samples. Notice the two zones of coarse-sand to gravel interstratified with dune sand. The zones of gravel are derived from glacial outburst flooding, which was followed by periods of eolian activity
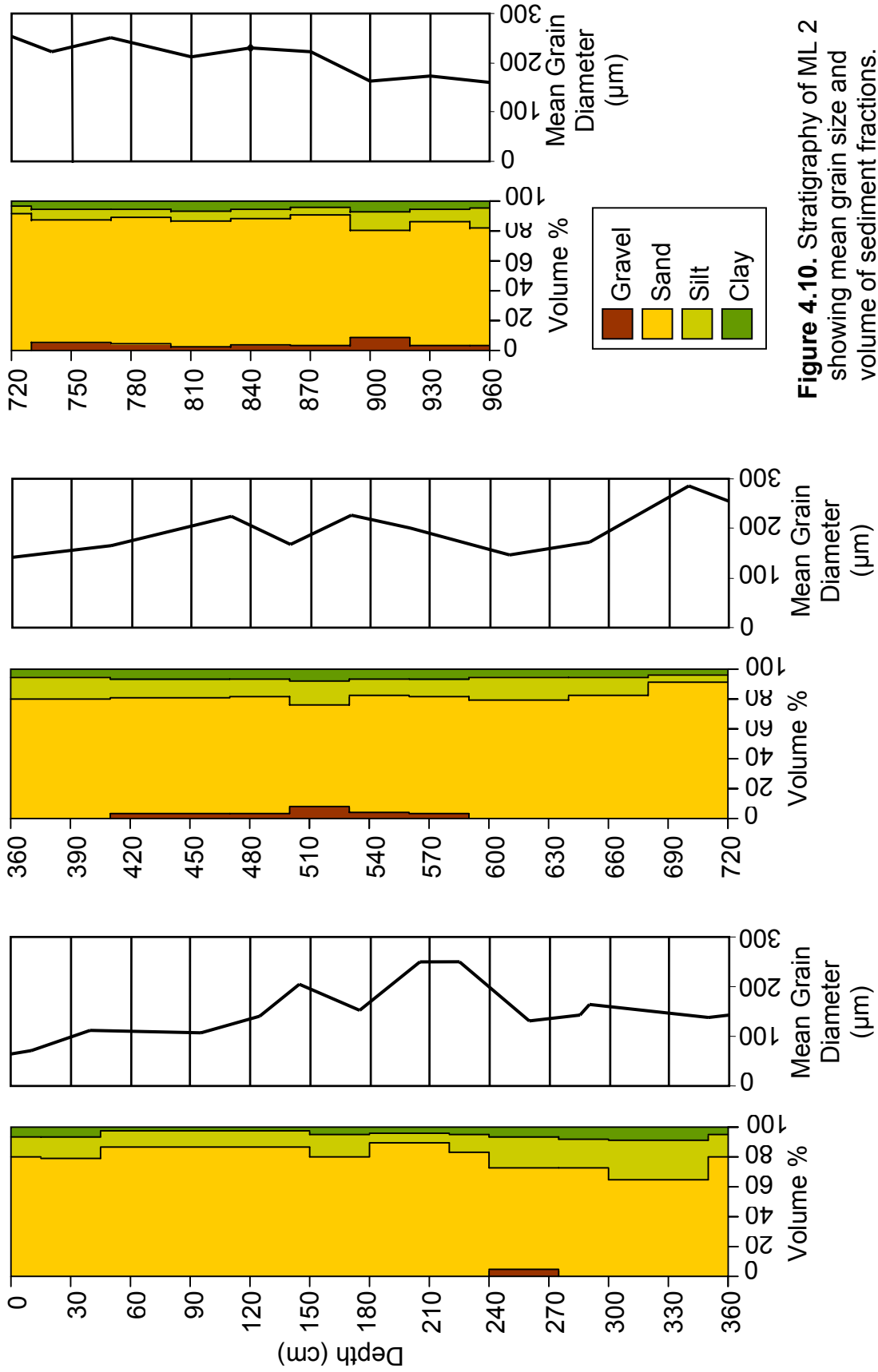
Figure 4.10. Stratigraphy of ML 2 showing mean grain size and volume of sediment fractions.
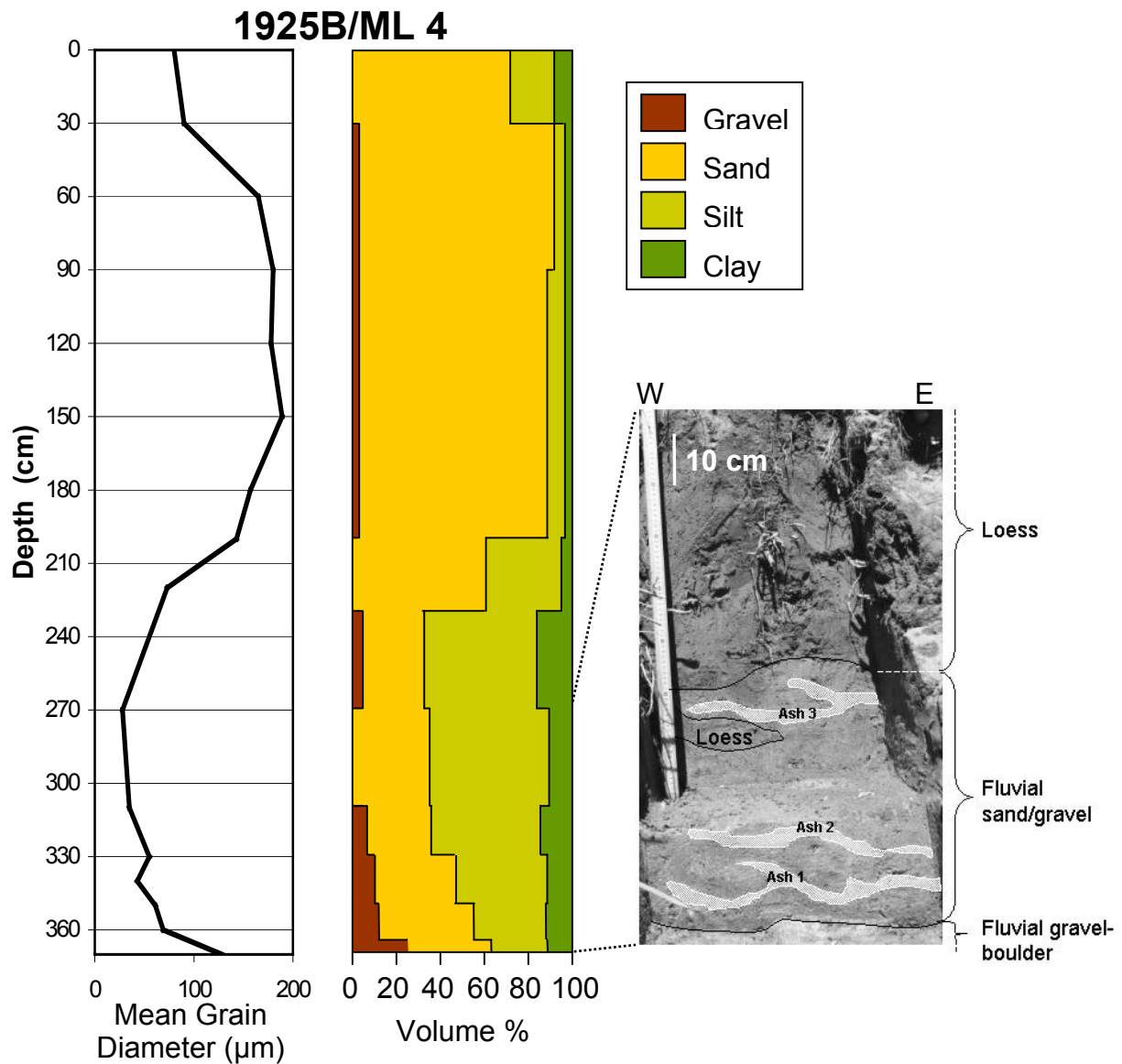
Figure 4.11. Graphs and highlighted photograph of ML 4 (1925B), shows stratigraphy and grain sizes of samples collected from the excavated face and an auger hole drilled behind excavated face. Total sediment thickness of 370 cm includes 40 cm of fluvial sands and gravels covered by 110 cm of loess that is covered by 220 cm of dune sand. This location indicates a change from fluvial sedimentation during outburst flooding to eolian sedimentation post-flooding. The loess being capped by dune sand indicates the migration of the eolian sands over this location.
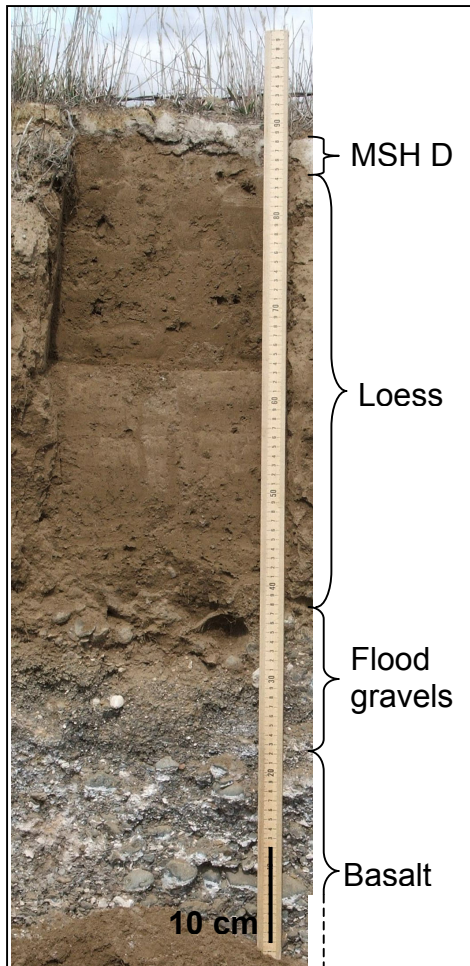
Figure 4.12. Photograph of ML 6, showing the typical stratigraphy on Wilbur Plateau and the area east of Quincy Basin. Approximately 50 cm of loess covering 0-50 cm of rounded basalt gravels often with carbonate coating all resting on basalt bedrock.

Figure 4.13. Section studied on Northrup Point (NP) on the east banks of Grand Coulee east of Steamboat Rock UTM 11T 0343659, 5303966. Recessed strata are medium- to coarse-grained sand interstratified in many fine-grained varves.
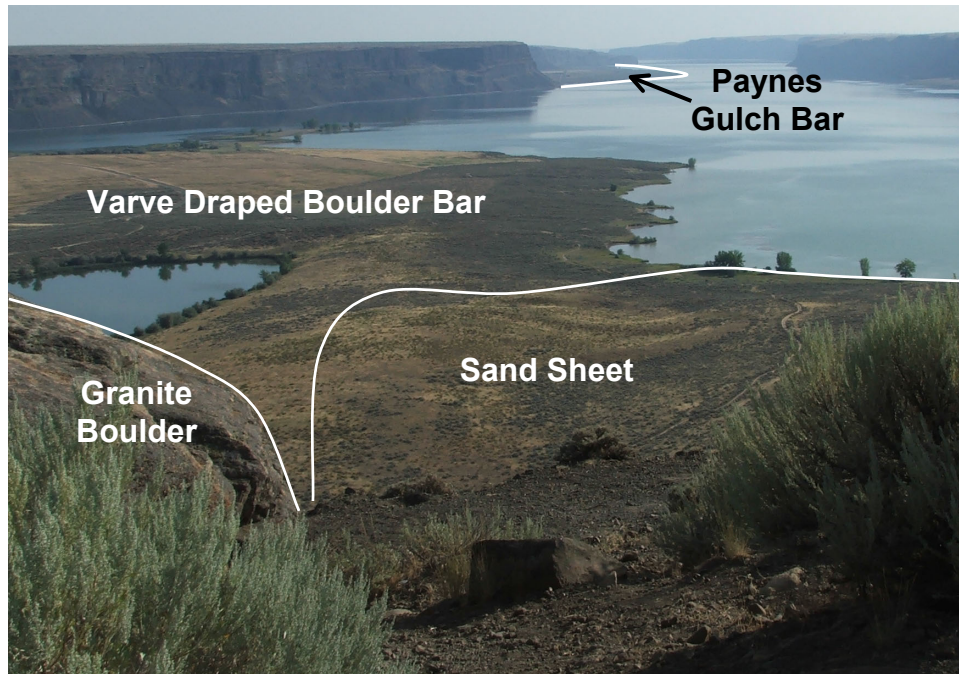
Figure 4.14. View south from the top of Steamboat Rock in Grand Coulee. Large granite boulder highlighted in left foreground. Large varve-draped point bar extends south and is covered by a thin dune sheet where indicated (Crosby and Carson, 1999). Paynes Gulch Bar, studied extensively by Atwater (1987) can be seen in the distance. Depth of coulee from rim to water is approximately 150 m.

CHAPTER FIVE

DISCUSSION

The use of mass accumulation rates (MARs), the distribution of eolian deposits and textural and chemical characteristics of potential source deposits gives insight into the eolian activity and paleoclimate fluctuations during the late Quaternary on the northern Columbia Plateau. The knowledge of eolian and climatic histories is required to understand the relatively thin loess of the northern Columbia Plateau as well as the possibility for the eolian activity to produce climate-influencing atmospheric dust. Evaluation of geographic influences on airflow patterns and their effects on eolian redistribution of glacial outburst flood deposits is also required to fully understand loess deposition on the northern Columbia Plateau. Data presented in this discussion will be used to reconstruct the late Quaternary history of the northern Columbia Plateau, an example of a continental semi-arid to arid region where determination of paleoclimate is often limited by the lack of temporal resolution and stratigraphic continuity in the sedimentary record.

Loess Sources and Distribution

Mapping the relations between potential loess-producing source areas and eolian deposits (including loess) on the northern Columbia Plateau illustrates how important the spatial relations between these factors are to the generation of atmospheric dust.   L1 loess covers approximately 15,400 km^2 of the northern Columbia Plateau (Figure 2.3), and is relatively thin, <3 m thick, when compared to the southern Columbia Plateau. The thickest loess deposits on the southern Columbia Plateau are >8

m thick and occur in areas downwind of thick and extensive slackwater rhythmites deposited in the Umatilla and Walla Walla Basins that are exposed to saltating sand grains (Sweeney, 2004; Sweeney et al., 2005). The relatively high competence of floodwaters flowing over the northern plateau promoted the bypass of fine-grained sediment that was transported and deposited on the southern plateau where it was reworked into thick loess deposits. As presented earlier the scarcity of fine-grained sediment along with the mantling of fine-grained, loess source, deposits by coarse sand to gravel deposits on the northern Columbia Plateau contributed to the accumulation of a relatively thin, <3 m thick, L1 loess deposit.

Several small and isolated outburst flood deposits account for the relatively thin L1 loess on the northern Columbia Plateau. The sources that have the greatest potential to produce loess are sand bodies in the Quincy Basin. These sand bodies are generated from fine-grained flood sediment that was reworked into eolian sand dunes and sand sheets. Additional source areas for L1 loess include loose sand-rich silt derived from outburst floods, lacustrine varves and alluvial deposits in the Columbia River Valley, Grand Coulee, Arbuckle Flat, and Wilson Creek. The thick rhythmite successions in Lind Coulee also are a potential source for downwind loess (Grolier and Bingham, 1978; Moody, 1987; Gaylord et al., 2004). The location of these six areas upwind of the thickest loess accumulations is further evidence that fine-grained deposits in these locations are loess sources. Loess sheets thicken to >1 m immediately downwind of these source locations and then thin to <50 cm within 20 km (Figure 4.2).

The potential source areas of the northern Columbia Plateau contain sufficient amounts of silt to supply adjacent loess deposits (Table 5.1). The average thickness of

L1 loess deposits determined from sampling sites within the study area is 30 cm. Loess covers 15,400 km^2 within the study area on the northern plateau. Multiplying the thickness by the area yields a total volume of loess within the study area of approximately 4.6 km^3. Estimates using field data displayed using a GIS reveal that loess blankets approximately 4,700 km^2 of the Wilbur Plateau and 2,500 km^2 of the area east of Quincy Basin. Auger data indicates that loess thickness on the Wilbur Plateau and in the area east of Quincy Basin is about 40 cm. Again, multiplying thickness times area yields a total L1 loess volume for the eastern two areas of the study area 2.9 km^3 while the volume of L1 loess throughout the rest of the study area equals approximately 1.7 km^3. Grain size analysis of the loess reveals that approximately 60% of the loess consists of silt, grain diameters of 4-63 μm (Figure 5.1; Appendices A and C). The total volume of silt needed to generate the loess deposits of Wilbur Plateau and the area east of Quincy basin is 1.7 km^3. The volume of silt, which is held in all the remaining northern plateau loess deposits, is then 1.0 km^3.

The eolian sand deposits within Quincy Basin cover approximately 1,100 km^2 based on grain size data of sampling locations. A conservative mean thickness of sand deposits within the Quincy basin is 7 m, making the total volume of dune sand 7.7 km^3. The grain size distributions of samples taken from the dune sand deposits show that on average 20% is silt, grain diameters of 4-63 μm (Figure 4.9; 4.10; 4.11; Appendices A and C). The total volume of silt available from Quincy Basin dune sand is 1.5 km^3 assuming fixed silt concentrations in dune sand. Silt originating from Quincy Basin would not likely be deposited as L1 loess on the Beezley Hills to the north or the Frenchman Hills to the south because of the south-southwest prevailing wind since the

LGM. Assuming grain size distributions of Quincy Basin sand deposits have remained constant since the onset of eolian activity these sand bodies could account for nearly all the silt held in Wilbur Plateau and east of Quincy Basin loess deposits. However, the assumption that silt concentrations within current sand deposits is the same as those at the onset of eolian activity is likely an oversimplification. A gradual decrease of silt concentration in eolian sand deposits would be expected without replenishment of silt-rich source sediment. Using present day silt concentrations thus yields a low estimate for the historic volume of silt within the source deposits. This makes it even more plausible that Quincy Basin eolian sands alone could have had enough silt to source all the eastern study area loess deposits.

Less extensive contributors of silt for loess deposition on the northern Columbia Plateau are outburst flood slackwater deposits, lacustrine varves and recent alluvial sand deposits in Grand Coulee, Lind Coulee, Wilson Creek and the sand sheet covering Arbuckle Flat. The total volume and silt concentrations of these additional source areas are not well constrained due to the small extent and discontinuous nature of these deposits in this study area. A reasonable silt volume estimate for these source areas is 0.1-0.4 km^3 (Table 5.1). It thus seems plausible that there was a surplus of silt needed to produce the loess deposits in the eastern half of the study area based on the low Quincy Basin silt estimate and the inclusion of additional source areas.

The amount of silt required to produce the loess deposits of the Frenchman and Beezley Hills and those on the western margin of the Quincy Basin is less certain. The bulk of the silt most likely comes from outburst flood and recent alluvial deposits within the Columbia River Valley since the thickest deposits are within 10 km of the river

valley. A large gravel bar, Crescent Bar, within the Columbia River Valley is capped by a fine-grained slackwater rhythmite. The proximity of 2023D to Crescent Bar makes it reasonable to conclude that the 260 cm thick L1 loess deposit originates from the Crescent Bar slackwater deposit. A possible cause for such a thick deposit is the funneling and enhancement of prevailing southwest winds (Figure 5.2) through the relatively narrow and deep Columbia River Valley (Bullard et al., 2000). It is possible that an additional portion of the silt in the study area is more far-traveled, coming from the western Cascades or even China. Further bulk chemical and mineralogical study could yield additional insights into the existence of more far-traveled dust.

Mass Accumulation Rates

Mass accumulation rates (MARs) of loess were used to estimate, time-constrained, paleoatmospheric dust concentrations. Increases in MARs on the northern Columbia Plateau probably correspond with increased dust production that could have been prompted by increased aridity and/or an increase in windiness. MARs of loess were calculated to be >3,000 $g/m^2/yr$ and average 1,500 $g/m^2/yr$ on mid-continental North America (Bettis et al., 2003) and 1,000 $g/m^2/yr$ for the Chinese Loess Plateau (Sun et al., 2000). Extremely high MARs, up to 11,500 $g/m^2/yr$, occur in some locations in Nebraska (Roberts et al., 2003). MARs calculated for the southern Columbia Plateau reach values of 3,000 $g/m^2/yr$ immediately following the LGM (Sweeney et al., 2004). MARs calculated for the northern Columbia Plateau are much lower ranging from one to three orders of magnitude less than those reported above (Table 5.2).

MARs were calculated by multiplying the rate of accumulation m/yr by the bulk density of the loess as demonstrated elsewhere by Bettis et al. (2003). Average Palouse Loess bulk density is 1.40 g/cm^3 (Sweeney et al., 2004). Average L1 loess thickness on the Wilbur Plateau is 40 cm, which equals the total thickness of loess that has accumulated over the past 15,400 years. Dividing 40 cm by 15,400 years yields an accumulation rate of 2.6×10^{-5} m/yr. Multiplying this value by the estimated bulk density of 1.40 g/cm^3 yields an average MAR of 36 g/m^2/yr across the Wilbur Plateau as compared to approximately 1,500 g/m^2/yr on average for near source loess deposits on the great plains (Bettis et al., 2003).

Locally, higher MARs were calculated for relatively thick L1 deposits that contained identifiable tephras (Figure 5.3). A 110 cm L1 loess thickness at site 2432A, on the Wilbur Plateau, yields a MAR of 100 g/m^2/yr since the LGM. This site reveals that 80 cm of loess was deposited between MSH So (ca. 15.4 ka) and Glacier Peak (ca. 13.2 ka) tephras giving a MAR of 500 g/m^2/yr. This higher MAR indicates that accumulation accelerated soon after the LGM but then significantly decreased to 32 g/m^2/yr since ca. 13.2 ka. Locations 2324A and 2424A on the Waterville Plateau contain Glacier Peak tephra to a depth of 30-60 cm, indicating that MARs since ca. 13.2 ka ranged from 32-64 g/m^2/yr. The thickest L1 loess deposit on the northern plateau, site 2023D (west of the town of Quincy), yielded an average MAR of 240 g/m^2/yr since the LGM.

These calculated MARs from the northern Columbia Plateau suggest that dust production since the LGM was greatest between ca. 15.4 and 13.2 ka. Better stratigraphic constraints are needed to resolve millennial-scale accumulation rates,

however. Despite the lack of temporal resolution, it is evident that MARs on the northern plateau are much lower than those on the southern plateau. It is also reasonable to conclude from site 2432A that much higher MARs, up to 500 g/m^2/yr, occurred toward the end of the glacial period as opposed to the post-Glacier Peak interglacial period with MAR 32 g/m^2/yr.

A early to middle Holocene MAR increase would be expected due to decreased precipitation, increased temperature and a possible increase in wind velocity (Whitlock and Bartlein, 1997; Gaylord et al., 2001; O'Green and Busacca, 2001), but MARs could not be determined do to a lack of geochronologic indicators. There are however, limited stratigraphic data that indicate an increase in mean grain size in loess deposits between the LGM and recent loess deposition (Figure 5.4). The increase in grain size at sites 1725D in the Frenchman Hills, 2023D the northwest corner of Quincy Basin, 2425A on the Waterville Plateau and 2530C on the Wilbur Plateau are considered evidence for enhanced eolian activity during the early to middle Holocene. It is possible that this episode of enhanced loess activity corresponds with enhanced sand dune activity in the southern plateau at this same time that has been documented by Gaylord et al. (2001).

Source-Limiting Factors

Dust production is a function of grain size availability, percentage of vegetative cover, and moisture (Pye, 1987). As discussed earlier possible reasons for relatively little eolian silt production on the northern plateau include: 1) the bypass of fine-grained sediment over the northern plateau during outburst flooding, 2) widespread coarse sand to gravel of northern plateau sediment that has inhibited eolian transport, and 3) the

removal of soil material by outburst flooding that otherwise would have encouraged plant growth and associated loess accumulation.

The most prominent limiting factor for the generation of thick loess in the northern plateau has been the tendency for finer-grained flood sediment to bypass the area. The later winnowing (by wind and water) of the remaining fine-grained particles from outburst flood sediments left coarse-enriched, fines depleted source sediments on the northern plateau. Deposition of these fine-grained particles downstream in the southern plateau depocenters of the Yakima, Walla Walla and Pasco Basins prompted the generation of thick loess in that area.

The second most important limiting factor for the generation of thick loess on the northern plateau has been the incorporation of very coarse sand- and gravel-sized sediment that could not be transported by wind. This coarse, protective sediment cover inhibited dust production from potential loess sources that were buried beneath these coarse sediments. Coarse-grained deposits that mantle potential source material at seven study locations within the Quincy Basin, cover an area of approximately 250 km^2 (Figure 4.4).

The third most important source-limiting factor on thick loess deposition on the northern Columbia Plateau has been the erosion of existing fine-grained sediment and soil from the basalt bedrock. This erosion left unweathered, barren rock surfaces that could not support plant growth that otherwise might have enhanced rates of loess accumulation (Pye, 1995).

Loess Provenance

Bulk chemical compositions of potential source deposits and loess were used to help delineate the sources of northern Columbia Plateau loess. Research directed toward known loess sources provides data that is more robust and furthers our understanding of the relationship between eolian sources and sinks. X-ray fluorescence (XRF) analysis was used to connect sediment sources to their corresponding loess sinks. Major elemental concentrations, along with trace element chemistry from XRF analyses were successfully used elsewhere to determine source areas for eolian deposits including loess (Muhs et al., 1996; 1999; Muhs and Bettis, 2000; Zimbelman and Williams, 2002; Sweeney, 2004; Sweeney et al., 2004; Muhs and Benedict, 2006). The simplifying assumption used by these researchers has been that sediment contained in loess deposits originating from differing sources should yield different chemical signatures. An additional assumption has been that the mixing of two or more sediment sources should be evident if loess compositions fall between distinct source compositions.

In previous studies on the Great Plains of the United States and Alaska, immobile trace elements, Ti, Nb, Zr, Ce, and Y, provided the most reliable links between eolian sedimentary sources and eolian sinks (Muhs et al., 1996; 1999; Muhs and Bettis, 2000; Muhs and Benedict, 2006). These, along with other trace elements, were utilized in this study. Major elemental oxide weight percents of Fe, Al, Mg, Ca, Na and K were also compared to further resolve composition variations that could have been related to source areas. Bulk compositions of southern Columbia Plateau source deposits

analyzed by Sweeney (2004) were also compared to northern Columbia Plateau source and loess deposits (Figure 5.4).

Loess samples across the entire northern Columbia Plateau showed little chemical variation. This lack of variation made determination of sources for the loess very difficult. Chemical variation between the potential source sediments and the loess deposits further complicates connecting sources to loess sinks using bulk chemical data. The chemical differences between potential source sediment and loess is probably the result of mineralogical changes due to the mixing of source sediment during transport, preferential sorting of minerals and grain sizes and pedogenic development.

Ca and Mg oxides are major components of carbonate minerals and can be used to indicate relative carbonate concentrations. Higher MgO and CaO values in Quincy Basin source samples when compared to loess samples indicate there has been a loss of carbonate from source to sink (Figure 5.5). The most likely cause for this carbonate loss is the translocation of carbonate in the loess during soil development, a common process in arid western soils. Translocation in arid environments is often due slow sedimentation rates (Muhs and Bettis, 2000). Low MARs of loess on the northern Columbia Plateau enhance translocation and leads to lower carbonate concentrations in loess as compared to the potential source sediments.

K and Rb, major elements in feldspars, can be used to indicate ratios of potassium feldspar to alkali feldspar (Muhs and Benedict, 2006). K/Rb values remain quite constant across the entire Columbia Plateau and indicate the sediment samples contain similar feldspar ratios with the exception of two Grand Coulee sediment

58

samples and one southern Columbia Plateau flood sediment sample (Figure 5.6). The high K/Rb ratios in Grand Coulee sand dune and varve sediments point towards a higher concentration of potassium feldspar. The similarity of K/Rb ratios determined for both Quincy Basin sands and northern Columbia Plateau loess suggest that Quincy Basin is the dominant loess source.

Ti/Zr and Ti/Nb ratios are good provenance indicators (Muhs and Benedict, 2006). Ti occurs in heavy minerals such as titanite, rutile and ilmenite and Zr in zircon. Data collected from northern Columbia Plateau samples indicates a positive correlation between this loess and Quincy Basin and Grand Coulee sedimentary sources. The correlation between Ti/Zr and Ti/Nb indicates that northern Columbia Plateau loess is a mixture of Quincy Basin and Grand Coulee sediment and provides the best evidence for multiple loess sources on the northern plateau (Figure 5.6). The slightly higher Ti/Zr values in Quincy Basin could also be a reflection of preferential sorting of more dense, Ti- and Zr-rich, minerals such as zircon and titanite from less dense, Si- and K-rich, minerals such as quartz and feldspar.

There is a lack of convincing bulk mineralogical evidence to connect Quincy Basin sediment sources with a single loess deposit on the northern Columbia Plateau. XRF analysis of more samples from differing depths may yield better resolution of sediment chemistry within individual loess sinks. However, the general lack of variation between loess on both the northern and southern portions of the Columbia Plateau indicates the bulk composition of potential source material does not have sufficient chemical diversity to correlate sources to sinks across this relatively small region. Correlating eolian

sources to sinks using XRF derived bulk chemistry maybe too simplistic for the

Columbia Plateau deposits.

Climatic Significance

Eolian production of atmospheric dust provides detailed information that is

required for the reconstruction of past climate fluctuations. Aerosols, including eolian-

derived dust, influence climate by changing the global energy budget (Collins et al.,

2001). Determining the amount and the sources of atmospheric dust is important when

assessing paleoclimate fluctuations and constructing models for future climate changes.

Evidence from MARs indicates a particularly dusty period on the northern

Columbia Plateau during ice retreat following the LGM and early in the current

interglacial between ca. 15.4 and 13.2 ka. Evidence of enhanced dust production

following the Glacier Peak (ca. 13.2 ka) eruption is indicated by four locations that

contain zones of increased sand content within L1 loess (Figure 5.4). This increased

mean grain size may reflect increased aridity and windiness correlated with early to

middle Holocene aridity reported by other researchers (Whitlock and Bartlein, 1997;

Gaylord et al., 2001; O'Green and Busacca, 2001).

Climatic models that are currently being developed require more widespread and

detailed information regarding aerosol chemistry, aerosol source areas, geographic

variations of dust, and wind erodibility of potential sources (Collins et al, 2001; Grini et

al., 2005; Zender and Kwon, 2005). Factors that determine the warming or cooling of

the atmosphere include concentration, vertical distribution, mineralogy, and particle size

distribution of the dust (Harrison et al., 2001). This study provides climatic modelers

additional data that can be used to more accurately reproduce past climate conditions

and may help those who are attempting to predict future climate fluctuations.

Stratigraphic Grain Size Distributions of Selected Loess Sample Locations
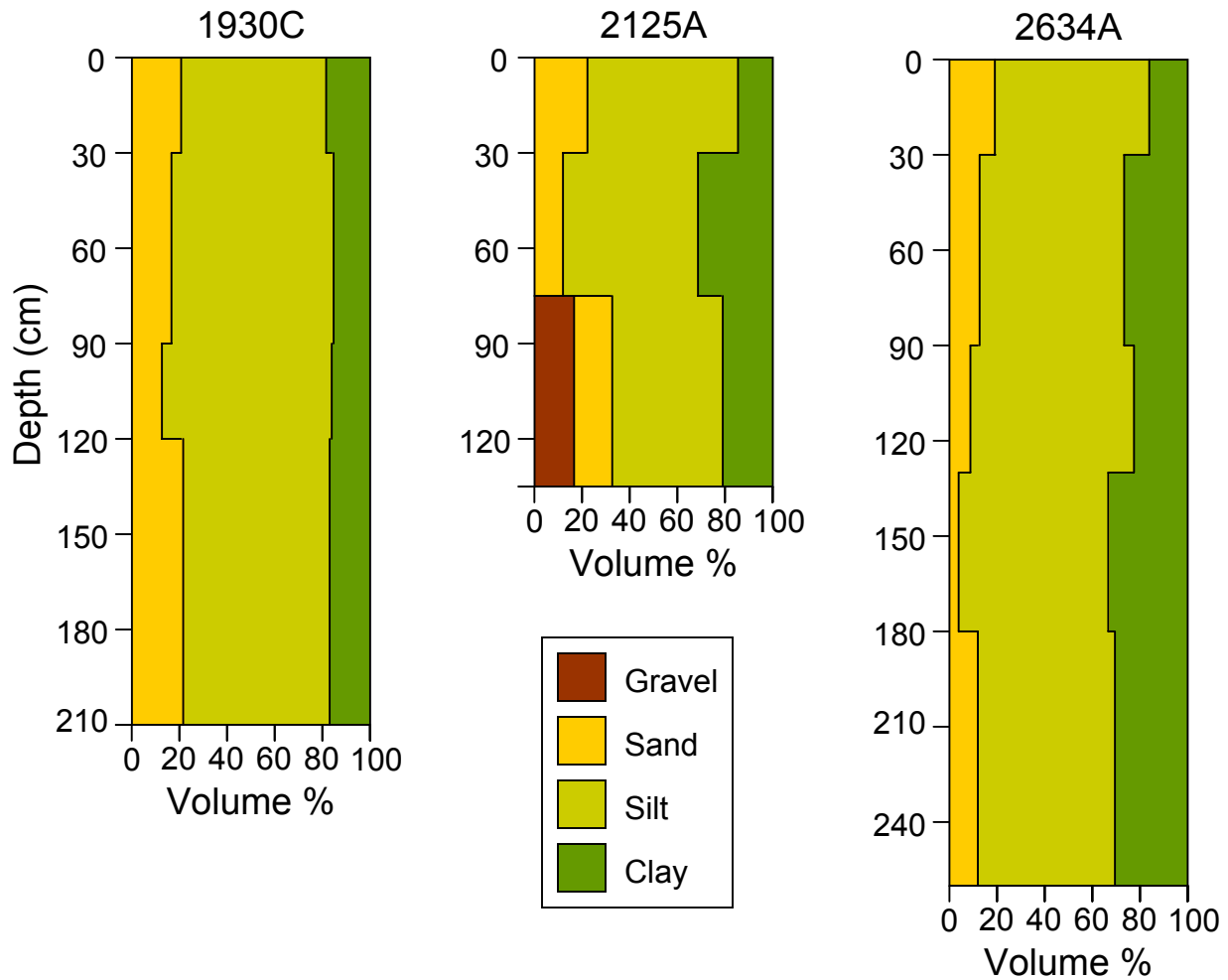
Figure 5.1. Stratigraphy of three loess deposits showing volume percentages of sediment fractions. Loess deposits in the study area average 60% silt.

L1 Loess Thickness and Possible Funneling of
Wind through the Columbia River Valley
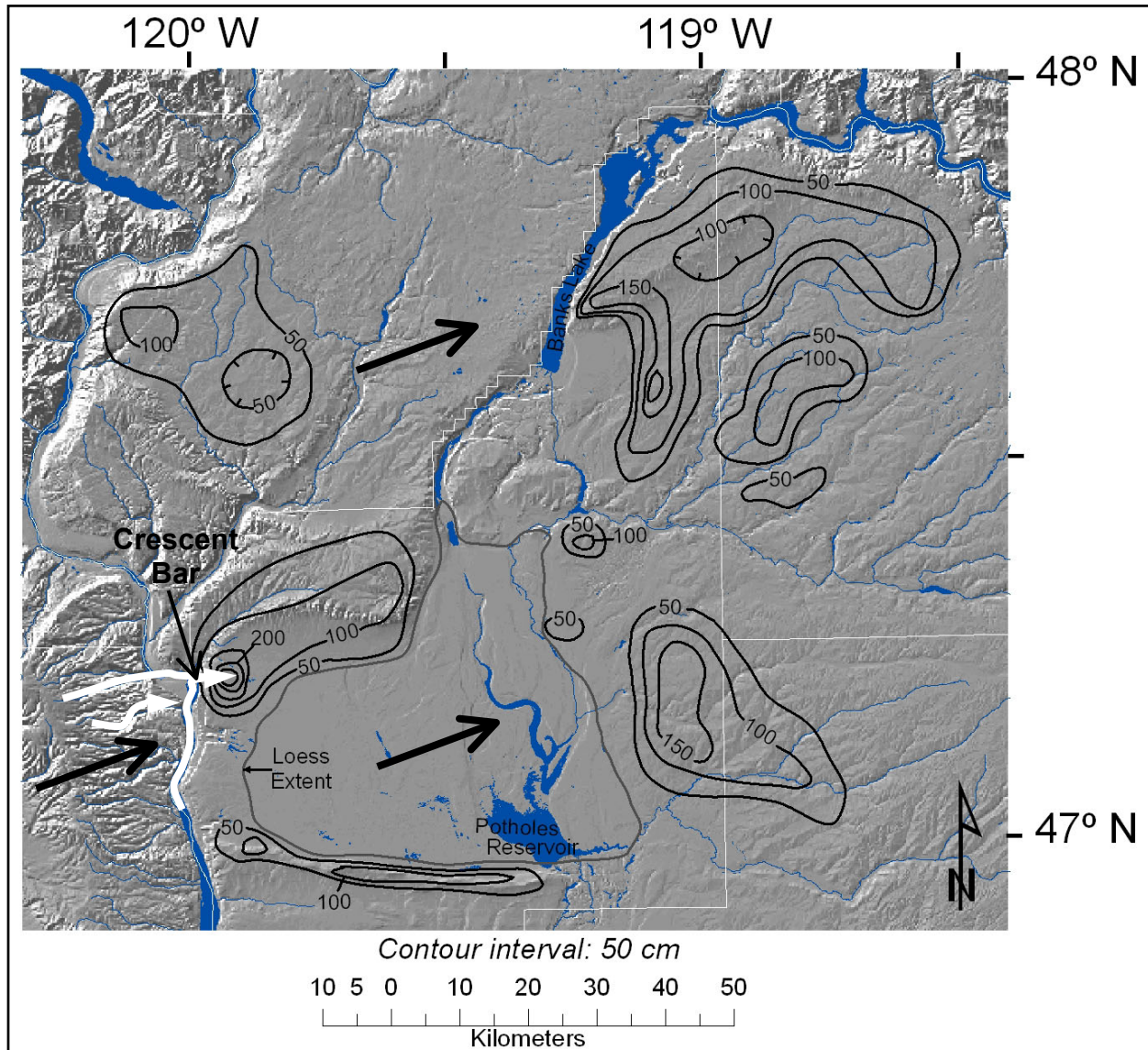
Figure 5.2. Isopach map of loess thickness. Notice the relatively thick L1 deposit in the northwest corner of Quincy Basin. Thick black arrows show prevailing winds across whole region. White arrows indicate speculated prevailing winds being channeled through the Columbia River Valley and over Crescent Bar.

Locations of Sites where MAR's were Determined
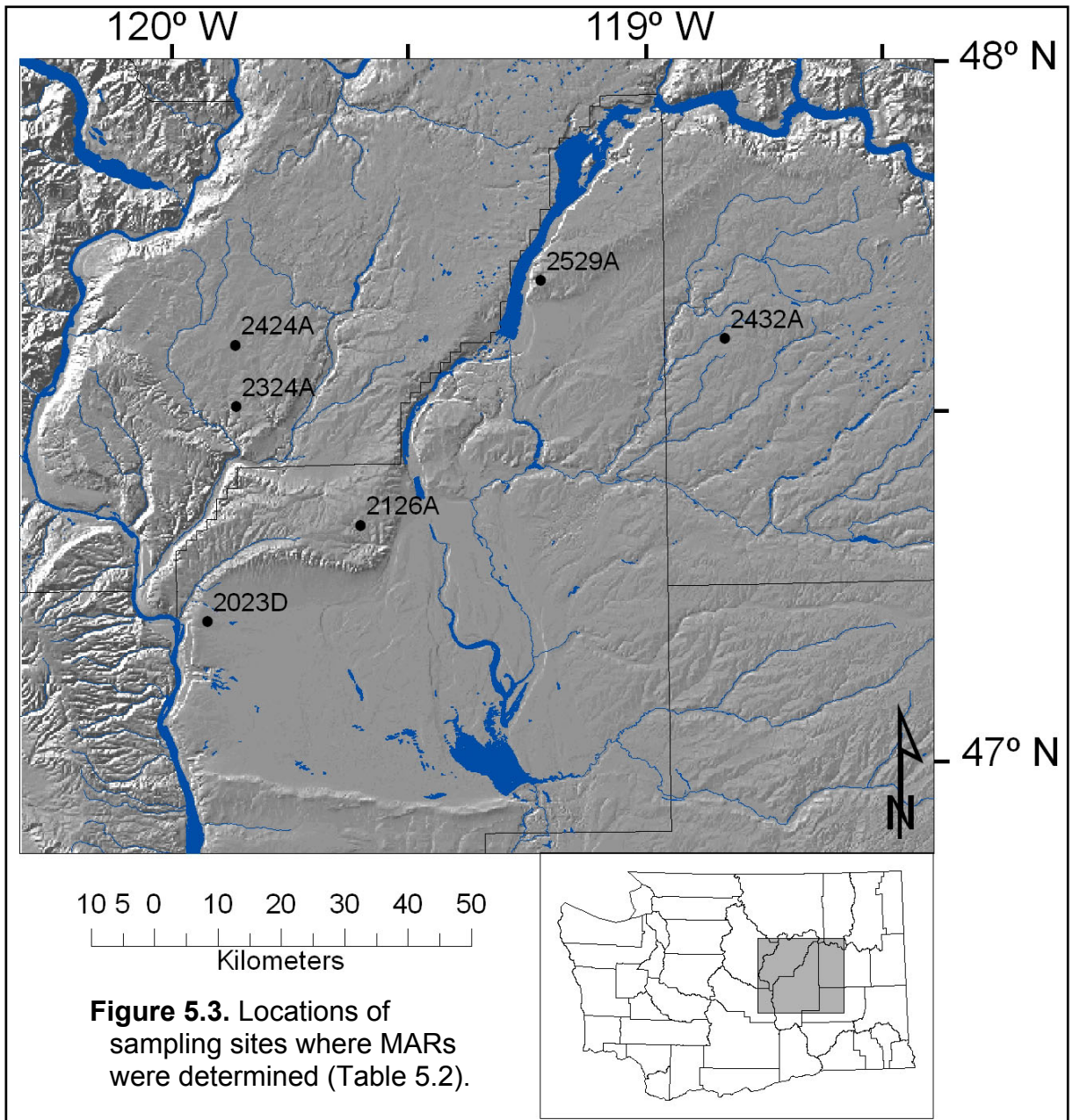
Figure 5.3. Locations of sampling sites where MARs were determined (Table 5.2).
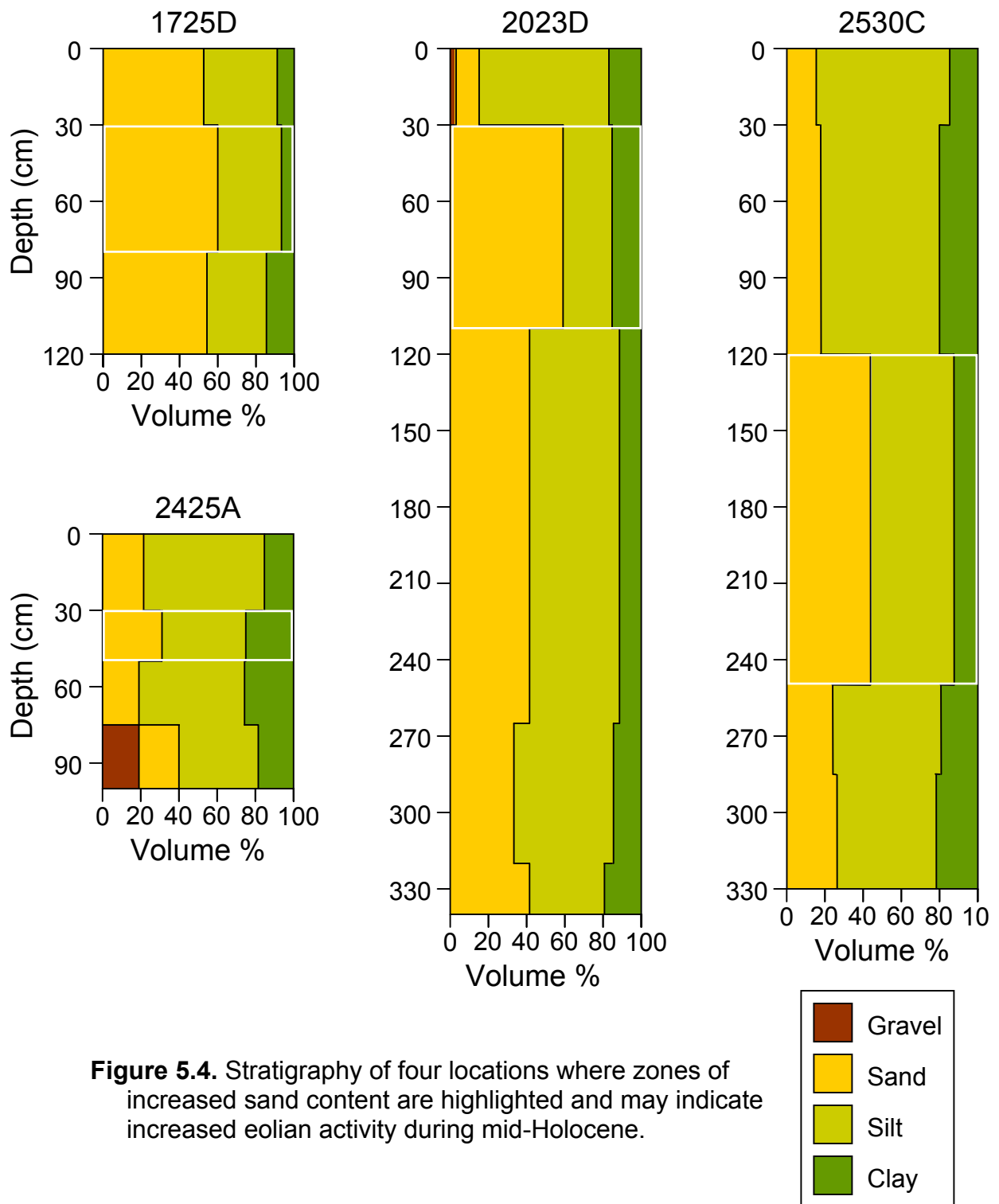
Figure 5.4. Stratigraphy of four locations where zones of increased sand content are highlighted and may indicate increased eolian activity during mid-Holocene.

Locations of Samples Analyzed Using XRF
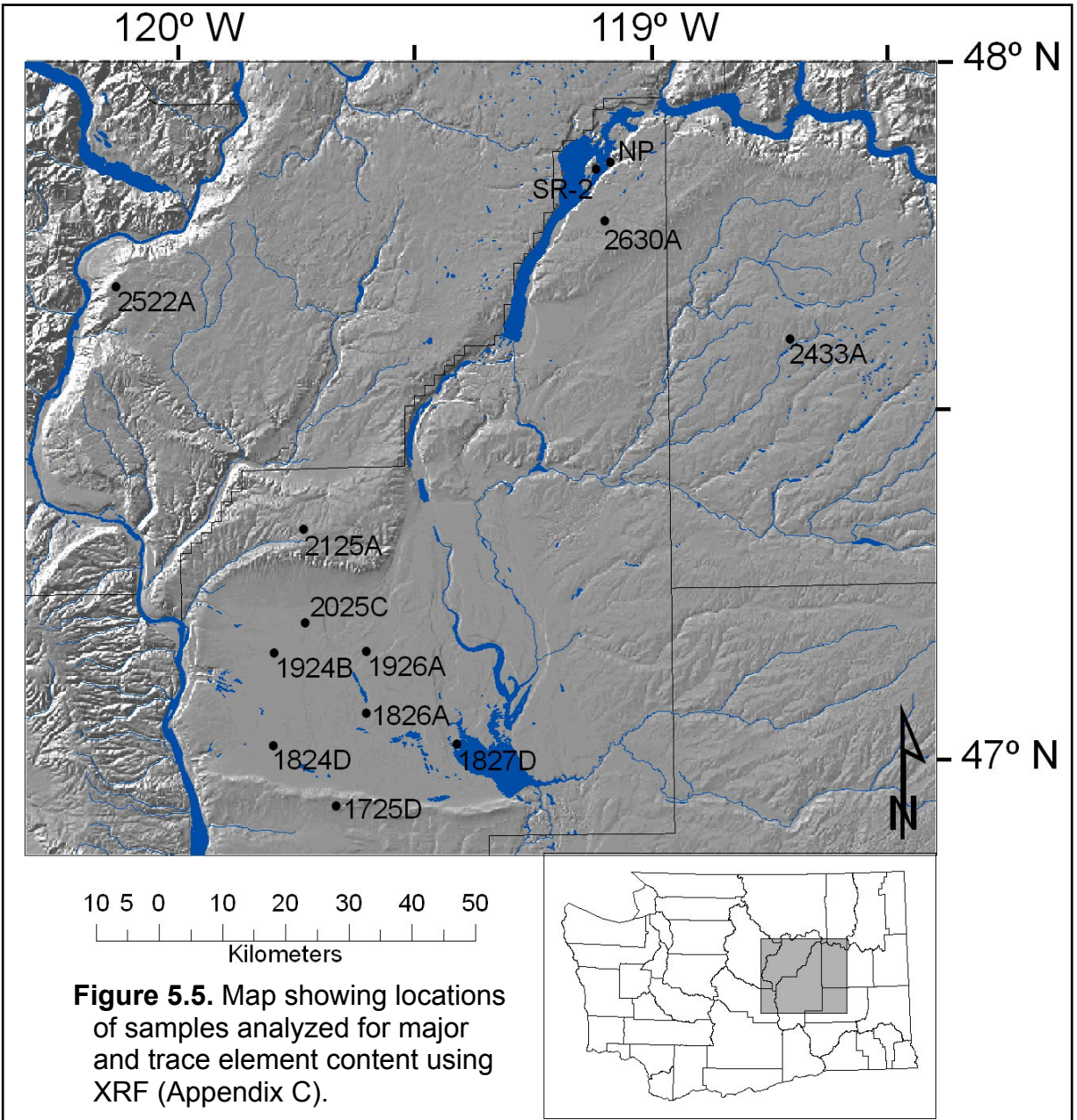
Figure 5.5. Map showing locations of samples analyzed for major and trace element content using XRF (Appendix C).
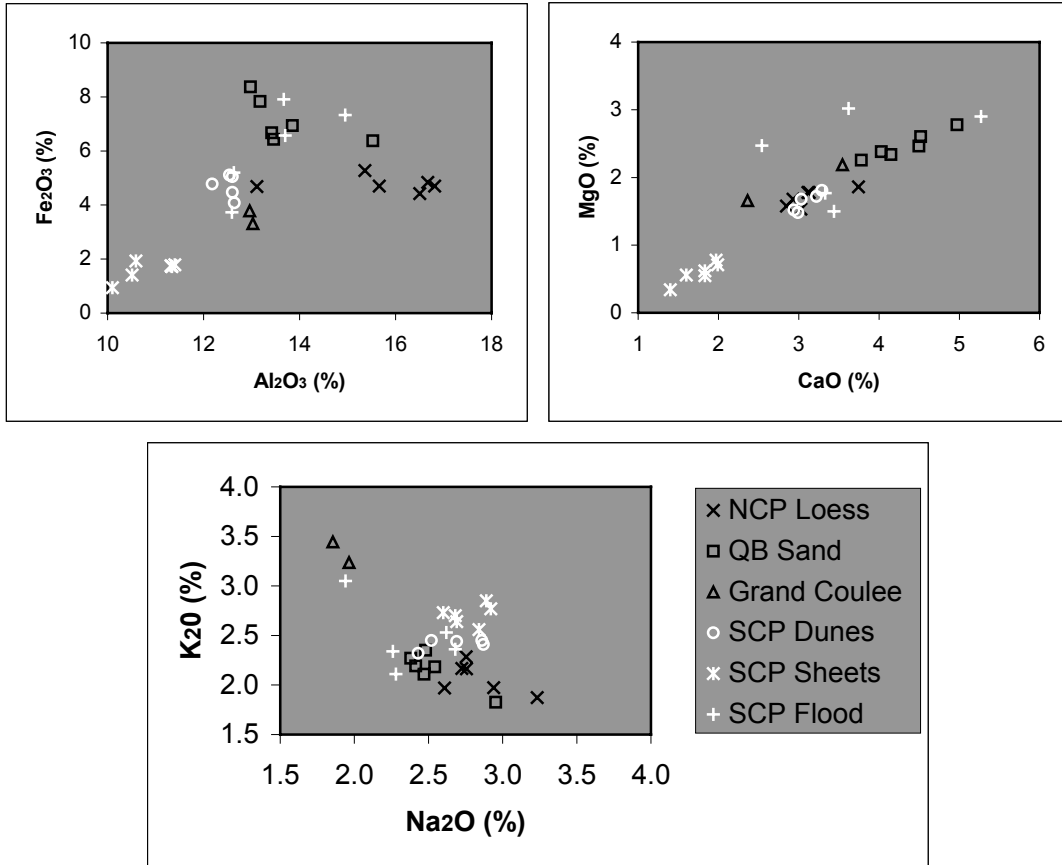
Figure 5.6. Comparison of elemental oxide weight percents of silt from several sediment samples from: northern Columbia Plateau (NCP), Quincy Basin (QB), Grand Coulee, and southern Columbia Plateau (SCP). SCP samples collected, analyzed and published by Sweeney (2004).
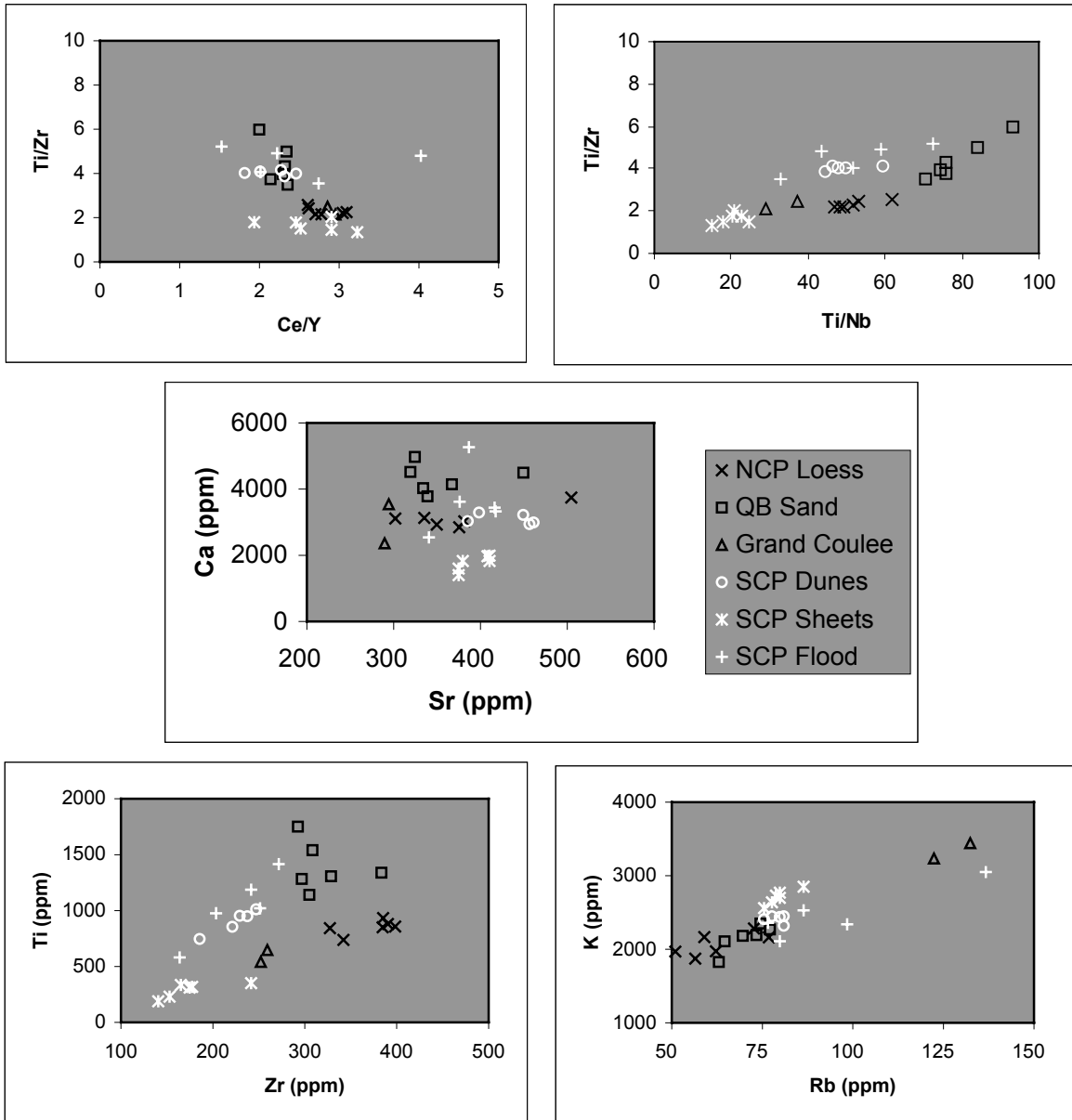
Figure 5.7. Comparison of trace element concentrations of silt for several sediment samples from: northern Columbia Plateau (NCP), Quincy Basin (QB), Grand Coulee, and southern Columbia Plateau (SCP). SCP samples collected, analyzed and published by Sweeney (2004).

Table 5.1. Estimated Volumes of Silt in Loess and Source Deposits

	Surface Area (km^2)	Average Thickness (cm)	Total Volume (km^3)	% Silt in Deposit	Total Volume of Silt (km^3)
Loess Deposits					
Wilbur Plateau	4,700	40	1.9	60	1.1
East of Quincy Basin	2,500	40	1.0	60	0.6
Remaining Deposits	8,200	20	1.7	60	1.0
Source Area					
Quincy Basin Sands	1,100	700	7.7	20	1.5
Remaining Potential Sources	40?	500-1500	0.2-0.6	60	0.1-0.4

Table 5.2: MARs of Loess at Selected Sites

	Thickness (m)	Duration (yr)	Accumulation Rate (m/yr)	Bulk Density (g/cm^3)	Mass Accumulation Rate (g/m^2/yr)
Avg. Waterville Plateau	0.30	15,400	1.9×10^{-5}	1.4	27
2126A	0.30	6,800	4.4×10^{-5}	1.4	62
2324A	0.60	13,200	4.5×10^{-5}	1.4	64
2424A	0.30	13,200	3.0×10^{-5}	1.4	32
Avg. Wilbur Plateau	0.40	15,400	2.6×10^{-5}	1.4	36
2432A	1.10	15,400	7.1×10^{-5}	1.4	100
2432A (pre-13.2 ka)	0.80	2,200	3.6×10^{-4}	1.4	509
2432A (post-13.2 ka)	0.30	13,200	2.3×10^{-5}	1.4	32
2529A	0.40	13,200	3.0×10^{-5}	1.4	42
Avg. Quincy Basin	0.20	15,400	1.3×10^{-5}	1.4	18
2023D	2.60	15,400	1.7×10^{-4}	1.4	240

CHAPTER SIX

CONCLUSIONS

Loess deposits on the northern Columbia Plateau are derived primarily from eolian reworking of outburst flood, eolian and alluvial sediment within the Quincy Basin. Less significant sources of loess deposits include the slackwater, eolian and alluvial deposits within the Columbia River Valley, Grand Coulee, Wilson Creek Valley and Lind Coulee. The thickest loess on the northern Columbia Plateau blankets the Wilbur Plateau northeast of Quincy Basin and the area east of Quincy Basin due primarily to prevailing west-southwest winds. Two anomalously thick loess sinks occur: east of and adjacent to the Columbia River on the western Waterville Plateau and: in the northwest corner of Quincy Basin. These two deposits were derived from slackwater deposits and recent Columbia River alluvium within the Columbia River Valley. It is proposed that these deposits were mobilized by winds that were funneled through the river valley.

MARs of loess on the northern Columbia Plateau are one to two orders of magnitude less than those on the southern Columbia Plateau. Differences in MARs has led to much thinner, 40 cm thick on average, L1 loess deposits on the northern Columbia Plateau while coeval loess on the southern Columbia Plateau is up to 800 cm thick (Sweeney, 2004; Sweeney et al., 2004; 2005). The bypassing of fine-grained, potential loess source, sediment during outburst flooding is the most significant factor for thinner northern Columbia Plateau loess. The stratigraphy of finer-grained loess source sediment below coarse sediment that cannot be transported by wind along with the erosion of existing fine-grained deposits during flooding are additional factors contributing to thinner northern Columbia Plateau loess.

71

The stratigraphies of eolian deposits on the northern Columbia Plateau confirm previously reported paleoclimate fluctuations. Tephra lenses and paleosols within loess and sand dune deposits on the northern plateau in association with MARs indicate a particularly dusty period immediately following the LGM and continuing into early interglacial times. Increases in sand content within L1 loess deposits are evidence of later enhanced eolian activity occurring during the mid-Holocene episode of increased aridity.

REFERENCES

Atwater, B.F., 1984, Periodic floods from glacial Lake Missoula into the Sanpoil arm of glacial Lake Columbia, northeastern Washington: Geology, v. 12, p. 464-467.

Atwater, B.F., 1986, Pleistocene glacial lake deposits of the Sanpoil River Valley, northeastern Washington: United States Geological Society Bulletin 1661, 39 pp.

Atwater, B.F., 1987, Status of glacial Lake Columbia during the last floods from glacial Lake Missoula: Quaternary Research, v. 27, p. 182-201.

Baker, V.R., 1973, Paleohydrology and sedimentology of Lake Missoula flooding in eastern Washington: Geological Society of America Special Paper 144, 79 pp.

Baker, V.R., and Bunker, R.C., 1985, Cataclysmic late Pleistocene flooding from glacial Lake Missoula; A review: Quaternary Science Reviews, v. 4, p. 1-41.

Barnosky, C.W., 1989, Postglacial vegetation and climate in the northwestern Great Plains of Montana: Quaternary Research, v. 31, p. 57-73.

Bartlein, P.J., Anderson, K.H., Anderson, P.M., Edwards, M.E., Mock, C.J., Thompson, R.S., Webb, R.S., Webb, T., III and Whitlock, C., 1998, Paleoclimate simulations for North America over the past 21,000 years: Features of the simulated climate and comparisons with paleoenvironmental data: Quaternary Science Reviews, vol. 17, p. 549-585.

Berger, G.W., and Busacca, A.J., 1995, Thermoluminescence dating of Late Pleistocene loess and tephra from eastern Washington and southern Oregon and implications for the eruptive history of Mount St. Helens: Journal of Geophysical Research, v. 100, p. 22,361-22,374.

Bettis, E.A., Muhs, D.R., Roberts, H.M. and Wintle, A.G., 2003, Last glacial loess in the conterminous USA: Quaternary Science Reviews, vol. 22, p. 1907-1946.

Björnsson, H., 1974, Explanation of jökulhlaups from Grímsvötn, Vatnajökull, Iceland: Jökull, vol. 24, p. 1-26.

Bjornstad, B.N., Fecht, K.R., and Pluhar, C.J., 2001, Long history of pre-Wisconsin, ice age cataclysmic floods: Evidence from southeastern Washington state: Journal of Geology, v. 109, p.695-713.

Blinnikov, M., Busacca, A., Whitlock, C., 2001, A new 100,000-year record from the Columbia Basin, Washington, U.S.A., *in* Meunier, J.D. and Colin, F., eds., Phytoliths - Applications in Earth Science and Human History. A.A. Balkema, Rotterdam. 384 pp.

Blinnikov, M., Busacca, A. and Whitlock, C., 2002, Reconstruction of the late Pleistocene grassland of the Columbia basin, Washington, USA, based on phytolith records in loess: Palaeogeography, Palaeoclimatology, Palaeoecology, vol. 177, p. 77-101.

Borchardt, G.A., Aruscavage, P.J., and Millard, Jr., H.T., 1972, Correlation of the Bishop Ash, a Pleistocene marker bed, using instrumental neutron activation analysis: Journal of Sedimentary Petrology, v. 42, p. 301-306.

Bretz, J.H., 1923, The Channeled Scabland of the Columbia Plateau: Journal of Geology, v. 31, p. 617-649.

Bretz, J.H., 1969, The Lake Missoula floods and the Channeled Scabland: Journal of Geology, vol. 77, p. 505-543.

Bretz, J.H., Smith, H.T.U., and Neff, G.E., 1956, Channeled Scabland of Washington; New data and interpretations: Geologic Society of America Bulletin, v. 67, p. 957-1049.

Bullard, J.E., Wiggs, G.F.S., and Nash, D.J., 2000, Experimental study of wind directional variability in the vicinity of a model valley: Geomorphology, v. 35, p. 127-143.

Busacca, A.J., 1989, Long Quaternary record in eastern Washington, U.S.A.; interpreted from multiple buried paleosols in loess: Geoderma Special Issue on Climate and Lithostratigraphic Significance of Paleosols, vol. 45, p. 105-122.

Busacca, A.J. and Montgomery, J.A., 1992, Field-landscape variation in soil physical properties of the northwest dryland crop production region, *in* Veseth, R. and Miller, B., eds., Precision Farming for Profit and Conservation: 10th Inland Northwest Conservation Farming Conference Proceedings, Washington State University, Pullman, p. 8-18.

Busacca, A.J., Nelstead, K.T., McDonald, E.V., and Purser, M.D., 1992, Correlation of distal tephra layers in loess in the Channeled Scabland and Palouse of Washington State: Quaternary Research, v. 37, p. 281-303.

Busacca, A.J., and McDonald, E.V., 1994, Regional sedimentation of Late-Quaternary loess on the Columbia Plateau: sediment source areas and loess distribution patterns: Washington Division of Geology and Earth Resources Bulletin, v. 80, p. 181-190.

Clague, J.J., Barendregt, R., Enkin, R.J., and Foit, F.F. Jr., 2003, Paleomagnetic and tephra evidence for tens of Missoula floods in southern Washington: Geology, v. 31, p. 247-250.

Collins, W.D., Rasch, P.J., Eaton, B.E., Khattatov, B., Lamarque, J.-F., and Zender, C.S., 2001, Forecasting aerosols using a chemical transport model with assimilation of satellite aerosol retrievals: Methodology for INDOEX: Journal of Geophysical Research, vol. 106, p. 7313–7336.

Cooke, R.V. and Warren, A., 1973, Geomorphology in Deserts: University of California Press, Berkley, 374 pp.

Crosby, C.J. and Carson, R.J., 1999, Geology of Steamboat Rock Grand Coulee, Washington: Washington Geology, v. 27, no. 2/3/4, p. 3-8.

Department of the Interior: Bureau of Reclamation, 2004, Federal Register, Vol. 69, No. 101, p. 29754-29755.

Foit, F.F., Jr., Mehringer, P.J., Jr., and Sheppard, J.C., 1993, Age, distribution and stratigraphy of Glacier Peak tephra in eastern Washington and western Montana, United States: Canadian Journal of Earth Sciences, v. 30, p. 535-552.

Franklin, J.F. and Dyrness, C.T., 1988, Natural Vegetation of Oregon and Washington, Oregon State University Press, Corvallis, OR, 464 pp.

Gaylord, D.R., Foit. F.F., Jr., Schatz, J.K. and Coleman, A.J., 2001, Smith Canyon dune field, Washington, U.S.A.: relation to glacial outburst floods, the Mazama eruption, and Holocene paleoclimate: Journal of Arid Environments, v. 47, p. 403-424.

Gaylord, D.R., Busacca, A.J., and Sweeney, M.R., 2003, The Palouse loess and the Channeled Scabland: a paired Ice-Age geologic system, *in* Easterbrook, D.J., ed., Quaternary Geology on the United States, INQUA 2003 Field Guide Volume, Desert Research Institute, Reno, NV, p. 123-134.

Gaylord, D.R., Sweeney, M.R., Busacca, A.J., and Foit, F.F., Jr., 2004, Post-LGM eolian history of the northern Columbia Plateau, Washington and relation glacial outburst flooding: Geological Society of America Abstracts with Programs, v. 36, no. 5, p. 68.

Gentry, H.R., 1979, Soil Survey of Grant County, Washington: United States Department of Agriculture, Soil Conservation Service, 329 pp.

Grini, A., Myhre, G., Zender, C. S., and Isaksen, I. S. A., 2005, Model simulations of dust sources and transport in the global troposphere: Journal of Geophysical Research, vol. 110, D02205, doi:10.1029/2004JD005037.

Grolier, M.J. and Bingham, J.W., 1978, Geology of parts of Grant, Adams, and Franklin counties, east-central Washington: State of Washington, Department of Natural Resources, Division of Geology and Earth Resources, Bulletin no. 71. 91 pp.

Gustafson, E.P., 1978, The vertebrate faunas of the Pliocene Ringold Formation, south-central Washington: Eugene, University of Oregon Museum of Natural History Bulletin 23, 62 pp.

Harrison, S.P., Kohfeld, K.E., Roelandt, C., and Claquin, T., 2001, The role of dist in climate changes today, at the last glacial maximum and in the future: Earth-Science Reviews, v. 54, p. 43-80.

Johnson, D.M., Hooper, P.R. and Conrey, R.M., 1999, XRF analysis of rocks and minerals for major and trace elements on a single low dilution Li-tetraborate fused bead: Advances in X-ray Analysis, v. 41, p 843-867.

Kovanen, D.J. and Slaymaker, O., 2004, Glacial imprints of the Okanogan Lobe, southern margin of the Cordilleran Ice Sheet: Journal of Quaternary Science, vol. 19, p. 547-565.

Kiver, E.P., Moody, U.L., Rigby, J.G., and Stradling, D.F., 1991, Late Quaternary stratigraphy of the Channeled Scabland and adjacent areas, *in* Morrison, R.B., ed., Quaternary nonglacial geology: Conterminous United States, Geology of North America, Boulder, Colorado, Geological Society of America, v. K-2, p. 238-245.

Ludwig, S.L., 1987, Sand within the silt; The source and deposition of loess in eastern Washington [M.S. thesis]: Pullman, Washington State University, 120 pp.

McDonald, E.V., and Busacca, A.J., 1992, Late Quaternary stratigraphy of loess in the Channeled Scabland and Palouse regions of Washington State: Quaternary Research, v. 38, p. 141-156.

Millineaux, D.R., 1986, Summary of pre-1980 tephra-fall deposits from Mount St. Helens, Washington state, USA: Bulletin of Volcanology, v. 48, p. 17-26

Moody, U.L., 1987, Late Quaternary stratigraphy of the Channeled Scabland and adjacent areas [Ph.D. Thesis]: Moscow, University of Idaho, 419 pp.

Muhs, D.R., Stafford, T.W., Jr., Cowherd, S.D., Mahan, S.A., Kihl, R., Maat, P.B., Bush, C.A., and Nehring, J., 1996, Origin of the late Quaternary dune fields of northeastern Colorado: Geomorphology, v. 17, p. 129-149.

Muhs, D.R., Aleinikoff, J.N., Stafford, T.W., Jr., Kihl, R., Been, J., Mahan, S.A., and Cowherd, S.D., 1999, Late Quaternary loess in northeastern Colorado, Part I; Age and paleoclimatic significance: Geological Society of America Bulletin, vol. 11, p. 1861-1875.

Muhs, D.R. and Bettis, E.A., 2000, Geochemical variations in Peoria Loess of western Iowa indicate paleowinds of mid-continent North America during last glaciation: Quaternary Research, vol. 53, p. 49-61.

Muhs, D.R. and Benedict, J.B., 2006, Eolian additions to late Quaternary alpine soils, Indian Peaks Wilderness Area, Colorado, Colorado front range: Arctic, Antarctic and Alpine Research, vol. 38, p. 120-130.

Newcomb, R.C., Strand, J.R., and Frank, F.J., 1972, Geology and groundwater characteristics of the Hanford reservation of the U.S. Atomic Energy Commission: U.S. Geological Survey Professional Paper 717, 78 pp.

O'Geen, A.T., and Busacca, A.J., 2001, Faunal burrows as indicators of Paleo-vegetation in eastern Washington, USA: Palaeogeography Palaeoclimatology Palaeoecology, v. 169, p. 23-37.

Packer, D.R., 1979, Paleomagnetism and age dating of the Ringold Formation and loess deposits in the State of Washington: Oregon Geology, v. 41, p. 119-132.

Petrone, A., 1970, The Moses Lake sand dunes [M.S. Thesis]: Washington State University, Pullman, 89 pp.

Pluhar, C.J., Bjornstad, B.N., Reidel, S.P. Coe, R.S., and Nelson, P.B., 2006, Magnetostratigraphic evidence from the Cold Creek bar for onset of ice-age cataclysmic floods in eastern Washington during the Early Pleistocene: Quaternary Research, vol. 65, p. 123-135.

Pye, K., 1987, Aeolian Deposits and Dust Deposits: Academic Press, London, 334 p.

Pye, K., 1995, The nature, origin and accumulation of loess: Quaternary Science Reviews, v. 14, p. 653-667.

Richardson, C.A., McDonald, E.V., and Busacca, A.J., 1997, Luminescence dating of loess from the northwest United States: Quaternary Science Reviews, v. 16, p. 403-415.

Richardson, C.A., McDonald, E.V., and Busacca, A.J., 1999, A luminescence chronology for loess deposition in Washington state and Oregon, USA: Zeitschrift fur Geomorphologie, v. 116, p. 77-95.

Riedel, S.P., 1984, The Saddle Mountains; The evolution of an anticline in the Yakima Fold Belt: American Journal of Science, v. 284, p. 972-978.

Roberts, H.M., Muhs, D.R., Wintle, A.G., Duller, G.A.T., and Bettis, E.A. III, 2003, Unprecedented last glacial mass accumulation rates determined by luminescence dating of loess from western Nebraska: Quaternary Research, v. 59, p. 411-419.

Rose, W.I., Riley, C.M. and Dartevelle, S., 2003, Sizes and shapes of 10-Ma distal fall pyroclasts in the Ogallala Group, Nebraska: The Journal of Geology, vol. 111, p 115–124.

Seamless Data Distribution System, October 28, 2004, U.S. Department of the Interior: U.S. Geological Survey, <http://seamless.usgs.gov>.

Shaw, J., Munro-Stasiuk, M., Sawyer, B., Beaney, C., Lesemann, J.-E., Musacchio, A., Rains, B. and Young, R.R., 1999. The Channeled Scabland; back to Bretz?: Geology, vol. 27, p. 605-608.

Smith, G.A., 1993, Missoula flood dynamics and magnitudes inferred from sedimentology of slack-water deposits on the Columbia Plateau: Geological Society of America Bulletin, v. 105, p. 77-100.

Smith, L.N., 2006, Stratigraphic evidence for multiple drainings of glacial Lake Missoula along the Clark Fork River, Montana, USA: Quaternary Research, v. 66, p. 311-322.

Sun, X. Li, X., Luo, Y. and Chen, X., 2000, The vegetation and climate at the last glaciation on the emerged continental shelf of the South China Sea: Palaeogeography, Palaeoclimatology, Palaeoecology, vol. 160, p. 301-316.

Swanson, D.A., Wright, T.L., Hooper, P.R., and Bentley, R.D., 1979, Revisions in stratigraphy nomenclature of the Columbia River Basalt Group: United State Geological Survey Bulletin 1457-G, 59 pp.

Sweeney, M.R., 2004, Sedimentology, paleoclimatology, and geomorphology of Late Pleistocene-Holocene paired eolian system, Columbia Plateau [Ph.D. Thesis]: Pullman, Washington State University, 204 pp.

Sweeney, M.R., Busacca, A.J., Richardson, C.A., Blinnikov, M., and McDonald, E.V., 2004, Glacial anticyclone recorded in Palouse loess of northwestern United States: Geology, vol. 32, p. 705-708.

Sweeney, M.R., Busacca, A.J., and Gaylord, D.R., 2005, Topographic and climatic influences on accelerated loess accumulation since the last glacial maximum in the Palouse, Pacific Northwest, USA: Quaternary Research, vol. 63, p. 261-273.

Tolan, T.L., Reidel, S.P., Beeson, M.H., Anderson, J.L., Fecht, K.R., and Swanson D.A., 1987, Revisions of the aerial extent and volume of the Columbia River Basalt Group (CRBG): Geological Society of America Abstracts with Programs, v. 19, p. 458.

Waitt, R.B., Jr., 1980, About forty last-glacial Lake Missoula jökulhlaups through southern Washington: Journal of Geology, v. 88, p. 653-679.

Waitt, R.B., Jr., 1983, Tens of successive, colossal Missoula floods at north and east margins of the Channeled Scabland: U.S. Geological Survey Open-File Report, 83-671, 29 pp.

Waitt, R.B., Jr., 1985, Case for periodic, colossal jökulhlaups from Pleistocene glacial Lake Missoula: Geological Society of America Bulletin, v. 96, p. 1271-1286.

Waitt, R.B., Jr., 1994, Scores of gigantic, successively smaller Lake Missoula floods through Channeled Scabland and Columbia Valley, *in* Swanson, D.A., and Haugerud, R.A., eds., Geologic field trips in the Pacific Northwest, Geological Society of America Annual Meeting, Boulder, Colorado, v. K1, 88 pp.

Waitt, R.B. and Atwater, B.F., 1989, Chapter 5: Stratigraphy and geomorphic evidence for dozens of last-glacial floods, *in* Breckenridge, R.M., ed., Glacial Lake Missoula and the Channeled Scabland, American Geophysical Union, Washington D.C., Field trip guidebook T 310, p. 37-55.

Whitlock, C. and Bartlein P.J., 1997, Vegetation and climate change in northwest America during the past 125 kyr: Nature, vol. 388, p. 57-61.

WSU Quaternary Research Lab Protocol, 2005, Particle-size analysis using Malvern Mastersizer S Laser Particle Diffractometer.

Zender, C. S., and Kwon, E. Y., 2005, Regional contrasts in dust emission responses to climate: Journal of Geophysical Research, vol. 110, D13201, doi:10.1029/2004JD005501.

Zimbelman, J.R., and Williams, S.H., 2002, Geochemical indicators of separate sources for eolian sands in the eastern Mojave Desert, California, and western Arizona: Geological Society of America Bulletin, vol.114, p. 490-496.

APPENDIX A:

STRATIGRAPHIC GRAIN SIZE DISTRIBUTION OF SELECTED SITES

2125A

2126A

2229C

2332A

2425A

2427A

2430A

2432A

2433A

Depth (cm)

Volume %

2628A

2630A

2534A

2633A

ML 2

ML 5
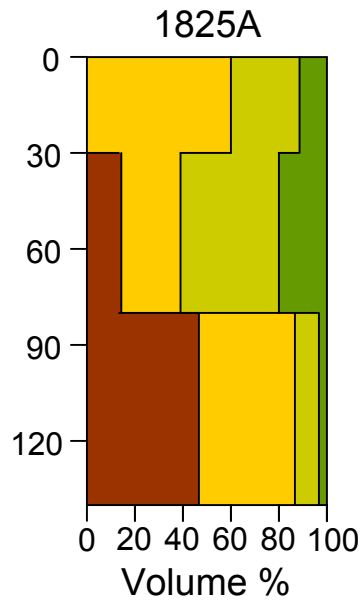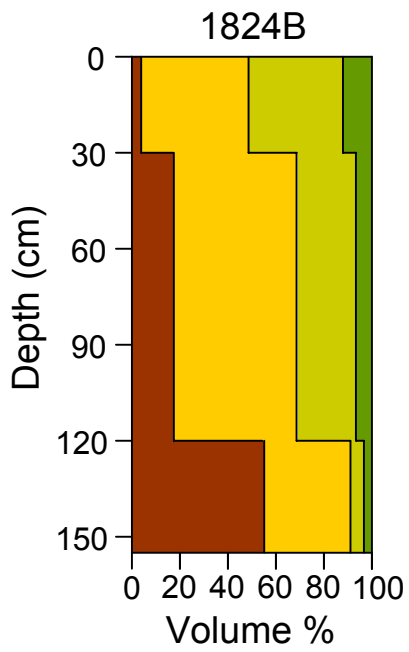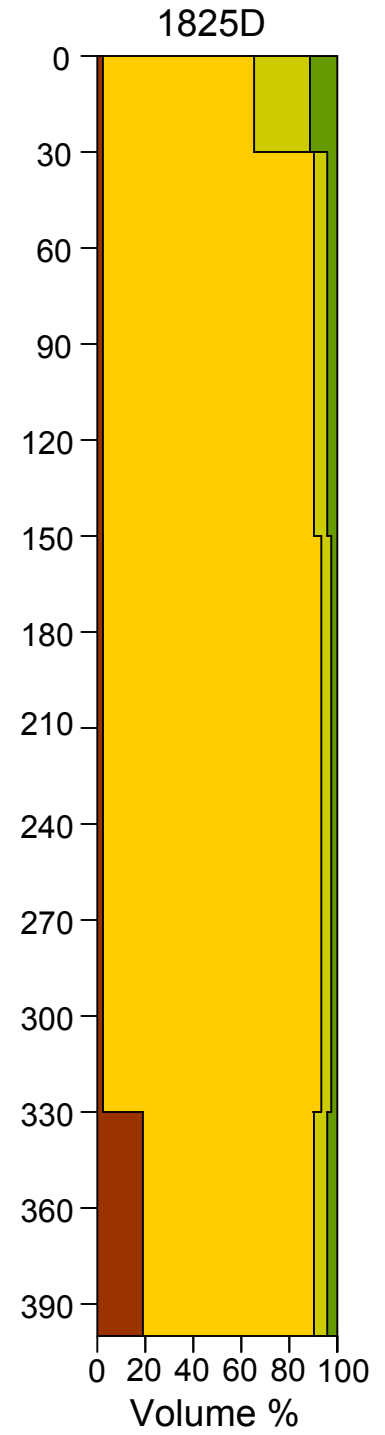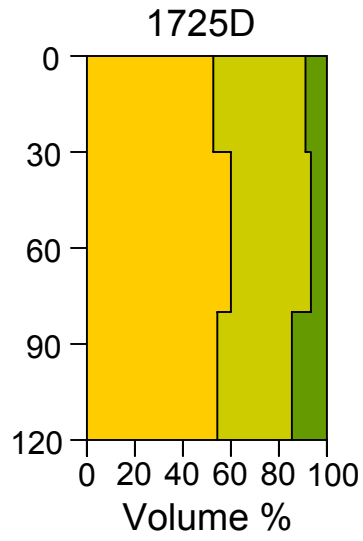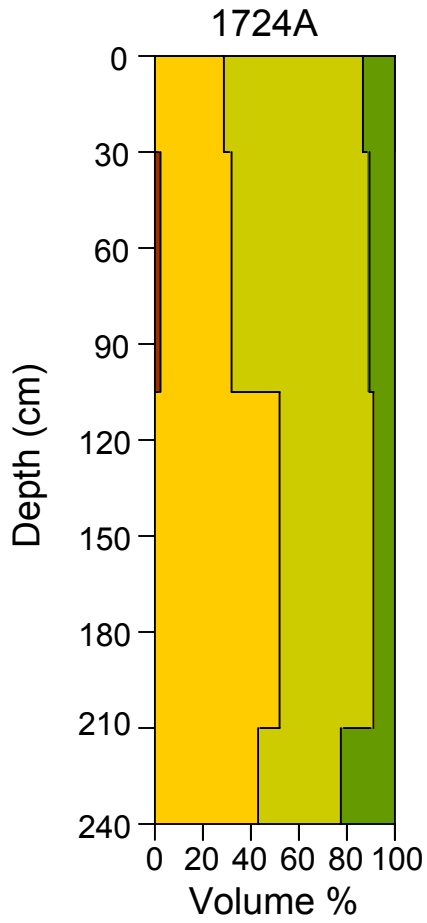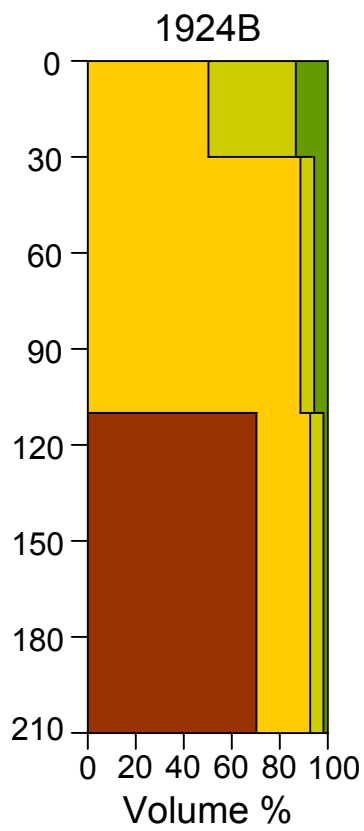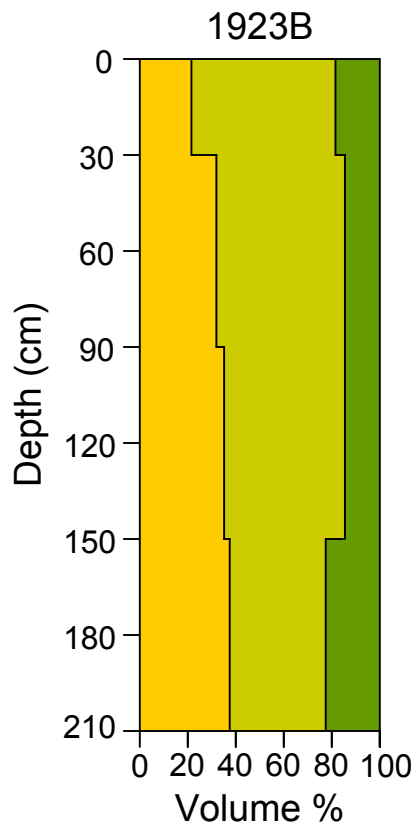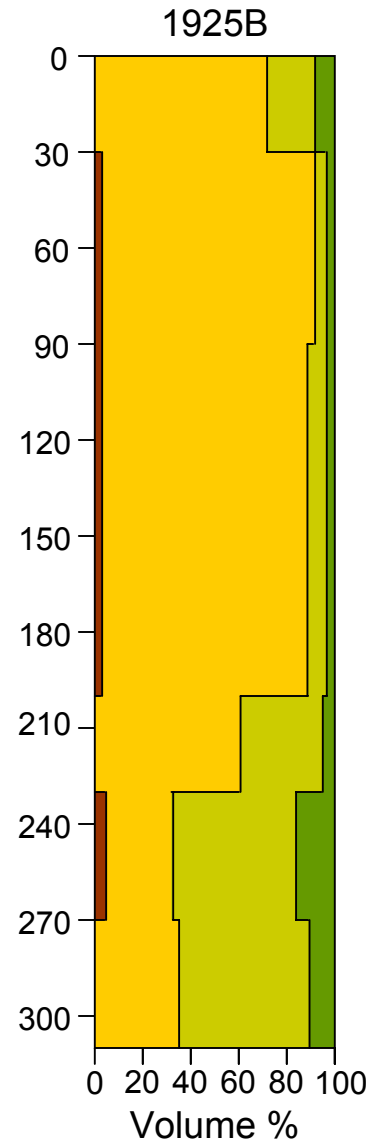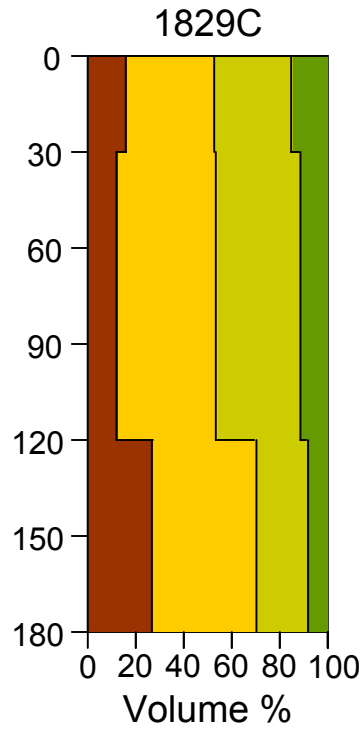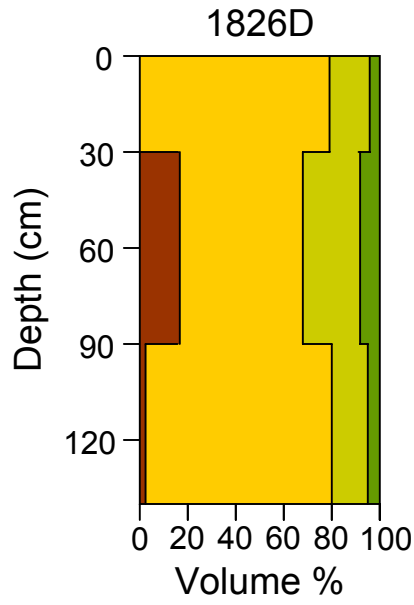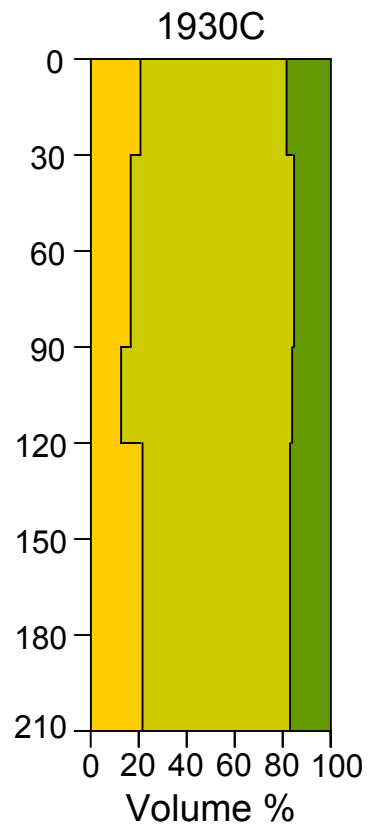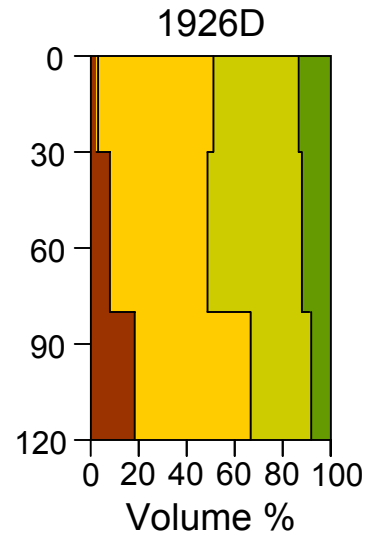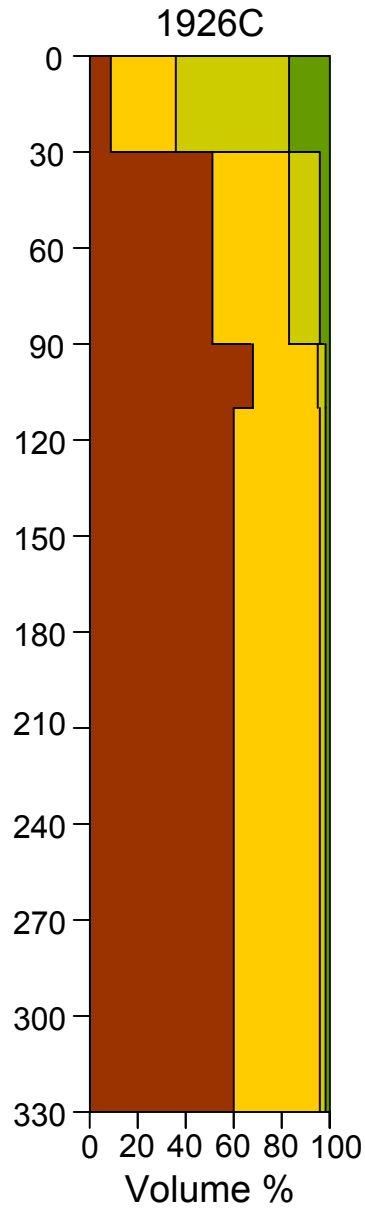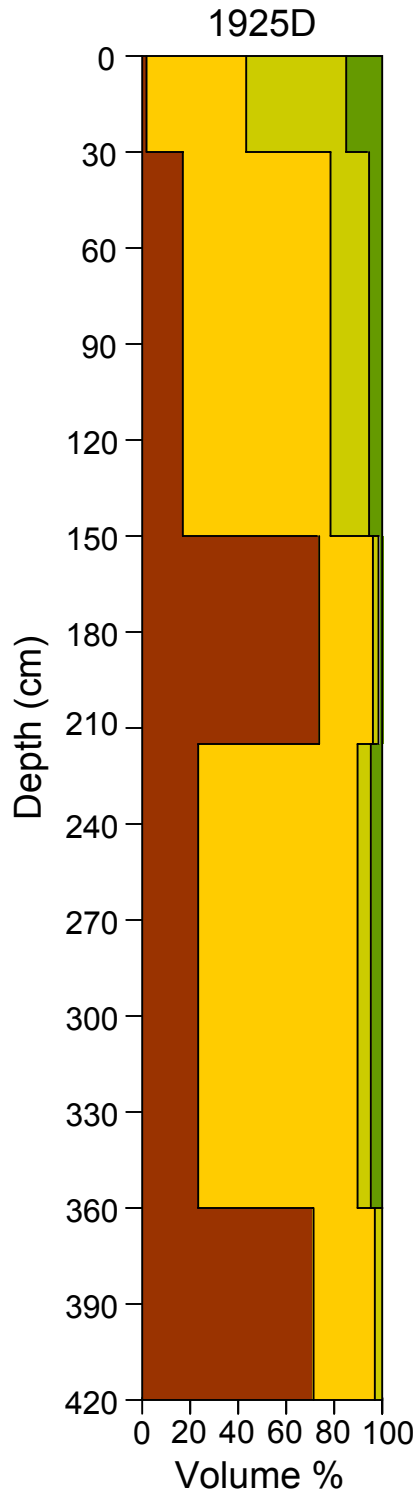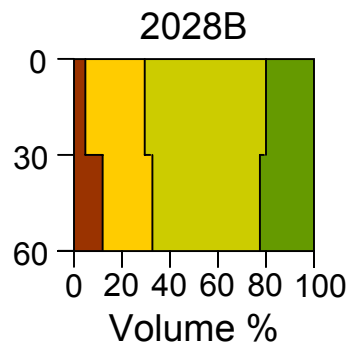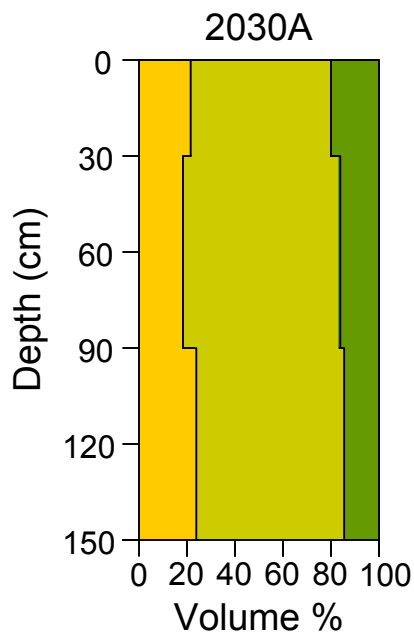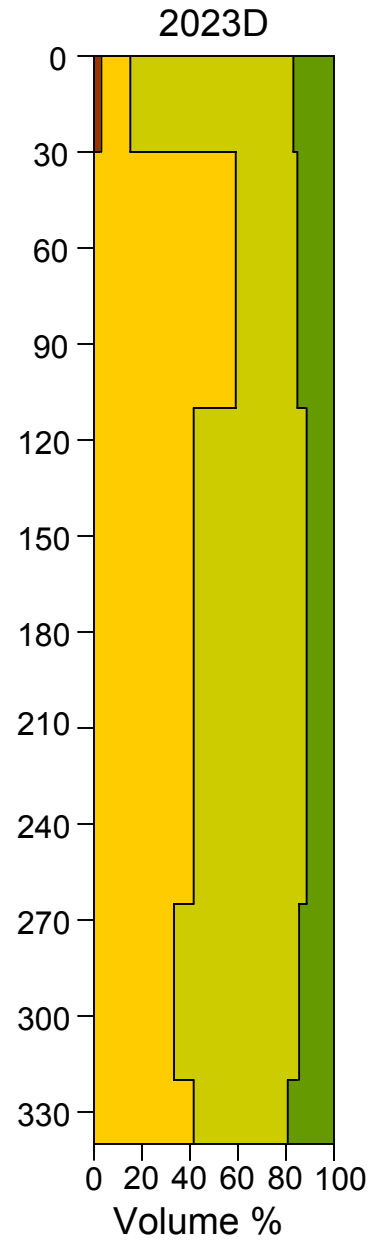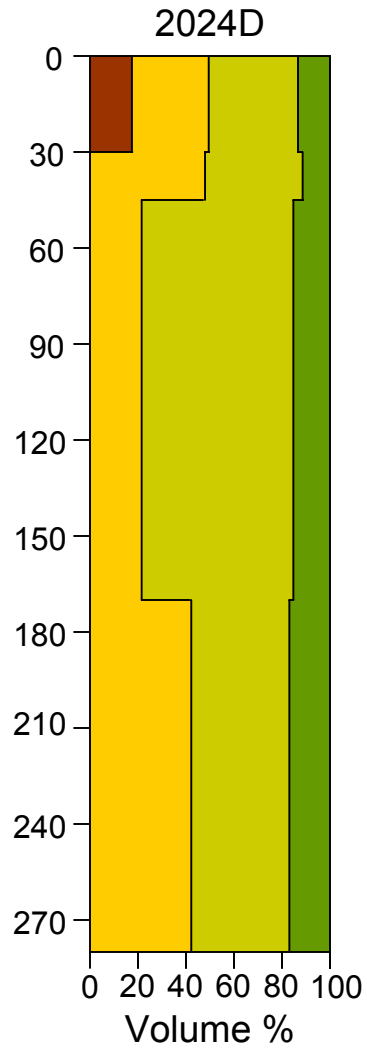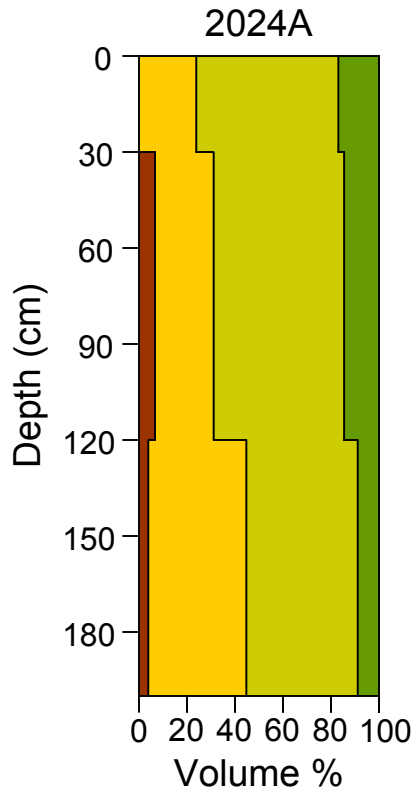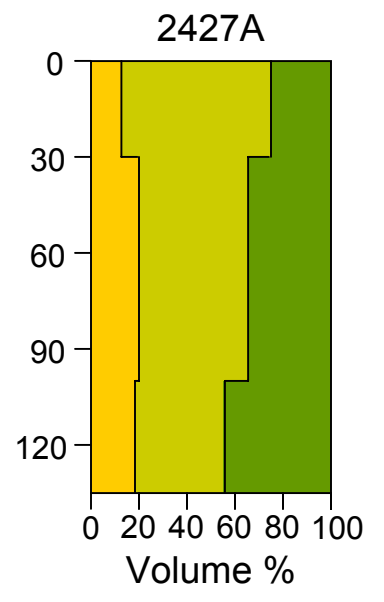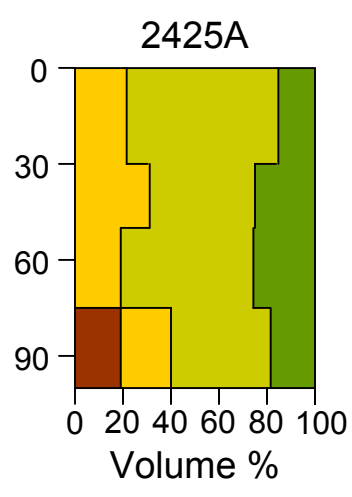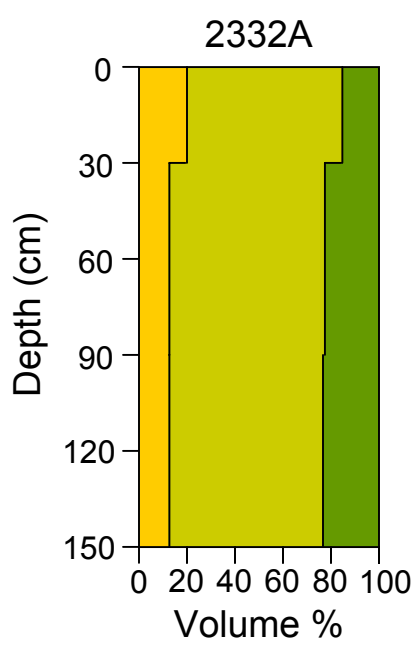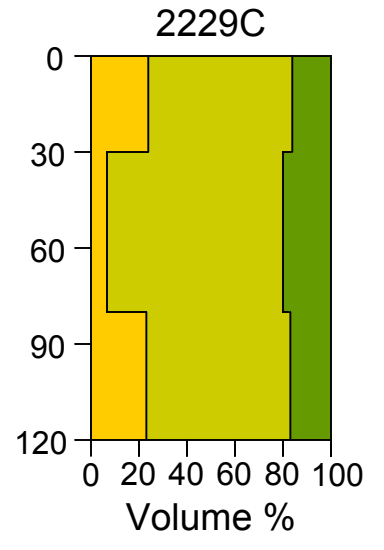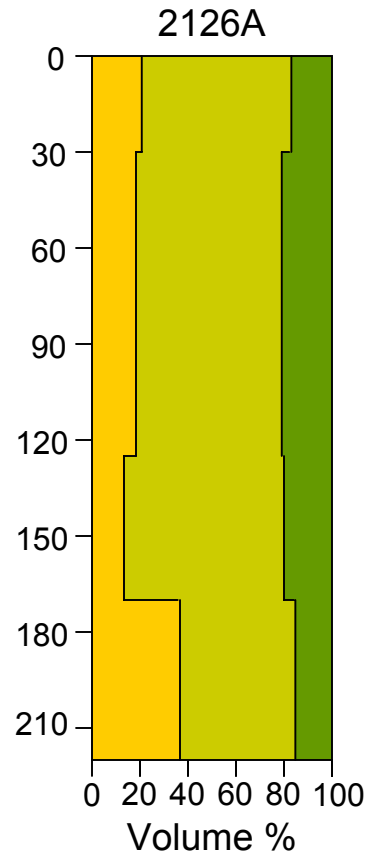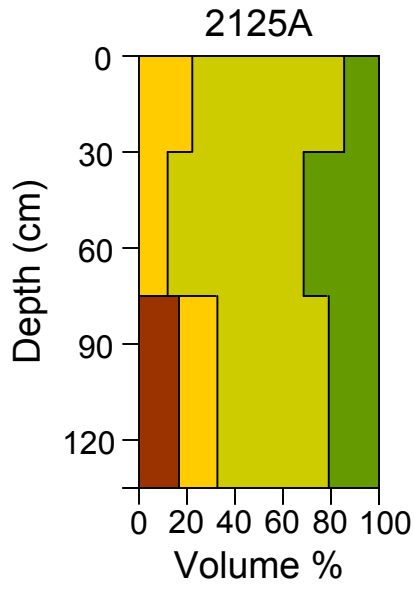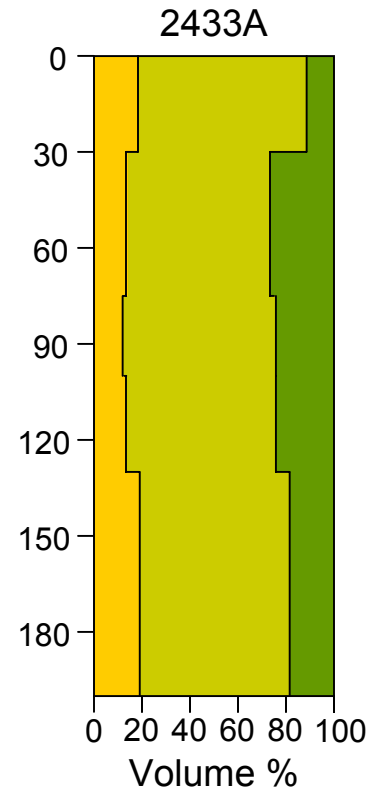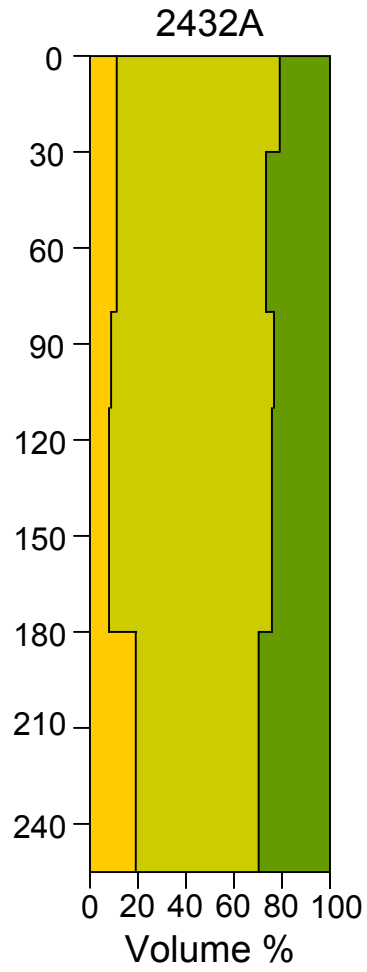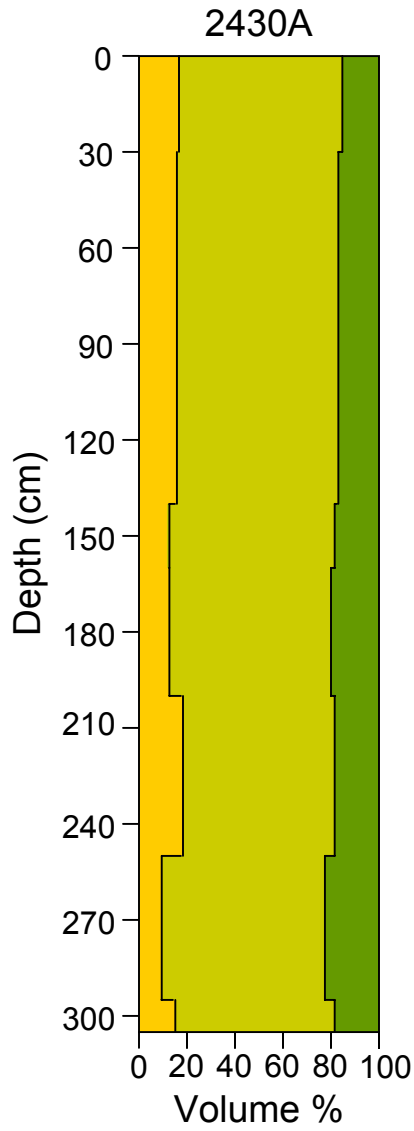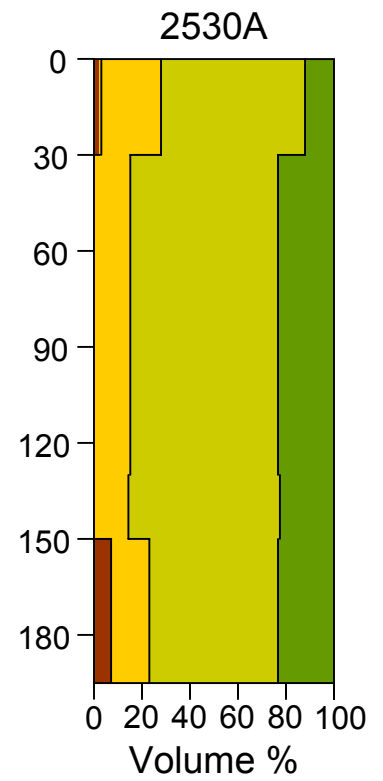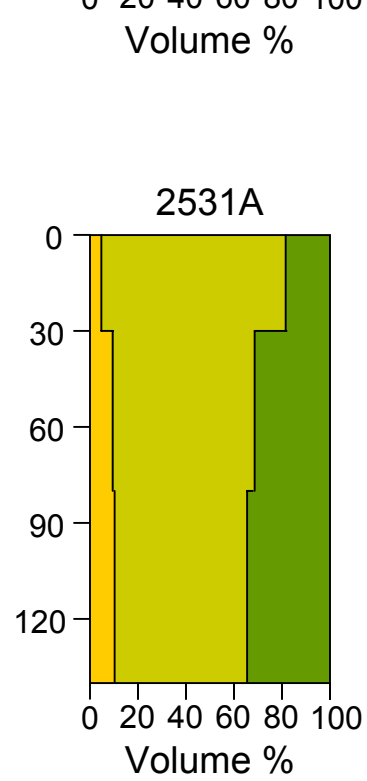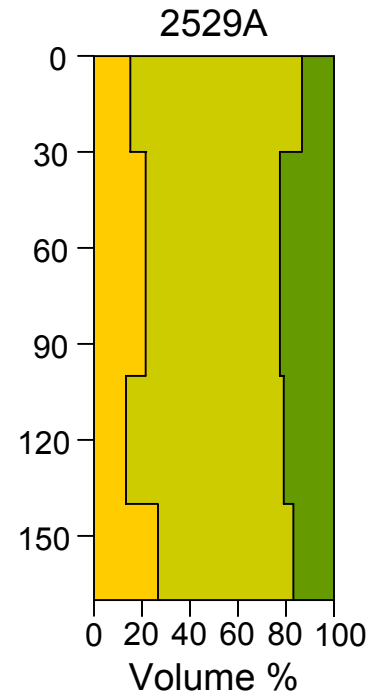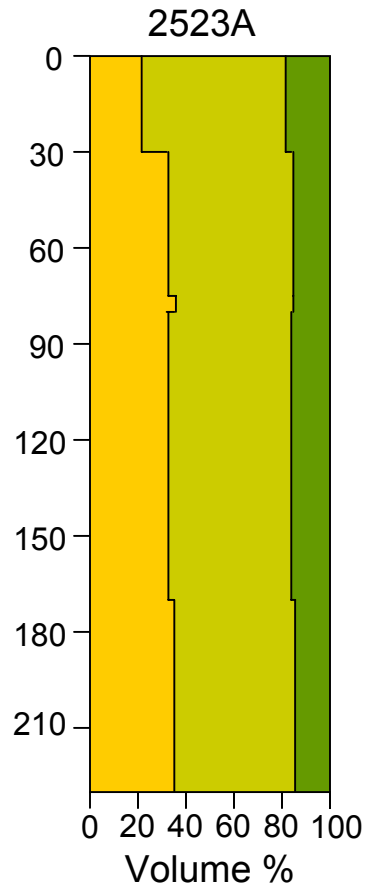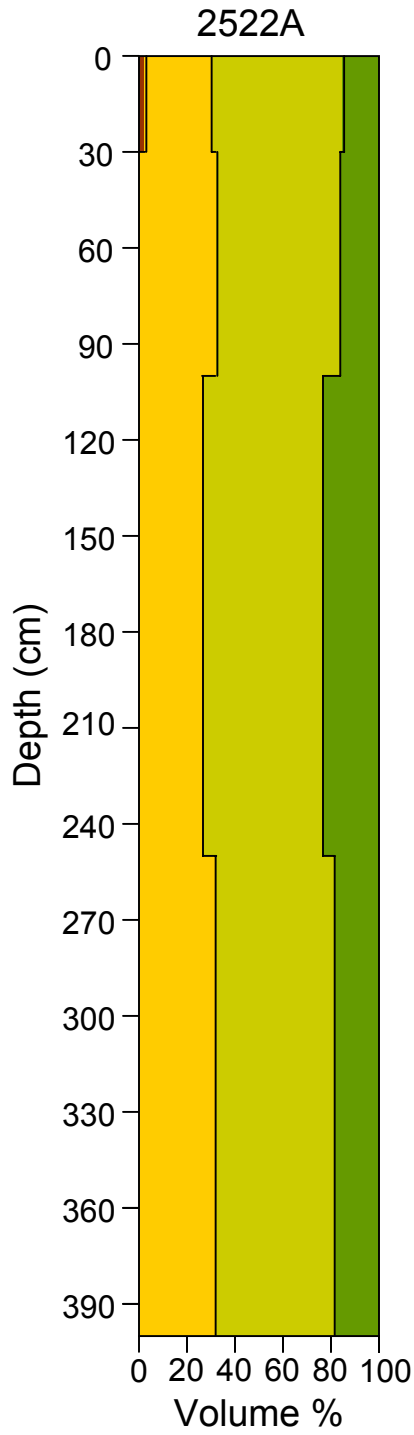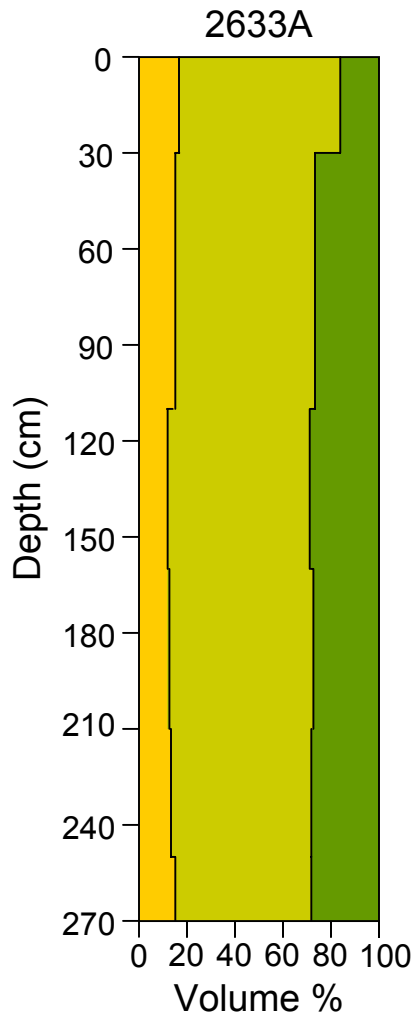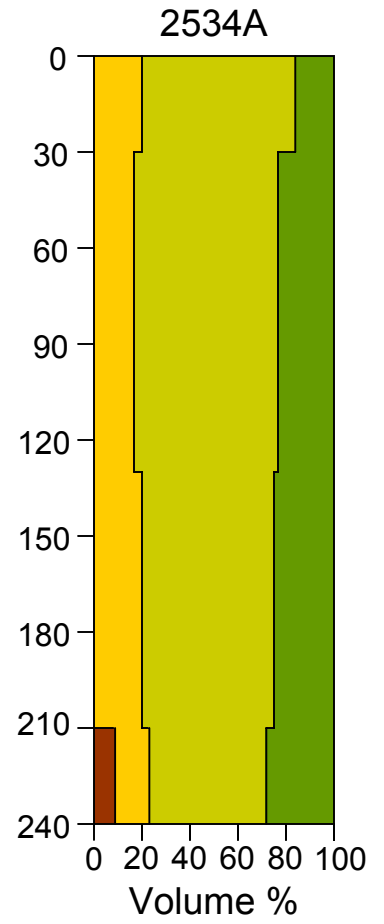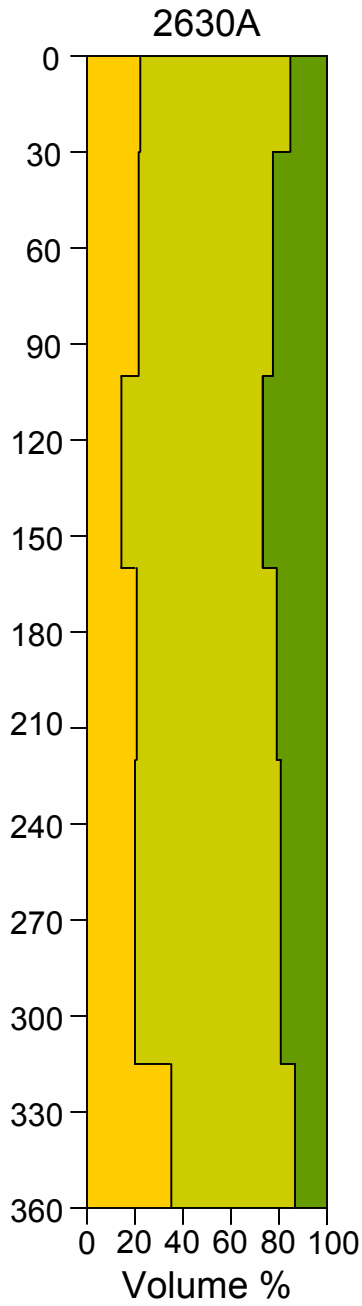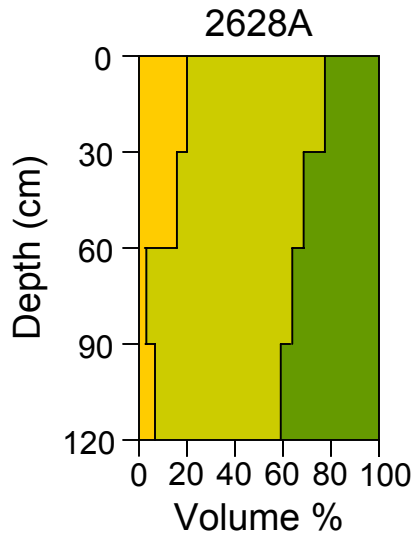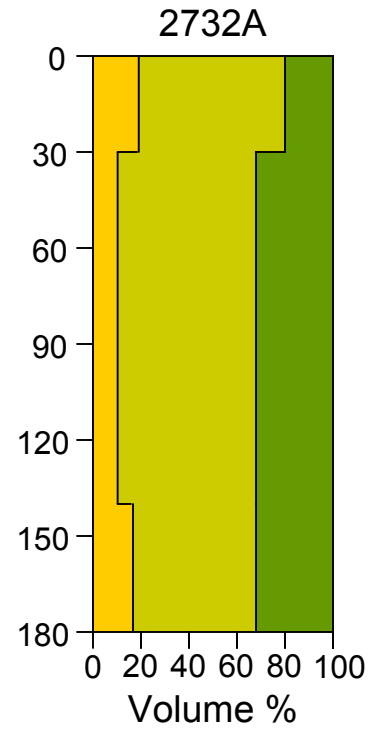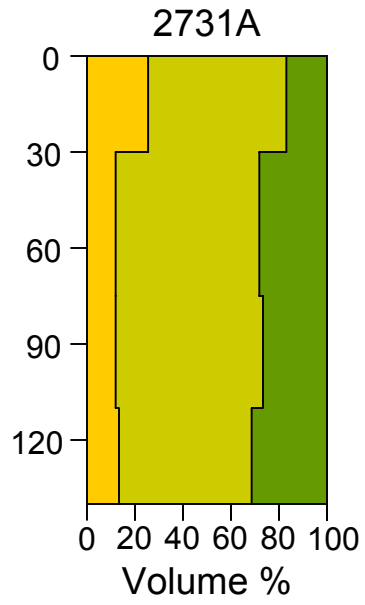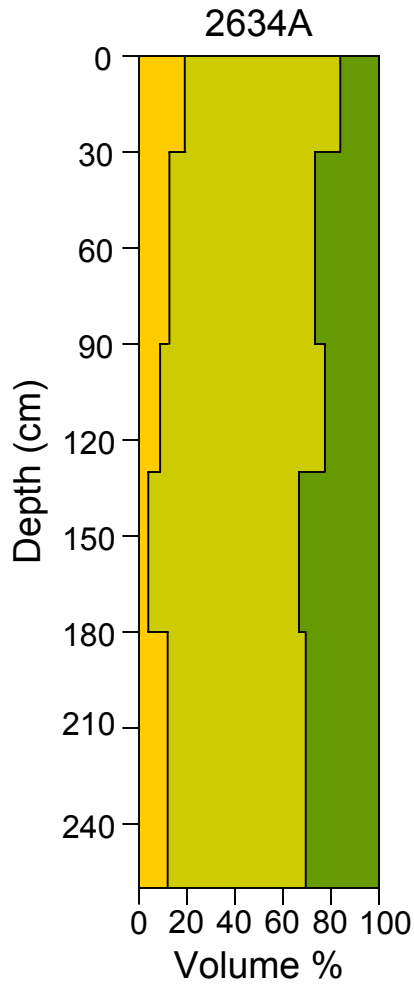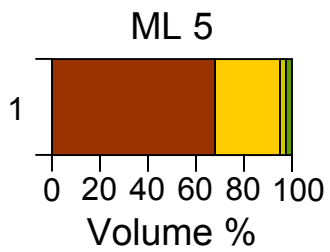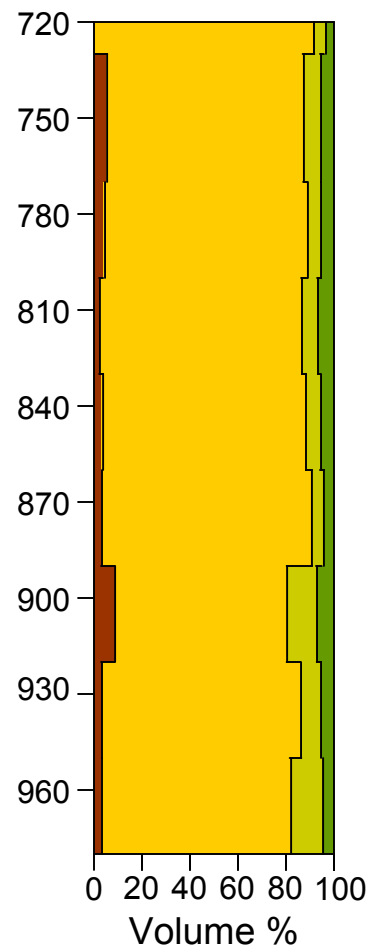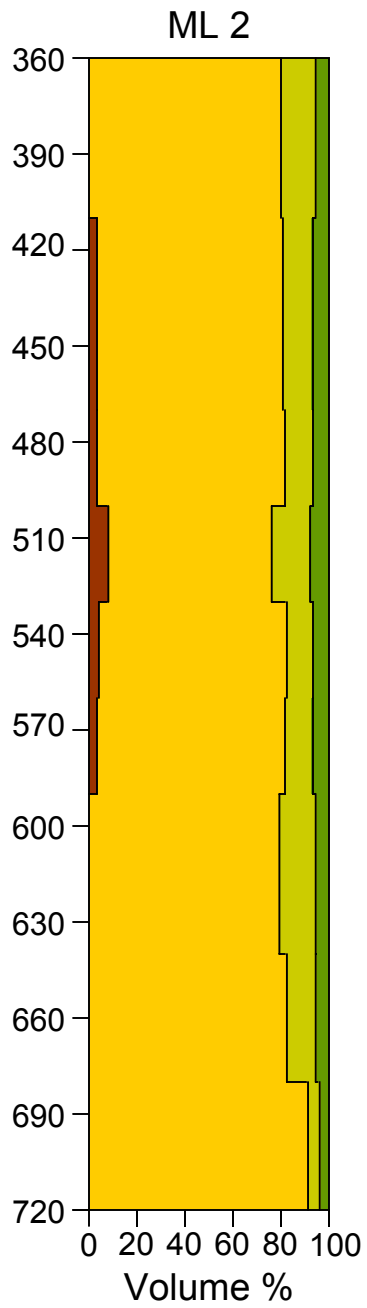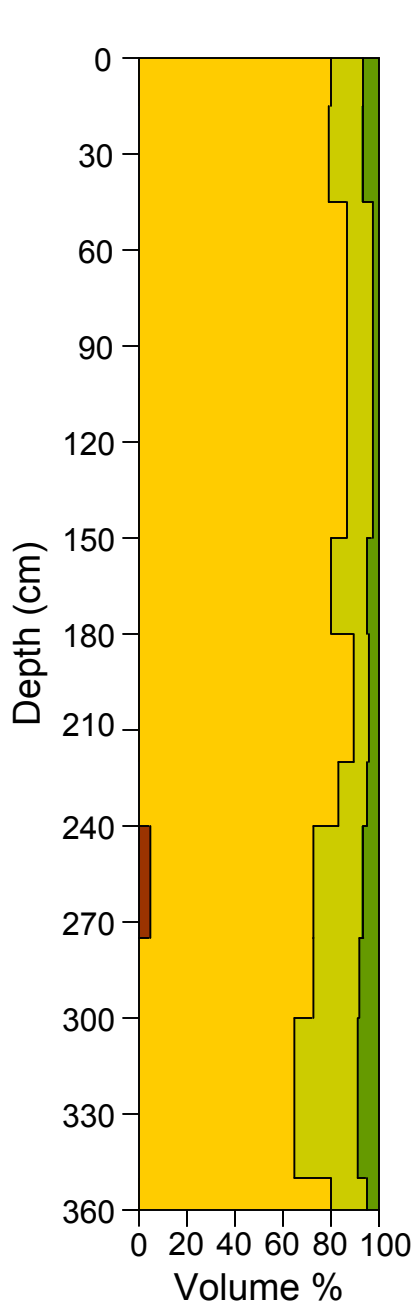
APPENDIX B:

TEPHRA ANALYSIS DATA

Oxide	ML2	ML3	ML4-1	ML4-2	ML4-3	1829C	2126A	2324A	2324A	2424A
SiO_2 (Wt%)	78.06	76.62	77.70	77.53	77.50	78.44	73.97	73.92	78.27	77.87
	(0.47)*	(0.0.21)	(0.27)	(0.40)	(0.30)	(0.45)	(0.58)	(0.31)	(0.39)	(0.46)
Al_2O_3	12.41	13.86	12.43	12.57	12.56	12.77	14.56	14.12	12.10	12.52
	(0.30)	(0.13)	(0.19)	(0.21)	(0.19)	(0.28)	(0.31)	(0.27)	(0.32)	(0.28)
Fe_2O_3	1.09	1.24	1.04	1.04	1.04	1.15	2.26	2.20	1.13	1.21
	(0.08)	(0.07)	(0.07)	(0.09)	(0.06)	(0.11)	(0.09)	(0.07)	(0.07)	(0.11)
TiO_2	0.21	0.14	0.22	0.21	0.21	0.22	0.47	0.46	0.22	0.22
	(0.02)	(0.02)	(0.02)	(0.02)	(0.03)	(0.02)	(0.02)	(0.03)	(0.01)	(0.01)
Na_2O	3.47	3.84	3.66	3.73	3.81	2.68	3.58	4.17	3.35	3.31
	(0.16)	(0.12)	(0.09)	(0.11)	(0.10)	(0.17)	(0.51)	(0.21)	(0.04)	(0.09)
K_2O	3.27	2.25	3.62	3.59	3.52	3.21	2.72	2.81	3.52	3.12
	(0.26)	(0.08)	(0.09)	(0.12)	(0.22)	(0.47)	(0.06)	(0.07)	(0.17)	(0.26)
MgO	0.22	0.32	0.19	0.20	0.19	0.23	0.49	0.48	0.25	0.28
	(0.05)	(0.03)	(0.04)	(0.04)	(0.06)	(0.05)	(0.03)	(0.03)	(0.09)	(0.04)
CaO	1.13	1.65	0.99	0.99	1.03	1.15	1.66	1.61	1.03	1.26
	(0.13)	(0.04)	(0.10)	(0.12)	(0.18)	(0.13)	(0.07)	(0.08)	(0.09)	(0.18)
Cl	0.15	0.09	0.15	0.14	0.14	0.15	0.20	0.23	0.13	0.21
	(0.03)	(0.03)	(0.03)	(0.03)	(0.02)	(0.04)	(0.02)	(0.03)	(0.02)	(0.06)
Total**	100	100	100	100	100	100	100	100	100	100
Number of Shards Analyzed	20	34	16	17	6	14	10	9	4	6
Tephra ID	Glacier Peak G[3]	MSH Sg[7]	Glacier Peak[4]	Glacier Peak[4]	Glacier Peak[4]	Glacier Peak G[5]	Mazama[1]	Mazama[2]	Glacier Peak[4]	Glacier Peak[6]
Similarity Coefficient***	0.97	0.97	0.98	0.98	0.98	0.95	0.96	0.98	0.96	0.97

* Standard deviations of the analyses given in parentheses
** Analyses normalized to 100 weight percent
*** Borchardt (1972)

92

Oxide	2432A-30	2432A-110	2529A	Mazama[1]	Glacier Peak G[3]	Glacier Peak[4]	Glacier Peak G[5]	Glacier Peak[6]	MSH Sg[7]	MSH So[8]
SiO$_2$ (Wt%)	77.62 (0.32)	77.27 (0.47)	77.65 (0.29)	73.08	78.48	77.71	77.73	77.39	76.78	77.42
Al$_2$O$_3$	12.76 (0.18)	13.32 (0.42)	12.74 (0.12)	14.55	11.93	12.42	13.05	12.95	13.82	13.25
Fe$_2$O$_3$	1.25 (0.10)	1.13 (0.24)	1.21 (0.11)	2.37	1.06	1.07	1.19	1.32	1.31	1.25
TiO$_2$	0.23 (0.02)	0.14 (0.06)	0.23 (0.02)	0.44	0.20	0.20	0.19	0.20	0.17	0.18
Na$_2$O	3.24 (0.15)	3.70 (0.44)	3.12 (0.14)	4.19	3.57	3.69	3.04	3.33	3.67	3.76
K$_2$O	3.32 (0.18)	2.60 (0.24)	3.27 (0.19)	2.71	3.28	3.51	3.17	3.15	2.24	2.31
MgO	0.28 (0.03)	0.30 (0.05)	0.27 (0.03)	0.49	0.23	0.19	0.27	0.25	0.32	0.28
CaO	1.21 (0.08)	1.42 (0.11)	1.22 (0.07)	1.70	1.21	1.06	1.21	1.27	1.58	1.42
Cl	0.18 (0.02)	0.12 (0.07)	0.20 (0.04)	0.18	n.d.	0.15	0.18	0.18	0.08	0.10
Total	100	100	100	100	100	100	100	100	100	100
Number of Shards Analyzed	10	9	14	29		25	25	30	22	22

Tephra ID	Glacier Peak[5]	MSH So[8]	Glacier Peak[5]
Similarity Coefficient****	0.97	0.95	0.97

[1] Mazama. Kearns Basin, MT; Foit et al. (1993)
[2] Mazama. Mirror Lake, ID; Betty Arens (unpublished)
[3] Glacier Peak G. Barnosky et al. (1989)
[4] Glacier Peak. East Wenatchee, WA; Foit et al. (1993)

[5] Glacier Peak G Std. Trinity Mine, WA; Foit et al. (1993)
[6] Glacier Peak. Lost Creek Pass, MT; Foit et al. (1993)
[7] MSH Sg. Yakima Valley, WA; Clague et al. (2003)
[8] MSH So. Walla Walla Valley, WA; Clague et al. (2003)

APPENDIX C:

XRF GEOCHEMICAL DATA

Unnormalized Major Elements (Weight %)

	Loess					Grand Coulee		Quincy Basin					
	1725D	2125A	2433A	2522A	2630A	NP4	SR2	1824D	1826A	1827D	1924B	1926A	2025C
SiO2	69.09	62.27	64.48	64.18	63.50	66.71	70.72	64.83	62.14	62.12	63.41	62.02	64.72
TiO2	0.825	0.772	0.803	0.703	0.794	0.603	0.519	1.236	1.469	1.695	1.246	1.090	1.283
Al2O3	12.50	15.42	14.67	15.73	15.56	12.10	12.51	12.97	12.58	12.57	13.21	14.84	12.87
FeO*	4.34	4.31	4.40	4.21	4.52	3.53	3.18	6.20	7.48	8.11	6.61	6.09	6.40
MnO	0.080	0.094	0.091	0.098	0.097	0.068	0.053	0.111	0.128	0.134	0.119	0.104	0.113
MgO	1.67	1.41	1.57	1.77	1.47	2.04	1.59	2.25	2.49	2.69	2.27	2.35	2.16
CaO	2.98	2.77	2.74	3.57	2.66	3.31	2.27	4.00	4.31	4.82	3.84	4.30	3.62
Na2O	2.54	2.70	2.58	3.08	2.57	1.83	1.78	2.45	2.37	2.39	2.30	2.82	2.28
K2O	1.86	1.81	2.14	1.78	2.02	3.02	3.31	2.10	2.25	2.04	2.09	1.75	2.18
P2O5	0.171	0.141	0.183	0.177	0.146	0.134	0.111	0.244	0.288	0.311	0.254	0.217	0.247
Sum	96.06	91.69	93.66	95.31	93.33	93.35	96.04	96.40	95.50	96.88	95.35	95.59	95.87

Normalized Major Elements (Weight %)

	Loess					Grand Coulee		Quincy Basin					
	1725D	2125A	2433A	2522A	2630A	NP4	SR2	1824D	1826A	1827D	1924B	1926A	2025C
SiO2	71.92	67.91	68.84	67.34	68.04	71.46	73.64	67.25	65.07	64.11	66.50	64.88	67.51
TiO2	0.859	0.842	0.857	0.737	0.851	0.646	0.540	1.282	1.539	1.750	1.306	1.140	1.338
Al2O3	13.01	16.81	15.66	16.50	16.67	12.96	13.03	13.46	13.18	12.98	13.85	15.53	13.42
FeO*	4.52	4.70	4.70	4.42	4.84	3.78	3.31	6.43	7.83	8.37	6.94	6.38	6.67
MnO	0.084	0.102	0.097	0.103	0.104	0.073	0.055	0.115	0.134	0.139	0.125	0.109	0.117
MgO	1.74	1.53	1.68	1.86	1.58	2.19	1.66	2.34	2.60	2.78	2.38	2.46	2.25
CaO	3.10	3.03	2.93	3.74	2.85	3.54	2.36	4.15	4.52	4.97	4.03	4.50	3.78
Na2O	2.64	2.94	2.75	3.23	2.76	1.96	1.85	2.54	2.48	2.47	2.41	2.95	2.38
K2O	1.94	1.97	2.29	1.87	2.16	3.24	3.44	2.18	2.35	2.11	2.19	1.83	2.27
P2O5	0.178	0.154	0.196	0.186	0.156	0.143	0.116	0.253	0.302	0.321	0.267	0.227	0.257
Total	100.00	100.00	100.00	100.00	100.00	100.00	100.00	100.00	100.00	100.00	100.00	100.00	100.00

*Major elements are normalized on a volatile-free basis, with total Fe expressed as FeO.

95

Unnormalized Trace Elements (ppm)

	Loess					Grand Coulee		Quincy Basin					
	1725D	2125A	2433A	2522A	2630A	NP4	SR2	1824D	1826A	1827D	1924B	1926A	2025C
Ni	24	23	26	24	26	16	17	15	16	15	20	21	17
Cr	47	44	47	45	51	35	36	35	37	35	40	43	41
Sc	12	12	12	12	13	10	11	18	22	24	19	17	18
V	95	88	88	91	91	75	63	165	201	230	165	144	167
Ba	566	649	646	663	684	685	719	649	638	638	649	583	625
Rb	59	62	73	57	77	122	132	70	75	65	73	63	77
Sr	364	381	350	505	376	294	290	367	319	325	334	450	339
Zr	329	240	292	251	282	190	185	217	226	214	241	224	281
Y	25	22	27	21	26	26	26	27	31	32	29	25	29
Nb	15.3	9.5	12.4	11.0	12.1	12.1	13.0	11.8	12.8	13.1	12.3	10.5	13.3
Ga	15	19	18	20	20	16	16	17	17	17	18	20	17
Cu	16	24	26	18	25	12	11	16	19	18	28	29	18
Zn	64	67	68	67	69	55	46	80	88	91	91	99	84
Pb	14	15	18	13	16	18	16	14	12	13	20	16	14
La	39	29	32	27	34	34	40	29	35	32	31	27	39
Ce	79	59	77	59	80	76	78	64	76	66	69	54	71
Th	9	7	10	6	9	10	9	8	8	6	6	6	8
Nd	34	27	33	28	34	33	35	32	35	32	31	25	34
U	5	3	2	2	2	5	2						
Bi	5	2	3	4	4	4	4						
Cs	7	5	5	6	8	6	7						
As	33	9	14	8	10	19	32						
sum tr.	1855	1797	1878	1936	1946	1752	1788	1833	1866	1866	1875	1856	1892

Normalized Trace Elements (ppm)

	Loess					Grand Coulee		Quincy Basin					
	1725D	2125A	2433A	2522A	2630A	NP4	SR2	1824D	1826A	1827D	1924B	1926A	2025C
NiO	30.7	29.4	32.7	30.3	33.0	20.5	22.1	19.5	20.2	19.0	25.7	26.3	22.0
Cr2O3	68.0	64.7	69.3	66.4	74.0	51.3	53.2	50.6	53.8	50.4	58.8	62.7	59.6
Sc2O3	17.8	18.7	17.8	17.6	19.5	15.6	16.1	27.8	33.7	36.7	29.6	26.4	27.9
V2O3	139.6	129.5	129.6	133.1	133.4	109.7	92.1	242.7	295.0	338.7	242.9	212.1	246.3
BaO	632.2	724.2	721.6	740.6	763.5	764.4	803.2	724.3	712.0	711.8	724.6	651.4	697.5
Rb2O	65.0	68.0	79.5	61.8	84.0	133.9	144.8	76.1	81.5	70.6	80.3	68.9	84.3
SrO	430.1	451.0	413.6	596.7	444.1	348.2	342.4	434.1	377.6	383.8	395.1	531.6	401.0
ZrO2	448.6	327.4	398.4	342.1	384.7	259.3	252.2	296.8	308.5	292.7	328.7	305.1	383.5
Y2O3	31.7	27.7	34.0	26.9	32.4	32.5	32.4	33.9	39.6	40.8	36.7	31.2	37.2
Nb2O5	21.9	13.6	17.7	15.7	17.3	17.3	18.6	16.9	18.3	18.7	17.6	15.0	19.0
Ga2O3	20.4	25.5	24.2	26.3	26.6	21.0	20.8	22.6	22.2	23.3	23.9	27.0	22.6
CuO	19.9	30.0	32.8	22.0	31.0	15.1	13.5	19.7	23.9	22.5	34.5	35.8	22.0
ZnO	80.3	84.2	85.3	84.3	85.8	69.1	58.1	99.7	110.1	114.4	114.0	124.1	104.8
PbO	15.0	15.6	19.2	14.2	17.3	19.5	17.1	15.1	13.2	14.2	21.1	17.7	15.0
La2O3	45.3	34.5	37.9	31.5	40.2	39.9	47.4	33.7	41.4	37.3	36.2	31.9	45.7
CeO2	97.2	72.2	94.5	72.8	98.6	92.8	95.6	78.7	92.8	81.5	84.2	66.9	87.6
ThO2	9.9	8.2	11.5	7.1	9.8	10.6	9.9	8.5	8.3	7.1	6.5	6.4	8.6
Nd2O3	40.1	31.7	38.4	32.8	40.1	38.4	40.5	37.6	41.3	37.6	35.7	28.6	39.3
U2O3	5.4	3.1	2.5	2.3	2.5	5.4	2.6						
Bi2O5	6.2	2.6	3.2	4.2	4.5	4.3	4.5						
Cs2O	6.9	5.4	4.8	5.9	8.0	6.7	7.8						
As2O5	50.5	13.7	20.9	12.4	15.6	29.8	49.7						
sum tr.	2219	2159	2260	2325	2338	2064	2083	2238	2293	2301	2296	2269	2324

97

APPENDIX D:

LOCATION AND GRAIN SIZE DATA

Site: **1723B**

Location (UTM): 11T 0276419, 5209368
Vegetation: Bunchgrass, Sage
Aspect/slope: Flat
Landscape: Top of Frenchman Hills

Depth (cm)	Mean grain size (Φ)	Clay %	Silt %	Sand %	Coarse %	Color
30	4.98	34.21	52.16	12.76	0.87	Dark yellowish brown
75	5.04	14.42	50.54	29.00	6.05	Light yellowish brown

Site: **1723D**

Location (UTM): 11T 0276298, 5204606
Vegetation: Bunchgrass
Aspect/slope: 160°/4°
Landscape: North slope Frenchman Hills

Depth (cm)	Mean grain size (Φ)	Clay %	Silt %	Sand %	Coarse %	Color
30	3.33	6.04	21.72	68.53	3.71	Grayish brown

Site: **1724A**

Location (UTM): 11T 0281300, 5209310
Vegetation: Orchard, Grass
Aspect/slope: 30°/4°
Landscape: North slope Frenchman Hills

Depth (cm)	Mean grain size (Φ)	Clay %	Silt %	Sand %	Coarse %	Color
30	5.23	13.85	57.00	27.99	1.17	Dark yellowish brown
105	4.91	11.09	56.78	28.23	3.90	Brownish yellow
210	4.30	8.27	40.99	50.75	0.00	Light yellowish brown
240	5.43	22.01	34.23	43.77	0.00	Light gray

Site: **1725A**

Location (UTM): 11T 0290938
Vegetation: Sage, Short grasses
Aspect/slope: Flat
Landscape: Sand sheet

Depth (cm)	Mean grain size (Φ)	Clay %	Silt %	Sand %	Coarse %	Color
30	3.04	4.08	13.96	81.96	0.00	Grayish brown
230	5.23	13.01	62.00	24.58	0.41	Olive gray

Site: 1725B
Location (UTM): 11T 0295858, 5208632
Vegetation: Sage, Short grasses
Aspect/slope: Flat
Landscape: Sand sheet

Depth (cm):	Mean grain size (Φ):	Clay %:	Silt %:	Sand %:	Coarse %:	Color:
30	2.58	2.24	8.42	89.34	0.00	Dark olive

Site: 1725D
Location (UTM): 11T 0295705, 5203863
Vegetation: Wheat
Aspect/slope: 0°/5°
Landscape: Draw on north facing slope

Depth (cm):	Mean grain size (Φ):	Clay %:	Silt %:	Sand %:	Coarse %:	Color:
30	4.39	8.84	40.52	50.64	0.00	Brown
80	3.77	5.95	32.62	61.43	0.00	Brown
115	4.63	14.47	30.70	54.83	0.00	Brown

Site: 1726A
Location (UTM): 11T 0300746, 5208663
Vegetation: Sage, Willows
Aspect/slope: Flat
Landscape: Sand dunes

Depth (cm):	Mean grain size (Φ):	Clay %:	Silt %:	Sand %:	Coarse %:	Color:
30	2.92	5.55	17.63	76.74	0.09	Dark olive gray
135	1.39	2.57	4.47	78.16	14.80	Black

Site: 1726B
Location (UTM): 11T 0305543, 5208266
Vegetation: Sage, Bunchgrass
Aspect/slope: Flat
Landscape: Sand sheet

Depth (cm):	Mean grain size (Φ):	Clay %:	Silt %:	Sand %:	Coarse %:	Color:
30	2.95	3.65	14.88	80.10	1.37	Dark olive
150	2.31	2.52	5.32	82.62	9.54	Dark olive
230	1.39	2.97	2.03	83.09	11.90	Black

Site: 1727D
Location (UTM): 11T 0315143
Vegetation: Wheat
Landscape: Frenchman Hills
Aspect/slope: 0°/2°

Depth (cm)	Mean grain size (Φ)	Clay %	Silt %	Sand %	Coarse %	Color
30	4.49	11.47	41.14	46.53	0.86	Brown
70	4.71	12.32	48.06	38.18	1.45	Brown

Site: 1823B
Location (UTM): 11T 0276910, 5219054
Vegetation: Potatoes
Landscape: Very low broad hills
Aspect/slope: 0°/2°

Depth (cm)	Mean grain size (Φ)	Clay %	Silt %	Sand %	Coarse %	Color
30	4.45	10.67	41.64	45.33	2.37	Brown
130	5.36	19.06	46.20	33.26	1.48	Brown

Site: 1823D
Location (UTM): 11T 0276644, 5214253
Vegetation: Sage, Bunchgrass
Landscape: Scabland
Aspect/slope: Flat

Depth (cm)	Mean grain size (Φ)	Clay %	Silt %	Sand %	Coarse %	Color
30	4.62	12.90	47.32	27.81	11.97	Yellowish brown

Site: 1824A
Location (UTM): 11T 0281790, 5218919
Vegetation: Hay
Landscape: Flat
Aspect/slope: Flat

Depth (cm)	Mean grain size (Φ)	Clay %	Silt %	Sand %	Coarse %	Color
30	5.21	15.40	52.56	26.86	5.19	Dark yellowish brown

Site: 1824B

Location (UTM): Vegetation: Landscape: Aspect/slope:
11T 0286612, 5218883 Hay Flat Flat

Depth (cm):	Mean grain size (Φ):	Clay %	Silt %	Sand %	Coarse %	Color:
30	4.49	11.49	39.60	44.61	4.29	Brown
115	2.66	6.49	24.46	50.97	18.08	Dark grayish brown
155	0.54	2.61	6.43	35.50	55.46	Olive gray

Site: 1824C

Location (UTM): Vegetation: Landscape: Aspect/slope:
11T 0281521, 5214116 Short grasses Flat Flat

Depth (cm):	Mean grain size (Φ):	Clay %	Silt %	Sand %	Coarse %	Color:
30	4.96	12.93	50.14	36.49	0.44	Dark yellowish brown

Site: 1824D

Location (UTM): Vegetation: Landscape: Aspect/slope:
11T 0286266, 5213930 Hay Flat Flat

Depth (cm):	Mean grain size (Φ):	Clay %	Silt %	Sand %	Coarse %	Color:
30	3.83	8.16	25.39	65.63	0.81	Dark brown
75	3.95	10.69	29.87	50.32	9.13	Very dark grayish brown

Site: 1825A

Location (UTM): Vegetation: Landscape: Aspect/slope:
11T 0291267, 5218647 Wheat Very low hills 90°/6°

Depth (cm):	Mean grain size (Φ):	Clay %	Silt %	Sand %	Coarse %	Color:
30	4.09	11.14	27.67	60.08	1.11	Dark yellowish brown
80	4.81	20.23	41.29	24.63	13.85	Brown
140	0.91	3.46	9.16	41.16	46.22	Pale olive

Site: 1825B
Location (UTM): 11T 0296370, 5218588
Vegetation: Sage, Short grasses
Aspect/slope: Flat
Landscape: Sand sheet

Depth (cm):	Mean grain size (Φ):	Clay %:	Silt %:	Sand %:	Coarse %:	Color:
30	4.53	15.23	30.52	53.39	0.85	Dark brown

Site: 1825D
Location (UTM): 11T 0296071, 5213658
Vegetation: Sage, Short grasses
Aspect/slope: Flat
Landscape: Interdune

Depth (cm):	Mean grain size (Φ):	Clay %:	Silt %:	Sand %:	Coarse %:	Color:
30	3.63	10.60	24.82	62.94	1.64	Dark brown
150	2.08	3.55	5.84	88.57	2.05	Very dark gray
330	2.10	2.59	3.86	89.98	3.57	Very dark gray
400	1.51	3.92	5.94	71.10	19.04	Very dark grey

Site: 1826A
Location (UTM): 11T 0301215, 5218373
Vegetation: Reeds
Aspect/slope: Flat
Landscape: Interdune

Depth (cm):	Mean grain size (Φ):	Clay %:	Silt %:	Sand %:	Coarse %:	Color:
30	4.64	16.74	29.29	51.35	2.61	Very dark brown

Site: 1826B
Location (UTM): 11T0305984, 5218237
Vegetation: Sage, Short grasses
Aspect/slope: Flat
Landscape: Sand dunes

Depth (cm):	Mean grain size (Φ):	Clay %:	Silt %:	Sand %:	Coarse %:	Color:
30	4.61	15.46	33.00	49.07	2.47	Dark grayish brown
100	0.44	4.20	6.29	28.80	60.71	Dark gray

Site: **1826D**

Location (UTM): 11T 0305786, 5213352
Vegetation: Sage, Bunchgrass
Landscape: Sand sheet/dunes
Aspect/slope: Flat

Depth (cm):	Mean grain size (Φ):	Clay %:	Silt %:	Sand %:	Coarse %:	Color:
30	3.00	4.32	16.00	78.21	1.47	Olive
90	2.88	7.82	24.39	51.40	16.39	Light olive gray
140	2.35	4.58	13.76	79.18	2.49	Dark olive

Site: **1827A**

Location (UTM): 11T 0310828, 5218086
Vegetation: Sage, Short grasses
Landscape: Interdune
Aspect/slope: Flat

Depth (cm):	Mean grain size (Φ):	Clay %:	Silt %:	Sand %:	Coarse %:	Color:
30	3.73	10.14	26.49	60.86	2.51	Dark grayish brown
120	2.46	8.20	20.37	48.12	23.31	Dark grayish brown

Site: **1827D**

Location (UTM): 11T 0315231, 5212851
Vegetation: Sage, Bunchgrass
Landscape: Dunes
Aspect/slope: 170°/10°

Depth (cm):	Mean grain size (Φ):	Clay %:	Silt %:	Sand %:	Coarse %:	Color:
10	2.57	8.07	8.28	75.73	7.91	Light olive gray

Site: **1829C**

Location (UTM): 11T 0330095, 5212336
Vegetation: Corn
Landscape: Sand sheet
Aspect/slope: Flat

Depth (cm):	Mean grain size (Φ):	Clay %:	Silt %:	Sand %:	Coarse %:	Color:
30	3.72	13.58	33.59	36.02	16.81	Olive brown
120	3.86	10.92	35.14	40.66	13.30	Light yellowish brown
180	2.44	8.70	20.64	43.45	27.21	Light brownish gray

Site: 1923B
Location (UTM): 11T 0277228, 5228806
Vegetation: Fallow
Landscape: Flat
Aspect/slope: Flat

Depth (cm)	Mean grain size (Φ)	Clay %	Silt %	Sand %	Coarse %	Color
30	5.62	17.85	58.99	23.16	0.00	Yellowish brown
90	5.19	14.29	55.20	30.51	0.00	Yellowish brown
150	4.98	13.66	50.19	36.15	0.00	Light yellowish brown
205	5.54	21.71	40.07	38.23	0.00	Light gray

Site: 1924A
Location (UTM): 11T 0282165, 5228760
Vegetation: Hay
Landscape: Flat
Aspect/slope: Flat

Depth (cm)	Mean grain size (Φ)	Clay %	Silt %	Sand %	Coarse %	Color
30	4.42	12.47	35.85	45.94	5.74	Dark yellowish brown
75	4.42	11.10	40.99	39.36	8.54	Dark brown

Site: 1924B
Location (UTM): 11T 0286997, 5228571
Vegetation: Grain corn
Landscape: Flat
Aspect/slope: Flat

Depth (cm)	Mean grain size (Φ)	Clay %	Silt %	Sand %	Coarse %	Color
30	4.43	13.41	36.26	49.52	0.80	Dark brown
110	2.09	4.55	6.29	87.67	1.49	Dark olive gray
210	0.59	2.35	6.34	21.48	69.83	Dark brown

Site: 1924C
Location (UTM): 11T 0281917, 5223852
Vegetation: Sage, Bunchgrass
Landscape: Scabland
Aspect/slope: Flat

Depth (cm)	Mean grain size (Φ)	Clay %	Silt %	Sand %	Coarse %	Color
30	4.90	16.35	47.19	27.77	8.70	Yellowish brown

Site: **1925B**

Location (UTM): 11T 0296650, 5228234
Vegetation: Not vegetated
Landscape: Dunes
Aspect/slope: Flat

Depth (cm)	Mean grain size (Φ)	Clay %	Silt %	Sand %	Coarse %	Color
30	3.48	7.56	20.25	71.89	0.29	Olive
90	2.47	3.31	3.95	89.25	3.50	Olive
200	2.81	2.85	8.15	86.35	2.65	Olive gray
220	3.77	4.77	33.55	61.49	0.19	Brown
270	5.17	16.44	51.70	26.38		Dark brown
310	4.73	9.90	54.64	35.09	0.37	Dark brown

Site: **1925D**

Location (UTM): 11T 0296596, 5223656
Vegetation: Short grasses
Landscape: Sand sheet
Aspect/slope: Flat

Depth (cm)	Mean grain size (Φ)	Clay %	Silt %	Sand %	Coarse %	Color
30	4.75	15.04	41.12	42.35	1.49	Dark brown
150	2.30	5.20	16.28	61.40	17.12	Very dark grayish brown
215	-0.26	1.35	1.47	22.93	74.25	Black
360	1.03	3.87	5.74	66.27	24.12	Very dark gray
420	-0.27	0.60	1.06	25.62	72.71	Black

Site: **1926A**

Location (UTM): 11T 0301580, 5228152
Vegetation: Short grasses
Landscape: Flat
Aspect/slope: Flat

Depth (cm)	Mean grain size (Φ)	Clay %	Silt %	Sand %	Coarse %	Color
30	2.84	9.98	27.58	30.24	32.20	Yellowish brown

Site: 1926C

Location (UTM): 11T 0301340, 5223273
Vegetation: Hay
Aspect/slope: 10°/2°
Landscape: Low hills, Dunes

Depth (cm):	Mean grain size (Φ):	Clay %	Silt %	Sand %	Coarse %	Color:
30	4.39	16.86	47.90	25.90	9.33	Dark yellowish brown
90	1.11	4.00	12.59	33.40	50.01	Very dark gray
110	-0.30	1.32	3.36	27.26	68.05	Black
330	0.08	1.49	2.21	35.62	60.67	Black

Site: 1926D

Location (UTM): 11T 0306177, 5223140
Vegetation: Wheat
Aspect/slope: Flat
Landscape: Flat

Depth (cm):	Mean grain size (Φ):	Clay %	Silt %	Sand %	Coarse %	Color:
30	4.45	12.69	35.92	48.98	2.41	Dark grayish brown
80	4.25	11.32	40.40	39.87	8.41	Olive
120	2.90	8.19	26.86	46.66	18.29	Olive gray

Site: 1930C

Location (UTM): 11T 0340143, 5221737
Vegetation: Corn
Aspect/slope: 90°/2°
Landscape: Very low hills

Depth (cm):	Mean grain size (Φ):	Clay %	Silt %	Sand %	Coarse %	Color:
30	5.65	17.51	61.10	21.30	0.09	Brown
90	5.55	15.00	67.50	17.45	0.05	Brown
120	5.77	16.37	70.12	13.35	0.16	Very pale brown
210	5.61	17.48	60.17	22.17	0.18	Pale brown

Site: **1931A**

Location (UTM): 11T 0349902, 5226427
Vegetation: Bunchgrass
Landscape: Slope of coulee
Aspect/slope: 50°/20°

Depth (cm):	Mean grain size (Φ):	Clay %	Silt %	Sand %	Coarse %	Color:
30	2.34	15.00	54.42	30.58	0.00	Yellowish brown

Site: **2023D**

Location (UTM): 11T 0277431, 5233633
Vegetation: Lima beans
Landscape: Flat
Aspect/slope: Flat

Depth (cm):	Mean grain size (Φ):	Clay %	Silt %	Sand %	Coarse %	Color:
30	5.80	17.40	67.34	13.01	2.25	Dark yellowish brown
100	4.36	15.32	25.86	58.82	0.00	Dark brown
265	4.69	11.07	47.25	41.68	0.00	Dark yellowish brown
320	5.10	14.16	53.16	32.69	0.00	Brown
340	5.29	19.00	38.60	42.40	0.00	Light gray

Site: **2024A**

Location (UTM): 11T 0282503, 5238395
Vegetation: Carrots
Landscape: Flat (toe of Beasley Hills)
Aspect/slope: Flat

Depth (cm):	Mean grain size (Φ):	Clay %	Silt %	Sand %	Coarse %	Color:
30	5.53	17.17	58.60	23.85	0.37	Dark yellowish brown
120	5.11	13.71	55.69	24.53	6.07	Yellowish brown
200	4.36	8.50	47.02	40.95	3.53	Yellowish brown

Site: **2024C**
Location (UTM): 11T 0282299, 5233542
Vegetation: Fallow
Aspect/slope: Flat
Landscape: Flat

Depth (cm):	Mean grain size (Φ):	Clay %	Silt %	Sand %	Coarse %	Color:
30	5.60	18.89	55.11	25.54	0.45	Dark yellowish brown
90	5.06	14.72	50.98	28.11	6.19	Yellowish brown

Site: **2024D**
Location (UTM): 11T 0287182, 5233410
Vegetation: Potatoes
Aspect/slope: Flat
Landscape: Flat

Depth (cm):	Mean grain size (Φ):	Clay %	Silt %	Sand %	Coarse %	Color:
30	3.77	13.08	37.84	31.83	17.26	Dark brown
45	4.52	11.17	40.19	47.49	1.16	Dark brown
170	5.46	15.35	62.92	21.64	0.09	Brown
280	4.97	16.54	41.13	41.98	0.36	Brown

Site: **2025C**
Location (UTM): 11T 0292096, 5233229
Vegetation: Wheat
Aspect/slope: Flat
Landscape: Flat

Depth (cm):	Mean grain size (Φ):	Clay %	Silt %	Sand %	Coarse %	Color:
30	3.58	9.54	23.15	66.92	0.04	Brown
120	2.92	10.37	27.08	41.47	21.08	Light brownish gray

Site: **2025D**
Location (UTM): 11T 0296928, 5233095
Vegetation: Hay
Aspect/slope: Flat
Landscape: Flat

Depth (cm):	Mean grain size (Φ):	Clay %	Silt %	Sand %	Coarse %	Color:
30	5.27	18.04	50.78	26.04	5.14	Dark yellowish brown

Site: **2026A**

Location (UTM): 11T 0301874, 5238128
Vegetation: Hay
Aspect/slope: 220°/3°
Landscape: Toe slope of Beasley Hills
Color: Dark yellowish brown / Dark brown

Depth (cm):	Mean grain size (Φ):	Clay %	Silt %	Sand %	Coarse %
30	5.60	17.84	58.65	23.42	0.09
110	5.52	18.32	55.87	21.21	4.59

Site: **2026C**

Location (UTM): 11T 0301796, 5233004
Vegetation: Hay
Aspect/slope: Flat
Landscape: Flat
Color: Yellowish brown

Depth (cm):	Mean grain size (Φ):	Clay %	Silt %	Sand %	Coarse %
15	4.14	15.31	46.33	17.82	20.54

Site: **2027B**

Location (UTM): 11T 0316473, 5237866
Vegetation: Bunchgrass, Sage
Aspect/slope: Flat
Landscape: Alluvial fan
Color: Very dark grayish brown

Depth (cm):	Mean grain size (Φ):	Clay %	Silt %	Sand %	Coarse %
10	5.23	17.25	51.35	23.79	7.62

Site: **2028B**

Location (UTM): 11T 0326110, 5237186
Vegetation: Sage, Short grasses
Aspect/slope: Flat
Landscape: Low ridges trending N/S
Color: Brown / Brown

Depth (cm):	Mean grain size (Φ):	Clay %	Silt %	Sand %	Coarse %
30	5.53	20.38	50.00	24.94	4.68
60	5.24	21.97	45.15	20.60	12.28

Site: 2029D

Location (UTM): 11T 0335555, 5231663
Vegetation: Short grasses
Landscape: Draw
Aspect/slope: Flat

Depth (cm)	Mean grain size (Φ)	Clay %	Silt %	Sand %	Coarse %	Color
30	3.61	13.07	36.13	19.10	31.70	Dark brown

Site: 2030A

Location (UTM): 11T 0340626, 5236407
Vegetation: Bunchgrass
Landscape: Low rolling hills
Aspect/slope: 100°/3°

Depth (cm)	Mean grain size (Φ)	Clay %	Silt %	Sand %	Coarse %	Color
30	5.83	20.15	58.37	21.41	0.08	Yellowish brown
90	5.72	17.06	64.90	17.98	0.06	Light yellowish brown
150	5.31	13.90	61.57	24.54	0.00	Pale brown

Site: 2125A

Location (UTM): 11T 0292500, 5247959
Vegetation: Bunchgrass
Landscape: High rolling hills
Aspect/slope: 20°/12°

Depth (cm)	Mean grain size (Φ)	Clay %	Silt %	Sand %	Coarse %	Color
30	5.48	14.21	63.33	22.36	0.10	Yellowish brown
75	6.68	30.97	56.65	12.33	0.06	Pale brown
135	4.48	20.66	45.91	16.26	17.17	Pale brown

Site: 2126A

Location (UTM): 11T 0302239, 5247765

Vegetation: Short grasses

Landscape: Rolling hills

Aspect/slope: 100°/2°

Depth (cm):	Mean grain size (Φ):	Clay %	Silt %	Sand %	Coarse %	Color:
30	5.61	16.63	61.70	21.59	0.09	Dark yellowish brown
125	5.96	20.68	61.00	18.32	0.00	Dark yellowish brown
170	6.06	20.46	65.86	13.68	0.00	Yellowish brown
220	4.92	15.39	46.86	37.49	0.25	Yellowish brown

Site: 2127D

Location (UTM): 11T 0316595, 5242611

Vegetation: Bunchgrass, Few sage

Landscape: Alluvial fan

Aspect/slope: Flat

Depth (cm):	Mean grain size (Φ):	Clay %	Silt %	Sand %	Coarse %	Color:
10	4.28	18.50	38.27	23.92	19.31	Very dark grayish brown

Site: 2225A

Location (UTM): 11T 0292841, 5257660

Vegetation: Sage, Bunchgrass

Landscape: Low hills

Aspect/slope: Flat

Depth (cm):	Mean grain size (Φ):	Clay %	Silt %	Sand %	Coarse %	Color:
10	4.35	15.99	52.99	14.66	16.35	Brown

Site: 2229C

Location (UTM): 11T 0331381, 5221418

Vegetation: Bunchgrass

Landscape: Very low rolling hills

Aspect/slope: 110°/5°

Depth (cm):	Mean grain size (Φ):	Clay %	Silt %	Sand %	Coarse %	Color:
30	5.46	15.37	59.85	24.27	0.15	Brown
80	6.24	20.09	73.67	6.24	0.00	Light yellowish brown
120	5.60	17.46	59.54	23.00	0.00	Light yellowish brown

Site: 2231A
Location (UTM): 11T 0350853, 5255622
Vegetation: Sage, Bunchgrass
Aspect/slope: Flat
Landscape: Rim of coulee

Depth (cm):	Mean grain size (Φ):	Clay %:	Silt %:	Sand %:	Coarse %:	Color:
15	5.55	21.24	51.33	19.23	8.20	Dark yellowish brown

Site: 2232A
Location (UTM): 11T0360515, 5255218
Vegetation: Bunchgrass, Sparse sage
Aspect/slope: 160°/12°
Landscape: Terrace of coulee

Depth (cm):	Mean grain size (Φ):	Clay %:	Silt %:	Sand %:	Coarse %:	Color:
30	5.65	18.04	58.90	19.53	3.54	Brown

Site: 2324A
Location (UTM): 11T 0283507, 5267483
Vegetation: Wheat fallow
Aspect/slope: 225°/10°
Landscape: High rolling hills

Depth (cm):	Mean grain size (Φ):	Clay %:	Silt %:	Sand %:	Coarse %:	Color:
30	5.56	16.33	62.19	21.02	0.45	Yellowish brown
60	6.17	24.71	56.33	12.55	6.41	Light yellowish brown

Site: 2326A
Location (UTM): 11T 0302824, 5267084
Vegetation: Sage, Bunchgrass
Aspect/slope: 15°/8°
Landscape: Rolling hills

Depth (cm):	Mean grain size (Φ):	Clay %:	Silt %:	Sand %:	Coarse %:	Color:
30	5.96	17.16	71.08	10.85	0.90	Yellowish brown

Site: 2331A

Location (UTM): 11T 0351104, 5265321
Vegetation: Bunchgrass
Landscape: Rolling hills
Aspect/slope: 270°/4°

Depth (cm)	Mean grain size (Φ)	Clay %	Silt %	Sand %	Coarse %	Color
30	5.84	17.84	66.07	15.93	0.16	Yellowish brown
60	6.07	22.13	61.91	15.80	0.15	Yellowish brown

Site: 2332A

Location (UTM): 11T 0360774, 5264939
Vegetation: Wheat
Landscape: Rolling hills
Aspect/slope: 190°/6°

Depth (cm)	Mean grain size (Φ)	Clay %	Silt %	Sand %	Coarse %	Color
30	5.60	15.27	65.31	19.12	0.29	Brown
90	6.16	21.99	66.07	11.85	0.09	Yellowish brown
150	6.19	22.53	65.23	12.16	0.08	Yellowish brown

Site: 2334A

Location (UTM): 11T 0380137, 5264389
Vegetation: Sage, Bunchgrass
Landscape: Scabland
Aspect/slope: Flat

Depth (cm)	Mean grain size (Φ)	Clay %	Silt %	Sand %	Coarse %	Color
25	4.10	14.50	46.89	11.15	27.46	Dark yellowish brown

Site: 2424A

Location (UTM): 11T 0283821, 5277225
Vegetation: Bunchgrass
Landscape: Low rolling hills
Aspect/slope: 320°/1°

Depth (cm)	Mean grain size (Φ)	Clay %	Silt %	Sand %	Coarse %	Color
30	4.65	9.67	55.13	33.88	1.32	Yellowish brown
40	6.59	32.24	48.57	19.19	0.00	Yellowish brown

Site: 2425A

Location (UTM): 11T 0293404, 5276929
Vegetation: Wheat
Aspect/slope: 110°/4°
Landscape: Very low hills

Depth (cm):	Mean grain size (Φ):	Clay %	Silt %	Sand %	Coarse %	Color:
30	5.49	14.5	63.24	21.85	0.41	Dark yellowish brown
50	5.81	25.12	45.21	29.67	0.00	Light yellowish brown
75	6.22	26.43	54.48	19.09	0.00	Brownish yellow
100	4.24	17.91	42.82	20.58	18.69	Brownish yellow

Site: 2427A

Location (UTM): 11T 0312893, 5276258
Vegetation: Grasses
Aspect/slope: Flat
Landscape: Low rolling hills

Depth (cm):	Mean grain size (Φ):	Clay %	Silt %	Sand %	Coarse %	Color:
30	6.53	25.22	62.04	12.14	0.60	Dark brown
100	6.47	34.34	46.23	18.53	0.90	Brown
135	6.89	45.06	37.04	17.71	0.19	Dark gray

Site: 2429A

Location (UTM): 11T 0332074, 5275656
Vegetation: Bunchgrass
Aspect/slope: Flat
Landscape: Scabland

Depth (cm):	Mean grain size (Φ):	Clay %	Silt %	Sand %	Coarse %	Color:
15	3.06	12.30	35.45	2.60	49.64	Dark brown

Site: 2429B

Location (UTM): 11T 0336885, 5275509
Vegetation: Bunchgrass
Aspect/slope: 180°/2°
Landscape: Very low hills

Depth (cm):	Mean grain size (Φ):	Clay %	Silt %	Sand %	Coarse %	Color:
30	4.71	11.85	55.38	20.18	12.60	Dark yellowish brown
70	2.88	27.13	26.87	36.35	27.13	Dark yellowish brown

Site: 2430A

Location (UTM): 11T 0341708, 5275337
Vegetation: Wheat
Landscape: Low hills
Aspect/slope: 0°/4°

Depth (cm)	Mean grain size (Φ)	Clay %	Silt %	Sand %	Coarse %	Color
30	5.67	15.08	67.67	17.25	0.00	Dark yellowish brown
140	5.76	16.68	67.34	15.98	0.00	Yellowish brown
170	5.94	17.85	69.54	12.61	0.00	Yellowish brown
200	6.10	20.08	67.27	12.64	0.00	Yellowish brown
250	5.78	18.00	64.03	17.97	0.00	Yellowish brown
295	6.23	22.13	68.47	9.39	0.00	Dark yellowish brown
305	5.96	18.95	66.24	14.81	0.00	Light yellowish brown

Site: 2432A

Location (UTM): 11T 0361026, 5274811
Vegetation: Bunchgrass
Landscape: Low hills
Aspect/slope: 170°/1°

Depth (cm)	Mean grain size (Φ)	Clay %	Silt %	Sand %	Coarse %	Color
30	6.30	21.25	68.27	10.47	0.00	Dark yellowish brown
80	6.39	25.65	62.96	11.39	0.00	Light yellowish brown
110	6.35	23.42	67.12	9.47	0.00	Yellowish brown
180	6.39	24.14	67.54	8.32	0.00	Yellowish brown
255	6.33	29.21	51.20	19.42	0.17	Yellowish brown

Site: 2433A

Location (UTM):
Vegetation: Bunchgrass
Landscape: Low hills
Aspect/slope: 150°/5°

Depth (cm)	Mean grain size (Φ)	Clay %	Silt %	Sand %	Coarse %	Color
30	5.42	11.09	71.04	17.87	0.00	Dark yellowish brown
75	6.37	26.29	59.46	14.26	0.00	Yellowish brown
100	6.33	24.09	64.67	11.24	0.00	Light yellowish brown
130	6.31	24.35	61.93	13.72	0.00	Light yellowish brown
200	5.76	18.33	63.11	18.56	0.00	Brownish yellow

Site: **2434A**

Location (UTM): 11T 0380390, 5274479
Vegetation: Sage, Bunchgrass
Aspect/slope: Flat
Landscape: Scabland

Depth (cm):	Mean grain size (Φ):	Clay %:	Silt %:	Sand %:	Coarse %:	Color:
30	4.09	12.72	50.35	7.96	28.96	Dark yellowish brown

Site: **2522A**

Location (UTM): 10T 0714835, 5286944
Vegetation: Wheat
Aspect/slope: Flat
Landscape: Rolling hills

Depth (cm):	Mean grain size (Φ):	Clay %:	Silt %:	Sand %:	Coarse %:	Color:
30	5.63	18.00	59.18	22.63	0.19	Dark yellowish brown
100	5.24	15.55	52.74	31.71	0.00	Yellowish brown
300	5.70	23.08	50.03	26.89	0.00	Yellowish brown
400	5.32	18.17	51.12	30.70	0.00	Yellowish brown

Site: **2523A**

Location (UTM): 10T 0724526, 5287259
Vegetation: Wheat fallow
Aspect/slope: 45°/3°
Landscape: High rolling hills

Depth (cm):	Mean grain size (Φ):	Clay %:	Silt %:	Sand %:	Coarse %:	Color:
30	5.23	14.98	55.01	28.07	1.94	Dark brown
75	5.12	14.99	51.99	33.02	0.00	Pale brown
80	4.95	14.55	48.88	36.57	0.00	Yellowish brown
170	5.22	15.93	50.91	33.16	0.00	Dark yellowish brown
230	5.01	13.80	50.04	36.16	0.00	Light yellowish brown

Site: 2524A
Location (UTM): 11T 0284073, 5286924
Vegetation: Short grasses
Landscape: Flat
Aspect/slope: Flat

Depth (cm)	Mean grain size (Φ)	Clay %	Silt %	Sand %	Coarse %	Color
30	5.11	11.06	60.06	28.69	0.18	Dark brown
60	5.01	16.49	49.01	33.70	0.79	Yellowish brown

Site: 2527A
Location (UTM): 11T 0313090, 5285913
Vegetation: Wheat fallow
Landscape: Rolling hills
Aspect/slope: 305°/5°

Depth (cm)	Mean grain size (Φ)	Clay %	Silt %	Sand %	Coarse %	Color
30	4.33	12.95	50.19	22.07	14.79	Very dark grayish brown

Site: 2528A
Location (UTM): 11T 0322699, 5285557
Vegetation: Bunchgrass
Landscape: Low rolling hills
Aspect/slope: Flat

Depth (cm)	Mean grain size (Φ)	Clay %	Silt %	Sand %	Coarse %	Color
30	5.17	14.88	56.67	22.89	5.56	Dark brown
60	5.48	22.24	49.19	22.12	6.45	Dark brown

Site: 2529A
Location (UTM): 11T 0332364, 5285298
Vegetation: Wheat
Landscape: Rolling hills
Aspect/slope: 350°/4°

Depth (cm)	Mean grain size (Φ)	Clay %	Silt %	Sand %	Coarse %	Color
30	5.69	13.16	71.64	15.10	0.10	Dark yellowish brown
100	5.79	21.63	56.34	22.02	0.00	Yellowish brown
140	6.08	21.11	65.42	13.38	0.09	Yellowish brown
170	5.43	17.45	55.84	26.70	0.00	Light yellowish brown

Site: 2529B

Location (UTM): 11T 0337189, 5285124
Vegetation: Wheat fallow
Landscape: Rolling hills
Aspect/slope: 220°/5°

Depth (cm)	Mean grain size (Φ)	Clay %	Silt %	Sand %	Coarse %	Color
30	6.08	17.63	72.39	9.98	0.00	Dark yellowish brown
120	6.15	24.70	58.01	17.29	0.00	Yellowish brown
195	6.22	25.19	59.75	15.06	0.00	Yellowish brown

Site: 2529D

Location: 11T 0337019, 5280322
Vegetation: Wheat
Landscape: Very low hills
Aspect/slope: Flat

Depth (cm)	Mean grain size (Φ)	Clay %	Silt %	Sand %	Coarse %	Color
30	3.39	11.35	31.85	44.89	11.93	Brown

Site: 2530A

Location (UTM): 11T 0342018, 5285042
Vegetation: Wheat fallow
Landscape: Rolling Hills
Aspect/slope: Flat

Depth (cm)	Mean grain size (Φ)	Clay %	Silt %	Sand %	Coarse %	Color
30	5.17	12.23	59.85	26.30	1.62	Dark yellowish brown
130	6.13	22.88	61.58	15.14	0.40	Yellowish brown
150	6.12	22.10	62.69	15.03	0.18	Yellowish brown
195	5.76	22.73	53.91	16.64	6.72	Yellowish brown

Site: **2530C**

Location (UTM): 11T 0341847, 5280187
Vegetation: Wheat fallow
Landscape: Low hills
Aspect/slope: Flat

Depth (cm):	Mean grain size (Φ):	Clay %	Silt %	Sand %	Coarse %	Color:
30	5.66	14.40	69.10	16.33	0.18	Dark brown
120	5.93	19.94	62.17	17.21	0.68	Yellowish brown
250	4.32	13.17	42.85	43.98	0.00	Dark yellowish brown
285	5.61	19.62	56.67	23.71	0.00	Olive
330	5.60	21.89	50.86	26.63	0.62	Olive

Site: **2531A**

Location (UTM): 11T 0351739, 5284728
Vegetation: Wheat
Landscape: Low rolling hills
Aspect/slope: Flat

Depth (cm):	Mean grain size (Φ):	Clay %	Silt %	Sand %	Coarse %	Color:
30	6.19	18.36	76.85	4.79	0.00	Dark yellowish brown
80	6.81	31.04	59.84	9.12	0.00	Yellowish brown
140	6.77	34.01	53.76	12.23	0.00	Light yellowish brown

Site: **2533A**

Location (UTM): 11T0370795, 5284354
Vegetation: Sage, Short grasses
Landscape: Scabland
Aspect/slope: Flat

Depth (cm):	Mean grain size (Φ):	Clay %	Silt %	Sand %	Coarse %	Color:
30	5.53	13.68	65.38	19.27	1.68	Dark yellowish brown
40	4.20	17.17	43.55	13.96	25.32	Yellowish brown

Site: 2534A
Location (UTM): 11T 0380513, 5284116
Vegetation: Wheat fallow
Landscape: Hills
Aspect/slope: 270°/5°

Depth (cm):	Mean grain size (Φ):	Clay %	Silt %	Sand %	Coarse %	Color:
30	5.56	15.50	64.21	19.85	0.43	Dark brown
130	6.09	23.22	59.24	17.14	0.41	Dark brown
210	6.11	25.38	54.25	19.99	0.38	Dark yellowish brown
240	6.19	28.75	48.38	14.14	8.72	Dark yellowish brown

Site: 2624A
Location (UTM): 11T 0284441, 5296601
Vegetation: Wheat
Landscape: Flat
Aspect/slope: Flat

Depth (cm):	Mean grain size (Φ):	Clay %	Silt %	Sand %	Coarse %	Color:
30	5.53	16.25	59.78	21.33	2.64	Dark brown
70	6.21	27.55	50.64	21.81	0.00	Brown

Site: 2625A
Location (UTM): 11T 0294068, 5296016
Vegetation: Wheat
Landscape: Ground moraine (Esker)
Aspect/slope: Flat

Depth (cm):	Mean grain size (Φ):	Clay %	Silt %	Sand %	Coarse %	Color:
30	5.08	16.30	51.18	26.25	6.27	Dark yellowish brown

Site: 2626A
Location (UTM): 11T 0303671, 5295820
Vegetation: Sage, Bunchgrass
Landscape: Low hills
Aspect/slope: Flat

Depth (cm):	Mean grain size (Φ):	Clay %	Silt %	Sand %	Coarse %	Color:
30	4.53	16.16	50.07	18.72	15.05	Dark yellowish brown

Site: 2627A
Location (UTM): 11T 0313426, 5295592
Vegetation: Sage, Bunchgrass
Aspect/slope: 40°/2°
Landscape: Low hills, Flat

Depth (cm):	Mean grain size (Φ):	Clay %	Silt %	Sand %	Coarse %	Color:
20	4.59	15.72	44.64	31.71	7.92	Dark brown

Site: 2628A
Location (UTM): 11T 0323049, 5295267
Vegetation: Bunchgrass
Aspect/slope: Flat
Landscape: Low rolling hills

Depth (cm):	Mean grain size (Φ):	Clay %	Silt %	Sand %	Coarse %	Color:
30	5.97	21.59	58.34	18.58	1.49	Very dark grayish brown
60	6.85	31.21	53.41	15.22	0.16	Gray
90	7.61	36.34	61.94	1.72	0.00	Olive gray
120	7.54	41.07	52.88	5.76	0.29	Olive gray

Site: 2629B
Location (UTM): 11T 0337499, 5294835
Vegetation: Bunchgrass, Sage
Aspect/slope: 0°/2°
Landscape: Scabland

Depth (cm):	Mean grain size (Φ):	Clay %	Silt %	Sand %	Coarse %	Color:
30	5.07	12.38	60.74	23.02	3.85	Dark brown
65	5.15	22.12	47.63	18.49	11.76	Brown

Site: 2630A

Location (UTM): 11T 0342346, 5294714
Vegetation: Wheat fallow
Landscape: Rolling hills
Aspect/slope: 280°/6°

Depth (cm)	Mean grain size (Φ)	Clay %	Silt %	Sand %	Coarse %	Color
30	5.49	14.92	62.70	22.39	0.00	Dark yellowish brown
100	5.89	22.21	56.46	21.32	0.00	Yellowish brown
160	6.43	27.31	58.38	14.30	0.00	Yellowish brown
220	5.85	20.76	58.74	20.50	0.00	Yellowish brown
315	5.81	19.39	60.99	19.07	0.55	Dark yellowish brown
360	4.80	13.37	51.81	34.82	0.00	Dark yellowish brown

Site: 2631A

Location (UTM): 11T 0352053, 5294478
Vegetation: Grasses
Landscape: Rolling hills
Aspect/slope: 40°/10°

Depth (cm)	Mean grain size (Φ)	Clay %	Silt %	Sand %	Coarse %	Color
30	5.73	19.61	58.73	21.16	0.50	Very dark brown
60	6.51	30.05	50.45	18069	0.80	Dark yellowish brown

Site: 2633A

Location (UTM): 11T 0371067, 5294095
Vegetation: Wheat
Landscape: Hills
Aspect/slope: 225°/1°

Depth (cm)	Mean grain size (Φ)	Clay %	Silt %	Sand %	Coarse %	Color
30	5.69	16.03	66.93	17.04	0.00	Dark yellowish brown
110	6.29	25.86	57.80	16.34	0.00	Dark yellowish brown
160	6.62	29.00	60.49	10.51	0.00	Yellowish brown
210	6.50	27.48	60.70	11.82	0.00	Brown
250	6.51	28.29	57.97	13.73	0.00	White
270	6.45	28.04	56.81	15.15	0.00	Yellowish brown

Site: **2634A**

Location (UTM):
11T 0380730, 5293888

Aspect/slope:
135°/7°

Vegetation:
Grasses

Landscape:
Rolling hills

Depth (cm):	Mean grain size (Φ):	Clay %	Silt %	Sand %	Coarse %	Color:
30	6.43	26.37	60.98	12.65	0.00	Dark yellowish brown
90	5.67	15.67	65.20	19.14	0.00	Light yellowish brown
110	6.31	22.49	68.50	9.01	0.00	Pale brown
180	6.97	33.42	63.28	3.30	0.00	Yellowish brown
260	6.69	29.99	59.23	10.78	0.00	Light yellowish brown

Site: **2727A**

Location (UTM):
11T 03113785, 5305218

Aspect/slope:
Flat

Vegetation:
Short grasses

Landscape:
Low hills

Depth (cm):	Mean grain size (Φ):	Clay %	Silt %	Sand %	Coarse %	Color:
30	4.51	13.68	40.00	42.11	4.22	Dark brown
65	4.27	12.68	47.29	31.17	8.86	Dark brown

Site: **2728A**

Location (UTM):
11T 0323371, 5304917

Aspect/slope:
295°/5°

Vegetation:
Sage, Bunchgrass

Landscape:
Rolling hills

Depth (cm):	Mean grain size (Φ):	Clay %	Silt %	Sand %	Coarse %	Color:
30	4.60	10.39	52.89	28.11	8.61	Dark brown

Site: 2731A

Location (UTM): 11T 0352365, 5304200
Vegetation: Sage, Short grasses
Aspect/slope: 270°/1°
Landscape: Low hills

Depth (cm):	Mean grain size (Φ):	Clay %	Silt %	Sand %	Coarse %	Color:
30	5.40	17.28	57.29	24.95	0.48	Dark yellowish brown
75	6.67	27.99	61.09	10.92	0.00	Light yellowish brown
110	6.60	27.38	61.61	11.02	0.00	Yellowish brown
140	6.67	30.48	55.42	13.23	0.88	Light yellowish brown

Site: 2732A

Location (UTM): 11T 0361602, 5304032
Vegetation: Wheat
Aspect/slope: Flat
Landscape: Low hills

Depth (cm):	Mean grain size (Φ):	Clay %	Silt %	Sand %	Coarse %	Color:
30	5.88	20.40	60.48	19.12	0.00	Dark yellowish brown
140	6.88	32.02	58.12	9.86	0.00	Brown
180	6.66	31.97	51.14	16.89	0.00	Yellowish brown

Site: 2825A

Location (UTM): 11T 0294663, 5315592
Vegetation: Wheat fallow
Aspect/slope: 80°/5°
Landscape: Rolling hills

Depth (cm):	Mean grain size (Φ):	Clay %	Silt %	Sand %	Coarse %	Color:
30	4.74	14.22	45.56	34.30	5.92	Very dark grayish brown
50						Very dark grayish brown

Site: 2826A

Location (UTM): 11T 0304542, 5315295
Vegetation: Wheat fallow
Aspect/slope: 250°/50°
Landscape: Ground Moraine (Hummocky)

Depth (cm):	Mean grain size (Φ):	Clay %	Silt %	Sand %	Coarse %	Color:
30	4.73	13.45	56.95	23.83	5.76	Brown

Site: 2828A
Location (UTM): 11T 0323615, 5314702
Vegetation: Sage, Bunchgrass
Landscape: Kame
Aspect/slope: 270°/15°

Depth (cm):	Mean grain size (Φ):	Clay %	Silt %	Sand %	Coarse %	Color:
30	5.38	19.13	51.79	23.85	5.22	Dark brown
55	3.94	13.05	36.17	40.76	10.02	Brown

Site: 2829A
Location (UTM): 11T 0331882, 5313892
Vegetation: Sage, Bunchgrass
Landscape: Ground moraine
Aspect/slope: Flat

Depth (cm):	Mean grain size (Φ):	Clay %	Silt %	Sand %	Coarse %	Color:
25	5.07	20.58	45.40	20.82	13.20	Dark brown

Site: ML 1
Location (UTM): 11T 0322595, 5220011
Vegetation: Sage, Short grasses
Landscape: Dunes
Aspect/slope: 340°/15°

Sample:	Mean grain size (Φ):	Clay %	Silt %	Sand %	Coarse %	Color:
1	3.02	6.78	12.53	80.50	0.20	Dark olive gray

Site: **ML 2**
Location (UTM): 11T 0293664, 5231352
Vegetation: Sage, Bunchgrass
Landscape: Dunes
Aspect/slope: 100°/10°

Sample:	Mean grain size (Φ):	Clay %	Silt %	Sand %	Coarse %	Color:
1	2.60	6.22	12.70	80.83	0.25	Olive gray
2	2.93	7.18	13.94	78.80	0.08	Olive gray
3	2.00	2.46	9.95	87.13	0.46	Light gray
4	2.01	2.37	9.93	86.75	0.95	Light gray
5	2.72	4.86	14.64	79.86	0.64	Light yellowish brown
6	2.29	3.58	7.28	88.14	1.01	Light yellowish brown
7	2.74	4.96	11.85	82.95	0.23	Light yellowish brown
8	3.22	6.69	21.21	67.55	4.55	Yellowish brown
9	3.14	8.29	18.67	72.05	0.99	Yellowish brown
10	3.78	9.08	26.10	64.55	0.27	Dark yellowish brown

Depth (cm):	Mean grain size (Φ):	Clay %	Silt %	Sand %	Coarse %	Color:
30	2.87	4.62	15.33	79.47	0.57	Olive gray
90	2.59	7.16	11.52	78.45	2.86	Very dark gray
150	2.15	5.87	10.60	80.69	2.84	Very dark gray
180	2.57	8.37	15.69	67.99	7.95	Dark olive gray
210	2.15	5.59	10.96	79.85	3.60	Dark olive gray
240	2.31	7.05	10.86	79.36	2.73	Dark olive gray
290	2.76	4.59	17.20	77.67	0.55	Dark olive gray
330	2.54	5.30	12.77	81.70	0.23	Dark olive gray
380	1.81	3.23	5.33	91.30	0.14	Dark olive gray
420	2.17	5.45	6.98	82.74	4.83	Dark olive gray
450	2.00	4.73	5.70	85.68	3.88	Dark olive gray
480	2.25	7.00	6.32	84.76	1.93	Dark olive gray
510	2.12	4.69	5.58	86.81	2.92	Dark olive gray
540	2.17	4.01	5.47	87.08	3.44	Dark olive gray
570	2.62	6.68	11.99	72.65	8.68	Dark olive gray
600	2.54	5.03	9.08	83.30	2.59	Dark olive gray
630	2.65	5.34	12.42	79.38	2.85	Dark olive gray

Site: ML 3

Location (UTM): 11T 0294847, 5233104
Vegetation: Not vegetated
Landscape: Dunes
Aspect/slope: Flat

Sample:	Mean grain size (Φ):	Clay %	Silt %	Sand %	Coarse %	Color:
1	4.00	8.89	33.54	57.38	0.20	Yellowish brown
2	4.08	6.41	41.87	51.72	0.00	Yellowish brown
3	2.53	7.88	19.15	55.05	17.92	Very dark gray

Site: ML 4

Location (UTM): 11T 0296650, 5228234
Vegetation: Not vegetated
Landscape: Dunes
Aspect/slope: Flat

Sample:	Mean grain size (Φ):	Clay %	Silt %	Sand %	Coarse %	Color:
1	2.97	38.98	25.63	10.83	24.56	Light brownish gray
2	3.85	11.97	32.53	43.20	12.30	Yellowish brown
3	4.03	12.40	32.02	47.59	7.99	Light brownish gray
4	4.54	13.06	44.44	34.86	7.64	Brown
5	4.20	11.48	41.31	37.02	10.19	Brown
6	4.91	14.77	49.38	30.24	5.61	Dark brown

Site: ML 5

Location (UTM): 11T 0311440, 5224603
Vegetation: Not vegetated
Landscape: Dry valley bottom
Aspect/slope: Flat

Sample:	Mean grain size (Φ):	Clay %	Silt %	Sand %	Coarse %	Color:
1	-0.10	1.36	1.33	29.00	68.31	Black

Site: ML 6
Location (UTM): 11T 0348185, 5224843
Vegetation: Bunchgrass
Landscape: Low hills
Aspect/slope: 340°/10°

Sample:	Mean grain size (Φ):	Clay %:	Silt %:	Sand %:	Coarse %:	Color:
1	4.51	12.80	48.02	25.10	14.09	Brown

Site: NP
Location (UTM): 11T 0343659, 5303966
Vegetation: Sage, Bunchgrass
Landscape: Coulee floor
Aspect/slope: Flat

Sample:	Mean grain size (Φ):	Clay %:	Silt %:	Sand %:	Coarse %:	Color:
1	6.55	18.59	78.33	3.08	0.00	Light olive gray
2	3.44	9.07	17.72	73.22	0.00	Very dark gray
3	2.73	4.87	15.09	77.55	2.50	Very dark gray
4	7.41	36.29	61.18	2.53	0.00	Light olive gray

Site: RT 1
Location (UTM): 11T 0357172, 5224546
Vegetation: Shorts grasses
Landscape: Low hills
Aspect/slope: 190°/15°

Sample:	Mean grain size (Φ):	Clay %:	Silt %:	Sand %:	Coarse %:	Color:
1	5.14	16.71	51.78	19.12	12.40	Yellowish brown

Site: RT 2
Location (UTM): 11T 0360746, 5216469
Vegetation: Short grasses
Landscape: Intermittent stream valley
Aspect/slope: 10°/10°

Sample:	Mean grain size (Φ):	Clay %:	Silt %:	Sand %:	Coarse %:	Color:
1	4.80	11.38	51.03	37.44	0.15	Brown
2	3.28	9.88	33.34	39.57	17.21	Brown
3	5.66	17.07	63.69	19.24	0.00	Dark brown

Site: **SR1**

Location (UTM):
11T 0340411, 5303440

Vegetation:
Sparse short grasses

Landscape:
Plateau

Aspect/slope:
Flat

Sample:
1

Mean grain size (Φ):
3.96

Clay %
13.08

Silt %
42.96

Sand %
26.18

Coarse %
17.77

Color:
Very dark brown

Site: **SR2**

Location (UTM):
11T 0341306, 5302921

Vegetation:
Sage

Landscape:
Dunes

Aspect/slope:
290˚/20˚

Sample:
1

Mean grain size (Φ):
1.71

Clay %
4.88

Silt %
4.39

Sand %
90.68

Coarse %
0.05

Color:
Light yellowish brown

130

APPENDIX E:

LABELED SAMPLE SITE LOCATION MAP